East Engineering

Journal of Research

of the

National Bureau of Standards

SEPTEMBER 1953

VOLUME 51 NUMBER 3

U. S. DEPARTMENT OF COMMERCE
Sinclair Weeks, Secretary
NATIONAL BUREAU OF STANDARDS
A. V. Astin, Director

SEPTEMBER • 1953
VOLUME • 51
NUMBER • 3

JOURNAL OF RESEARCH

of the

NATIONAL BUREAU OF STANDARDS

PERIODICALS OF THE NATIONAL BUREAU OF STANDARDS

The National Bureau of Standards is engaged in fundamental and applied research in physics, chemistry, mathematics, and engineering. Projects are conducted in thirteen fields: electricity, optics and metrology, heat and power, atomic and radiation physics, chemistry, mechanics, organic and fibrous materials, metallurgy, mineral products, building technology, applied mathematics, electronics, and radio propagation. The Bureau has custody of the national standards of measurement and conducts research leading to the improvement of scientific and engineering standards and of techniques and methods of measurement. Testing methods and instruments are developed; physical constants and properties of materials are determined; and technical processes are investigated.

JOURNAL OF RESEARCH

Internationally known as a leading scientific periodical, the Journal presents research papers by authorities in the specialized fields of physics, mathematics, chemistry, and engineering. Complete details of the work are presented, including laboratory data, experimental procedures, and theoretical and mathematical analyses. Annual subscription: domestic, $5.50; foreign, $6.75.

TECHNICAL NEWS BULLETIN

Summaries of current research at the National Bureau of Standards are published each month in the Technical News Bulletin. The articles are brief, with emphasis on the results of research, chosen on the basis of their scientific or technologic importance. Lists of all Bureau publications during the preceding month are given, including Research Papers, Handbooks, Applied Mathematics Series, Building Materials and Structures Reports, and Circulars. Each issue contains 12 or more two-column pages; illustrated. Annual subscription: domestic, $1.00; foreign, $1.35.

BASIC RADIO PROPAGATION PREDICTIONS

The Predictions provide the information necessary for calculating the best frequencies for communication between any two points in the world at any time during the given month. The data are important to all users of long-range radio communications and navigation, including broadcasting, airline, steamship, and wireless services, as well as to investigators of radio propagation and ionosphere. Each issue, covering a period of one month, is released three months in advance and contains 16 large pages, including pertinent charts, drawings, and tables. Annual subscription: domestic, $1.00; foreign, $1.25.

Order all publications from the Superintendent of Documents
U. S. Government Printing Office, Washington 25, D. C.

The printing of this publication has been approved by the Director of the Bureau of the Budget, May 12, 1953.

Journal of Research of the National Bureau of Standards Vol. 51, No. 3, September 1953 Research Paper 2440

Refractive Index of Cesium Bromide for Ultraviolet, Visible, and Infrared Wavelengths

William S. Rodney and Robert J. Spindler

The index of refraction of cesium bromide was measured at 37 wavelengths from 0.365 to 39.22 microns. The minimum deviation method was used, and the entire range was covered with a single instrument. The index changes approximately two units in the first decimal place over the wavelength range. The dispersion compares favorably with that of KRS–5 beyond 20 microns; and when the effects of inhomogeneity and reflection losses are considered, the resolving power of CsBr is probably better.

1. Introduction

Large crystals of cesium bromide of reasonably good optical quality have recently been successfully grown, providing a new material for infrared studies in the range beyond the 25-micron (μ) limit of KBr and out to about 40 μ, wherein lie many of the fundamental modes of vibrations of molecules. A mixed crystal of thallium bromide-iodide, known as KRS–5, was previously the only material available for use in this region.

In order to utilize fully any dispersive medium, spectroscopists must have a knowledge of the indices of refraction and dispersion for all wavelengths transmitted by the medium. Such data are also useful to physicists for evaluating theoretical dispersion equations and for studying the forces between the constituents of the crystal. The alkali-halides, having the cubic structure, are favorable subjects for such studies.

The authors are fortunate in having access to two samples of cesium bromide whose faces are about 1 sq in. One of these samples was grown by the Harshaw Chemical Co. of Cleveland, Ohio, and the other was grown at the National Bureau of Standards by Francis P. Phelps of the Mineral Products Division. The refractive indices of each of these samples were determined for 37 wavelengths ranging from 0.365 to 39.22 μ, the latter being near the infrared transmission limit of cesium bromide.

2. Instrument

The instrument (fig. 1) used in these experiments is a Gaertner precision spectrometer adapted for measuring indices of refraction for nonvisible radiation. The telescope and collimator objectives have been replaced by mirrors of the same focal length. The telescope eyepiece is replaced by a second, or exit, slit. The radiation is focussed on the exit slit by the telescope mirror, and the image of the slit on the prism face is formed on the detector by use of another mirror or a lens of KRS–5.

The infrared detectors employed are the lead sulfide photoconducting cell for the near ultraviolet, the visible, and the infrared to about 2.5 μ; and the Golay pneumatic detector beyond 2.5 μ to the limit of transmission of the window employed with this cell, which in this case is about 40 μ. The signal, chopped at the rate of 10 times a second, is amplified by a gated amplifier controlled by a photocell in the chopper unit. The amplified signal is recorded on a recording potentiometer.

The spectrometer is equipped with a set of gears, also shown in figure 1, in such ratio that when engaged the prism table rotates at one-half the rotation rate of the telescope and microscope ring. The gears may be readily engaged at will, and they maintain a condition of minimum deviation once it has been established for any line. The method of minimum deviation provides desirable features of high accuracy and simplicity of calculation as compared, for example, with methods where a constant angle of incidence is employed.

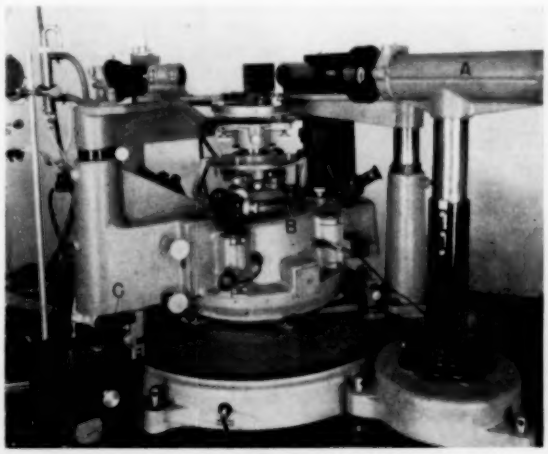

FIGURE 1. *Gaertner precision spectrometer.*

A, Auxiliary telescope is used to level and center the prism; B, gear system is used to maintain minimum deviation; C, driving mechanism for scanning. Entrance slit is partially hidden by telescope mirror directly above driving mechanism. Collimator mirror is hidden by the auxiliary telescope. Exit slit is seen between prism and auxiliary telescope.

267518—53—1

3. Procedure

To begin a series of measurements the refracting angle of the prism and the deviation angles at minimum deviation for several visible lines are measured on a Watts precision spectrometer by the usual methods and described in a previous paper [1].[1] Index of refraction values accurate to $\pm 1\times10^{-5}$ are easily attainable by this method [2]. Then an auxiliary telescope, figure 1, is used to level and center the prism with respect to the optical axis of the mirror system on the Gaertner spectrometer. Another auxiliary telescope is used to set a given line, usually the 0.6438 μ line of cadmium, at its minimum deviation position. The table is now clamped in this position. The mirror, acting as the telescope objective, is brought into the beam so that an image of this line falls on the exit slit, causing a deflection of the potentiometer pen. The scale position corresponding to maximum deflection of the pen is observed with the microscopes. This is repeated several times, and the microscope is set at the average of these readings and clamped. The gears are now engaged and the telescope and prism-table clamps released. A condition of minimum deviation will then prevail for other spectral lines.

Unfortunately, with this mirror system, one cannot directly observe the position of an undeviated beam or measure twice the minimum deviation, as is feasible in visual measurements. It is therefore necessary to compute the average reading for an undeviated beam by applying a few deviations, as observed visually on the Watts instrument, to the scale readings on the Gaertner spectrometer for the corresponding lines of the visual spectrum as determined by the use of the detector.

The spectra are now scanned by using a driving mechanism consisting of a synchronous motor and a gear segment attached to the telescope assembly. The spectra used are the emission lines of mercury and cadmium for the ultraviolet, visible, and infrared to about 2.3 μ, the absorption bands of polystyrene from approximately 3 to 15 μ [3], 1,2,4-trichlorobenzene from approximately 15 to 20 μ [3], and water-vapor bands for the rest of the range [4]. The bands of carbon dioxide at 4.2 and 14.9 μ are also used. The scanning serves to identify and locate the approximate scale position corresponding to these lines and bands. The actual measurements are made by the method used to determine precisely the scale position for the 0.6438 μ line. For some broad bands and for the region of low intensity, scale positions may be read from the graphs. This is done by using a relay to mark the graph at intervals varying from 1 min of arc to 15 sec of arc, depending on the speed at which the telescope is being driven.

4. Data

The refractive indices of the two crystals of cesium bromide were measured at room temperatures near 24° and 31° C. The temperature was determined by placing a calibrated mercury thermometer directly over the sample and observing the temperature at 1-min intervals with a telescope and averaging. This procedure was repeated several times each day, and the variations between these averages did not exceed ± 0.2 deg C. Indices were determined for 37 wavelengths, ranging from 0.365 to 39.22 μ, at each temperature. Temperature coefficients of refractive index were determined, and the indices at 24° and 31° C were adjusted to 27° and averaged for each sample. These average values were again averaged, giving the average for both samples. The average temperature coefficient for both samples is 7.9×10^{-5}/deg C.

Table 1 lists the indices at this temperature as obtained from the observations and as computed by means of eq 1.

$$n^2=a^2-k\lambda^2+\frac{p}{\lambda^2}+\frac{M}{\lambda^2-L^2}+\frac{m}{\lambda^2-l^2} \qquad (1)$$

where

λ = wavelength, microns
$a^2=5.640752$
$k=0.000003338$
$p=0.0018612$
$M=41110.49$
$L^2=(119.96)^2=14390.4$
$m=0.0290764$
$l^2=(0.15800)^2=0.024964$.

Although this equation has 7 constants, only 5 of them were determined by means of a simultaneous solution. The constants appearing in the denom-

TABLE 1. *Observed and computed data on index of refraction of* CsBr (27° C)

Wavelength (microns)	Observed index, n_0	Computed index, n_c	(n_0-n_c)
0.365015	1.75118	1.75113	$+5\times10^5$
.366288	1.75050	1.75045	+5
.404656	1.73344	1.73343	+1
.435835	1.72333	1.72335	−2
.546074	1.70190	1.70193	−4
.643847	1.69202	1.69204	−2
1.01398	1.67766	1.67766	0
1.12866	1.67584	1.67584	0
1.52952	1.67237	1.67238	−1
1.7011	1.67158	1.67157	+1
3.3610	1.66866	1.66866	0
4.258	1.66794	1.66793	+1
6.465	1.66587	1.66620	−33
9.724	1.66283	1.66285	−2
11.035	1.66118	1.66115	+3
14.29	1.65594	1.65599	−5
14.98	1.65474	1.65472	+2
15.48	1.65375	1.65375	0
17.40	1.64967	1.64974	−7
18.16	1.64795	1.64801	−6
20.57	1.64184	1.64197	−13
21.80	1.63846	1.63856	−10
22.76	1.63565	1.63573	−8
23.86	1.63234	1.63231	+3
25.16	1.62817	1.62802	+15
25.97	1.62521	1.62520	+1
26.63	1.62284	1.62282	+2
29.81	1.61034	1.61028	+6
30.54	1.60749	1.60713	+36
30.91	1.60591	1.60550	+41
31.70	1.60198	1.60192	+6
33.00	1.59584	1.59576	+8
34.48	1.58835	1.58831	+4
35.45	1.58284	1.58317	−33
35.90	1.58069	1.58071	−2
37.52	1.57183	1.57147	+36
39.22	1.55990	1.56106	−116

[1] Figures in brackets indicate the literature references at the end of this paper.

inators of two terms represent the infrared and ultraviolet absorption bands. The ultraviolet term, F, was determined by taking a weighted mean of several measured bands. The infrared term, L^2, is an estimate based on the measured and computed values of the infrared absorption bands of cesium chloride and is probably low.

Some obvious anomalies occur in the residuals, for instance, at wavelengths 6.465 and 35.45 μ. It is known that the first of these bands consists of several unresolved bands, indicating that the anomalous residual may be due to an inaccurate value for the wavelength. A value of 6.695 μ arrived at by taking a differently weighted average gives a more consistent value of n. The bands at 35.45 and 39.22 μ are quite broad, causing considerable difficulty in locating their minima.

Index of refraction as a function of wavelength is plotted in figure 2. This graph is particularly interesting as it shows the smoothness that results from taking data over a large range on a single instrument for a single sample and under the same conditions. It is hoped that consistent data such as these will lend themselves more readily to theoretical analysis. The total change in index amounts to approximately 2 units in the first decimal place over the wavelength range considered. The values plotted are the indices at 27° C. Differences between samples are small.

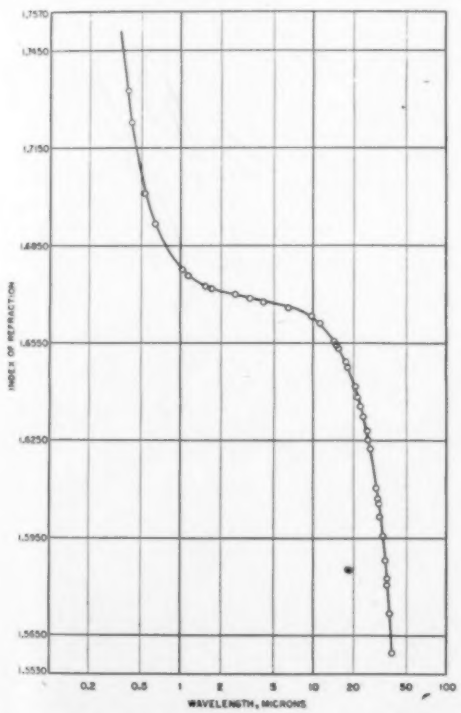

FIGURE 2. *Index of refraction of* CsBr *as a function of wavelength.*
Wavelength scale is logarithmically graduated.

The index values of the Phelps crystal are lower by several units in the fifth decimal than corresponding values for the Harshaw crystal. The only prior data available are 3 values in the visible spectral region given by Sprockoff [5] to only 4 decimal places at an unspecified temperature.

The preliminary values published by the authors [6] for only one of the crystals are in substantial agreement with values published in this paper. There are some changes and additions beyond 30 μ, and in many cases another significant figure has been added.

Equation (1) has been used for computing values of $n-1$ for cesium bromide that are listed in table 2. They are considered as the best values obtainable from the measurements here described and are probably accurate to within ± 1 or 2×10^{-5}, except for wavelengths longer than about 30 μ.

The dispersion $\Delta n/\Delta\lambda$ of CsBr is shown in figure 3. Both abscissa and ordinate are logarithmically graduated. The dispersion in the far infrared increases but remains less than in the visible region by a factor of 10. The values of $\Delta n/\Delta\lambda$ are plotted at the midpoint of the $\Delta\lambda$ increment.

Values for the dispersion of KBr and KRS–5 [7, 8] were also computed at various wavelengths and plotted for comparison purposes. We see that KRS–5 has a higher dispersion than CsBr throughout the spectral range considered. KBr has a higher dispersion than either from 10 to 25 μ, where it becomes opaque. This result would lead to the conclusion that KRS–5 is better than CsBr as a dispersive material, if the effects of its optical inhomogeneity and larger index could be ignored.

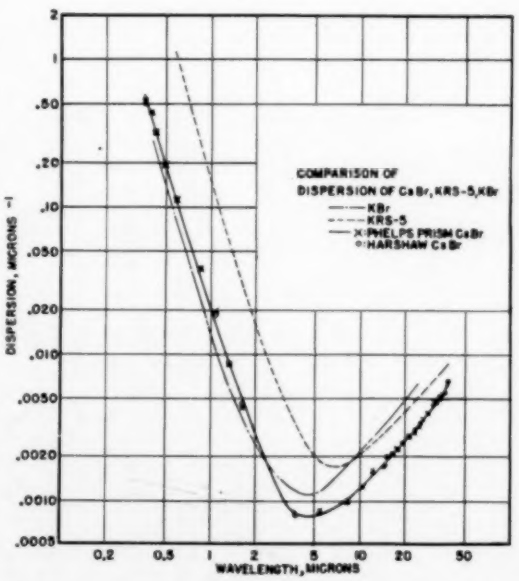

FIGURE 3. *Dispersion as a function of wavelength.*
Both abscissa and ordinate are logarithmically graduated.

TABLE 2. *Refractivity, $(n-1)\times 10^5$, of* CsBr *at 27° C*

This table gives the average refractivity of two samples of CsBr, one grown at the Harshaw Chemical Co. and one grown at the National Bureau of Standards.

Wavelength	Refractivity at wavelength (microns)—									
	.0	.1	.2	.3	.4	.5	.6	.7	.8	.9
0	------	------	------	------	73, 519	70, 896	69, 583	68, 825	68, 345	68, 022
1	67, 793	67, 624	67, 496	67, 397	67, 318	67, 254	67, 201	67, 157	67, 120	67, 088
2	67, 061	67, 036	67, 015	66, 996	66, 979	66, 963	66, 948	66, 935	66, 923	66, 911
3	66, 901	66, 890	66, 881	66, 871	66, 862	66, 853	66, 845	66, 837	66, 829	66, 821
4	66, 813	66, 805	66, 798	66, 790	66, 782	66, 775	66, 767	66, 760	66, 752	66, 745
5	66, 737	66, 730	66, 722	66, 715	66, 707	66, 699	66, 691	66, 683	66, 675	66, 667
6	66, 659	66, 651	66, 643	66, 634	66, 626	66, 617	66, 609	66, 600	66, 591	66, 582
7	66, 573	66, 564	66, 555	66, 545	66, 536	66, 526	66, 517	66, 507	66, 497	66, 487
8	66, 477	66, 467	66, 457	66, 446	66, 436	66, 425	66, 414	66, 403	66, 392	66, 381
9	66, 370	66, 359	66, 347	66, 335	66, 324	66, 312	66, 300	66, 288	66, 276	66, 263
10	66, 251	66, 238	66, 226	66, 213	66, 200	66, 187	66, 174	66, 160	66, 147	66, 134
11	66, 120	66, 106	66, 092	66, 078	66, 064	66, 050	66, 035	66, 021	66, 006	65, 991
12	65, 976	65, 961	65, 946	65, 931	65, 915	65, 900	65, 884	65, 868	65, 852	65, 836
13	65, 820	65, 804	65, 787	65, 770	65, 754	65, 737	65, 720	65, 703	65, 685	65, 668
14	65, 651	65, 633	65, 615	65, 597	65, 579	65, 561	65, 543	65, 524	65, 505	65, 487
15	65, 468	65, 449	65, 430	65, 411	65, 391	65, 372	65, 352	65, 332	65, 312	65, 292
16	65, 272	65, 251	65, 231	65, 210	65, 190	65, 169	65, 148	65, 126	65, 105	65, 084
17	65, 062	65, 040	65, 018	64, 996	64, 974	64, 952	64, 929	64, 907	64, 884	64, 861
18	64, 838	64, 815	64, 792	64, 768	64, 745	64, 721	64, 697	64, 673	64, 649	64, 625
19	64, 600	64, 576	64, 551	64, 526	64, 501	64, 476	64, 450	64, 425	64, 399	64, 374
20	64, 348	64, 322	64, 295	64, 269	64, 243	64, 216	64, 189	64, 162	64, 135	64, 108
21	64, 080	64, 053	64, 025	63, 997	63, 969	63, 941	63, 913	63, 884	63, 856	63, 827
22	63, 798	63, 769	63, 739	63, 710	63, 681	63, 651	63, 621	63, 591	63, 561	63, 530
23	63, 500	63, 469	63, 438	63, 407	63, 376	63, 345	63, 313	63, 282	63, 250	63, 218
24	63, 186	63, 154	63, 121	63, 089	63, 056	63, 023	62, 990	62, 957	62, 923	62, 890
25	62, 856	62, 822	62, 788	62, 754	62, 719	62, 685	62, 650	62, 615	62, 580	62, 545
26	62, 509	62, 474	62, 438	62, 402	62, 366	62, 330	62, 293	62, 256	62, 220	62, 183
27	62, 146	62, 108	62, 071	62, 033	61, 995	61, 957	61, 919	61, 881	61, 842	61, 803
28	61, 764	61, 725	61, 686	61, 646	61, 607	61, 567	61, 527	61, 487	61, 446	61, 406
29	61, 365	61, 324	61, 283	61, 242	61, 200	61, 158	61, 116	61, 074	61, 032	60, 990
30	60, 947	60, 904	60, 861	60, 818	60, 775	60, 731	60, 687	60, 643	60, 599	60, 555
31	60, 510	60, 465	60, 420	60, 375	60, 330	60, 284	60, 238	60, 192	60, 146	60, 100
32	60, 053	60, 007	59, 960	59, 912	59, 865	59, 817	59, 770	59, 722	59. 673	59, 625
33	59, 576	59, 527	59, 478	59, 429	59, 380	59, 330	59, 280	59, 230	59, 179	59, 129
34	59, 078	59, 027	58, 976	58, 924	58, 873	58, 821	58, 769	58, 717	58, 664	58, 611
35	58, 558	58, 505	58, 452	58, 398	58, 344	58, 290	58, 236	58, 181	58, 126	58, 071
36	58, 016	57, 960	57, 905	57, 849	57, 792	57, 736	57, 679	57, 622	57, 565	57, 508
37	57, 450	57, 392	57, 334	57, 276	57, 217	57, 158	57, 099	57, 040	56, 980	56, 920
38	56, 860	56, 800	56, 739	56, 678	56, 617	56, 556	56, 494	56, 432	56, 370	56, 308
39	56, 245	56, 182	56, 119	------	------	------	------	------	------	------

The results of practical tests on these materials [9] indicate that CsBr prisms gives better resolving power. This better resolving power could, largely, be due to better optical homogeneity of CsBr. The effects of higher index of KRS–5 also deserve some consideration because there are practical limits to the size of the crystals grown.

5. References

[1] R. J. Spindler and W. S. Rodney, J. Research NBS **49,** 253 (1952) RP2361.

[2] L. W. Tilton, BS J. Research **2,** 909 (1929) RP64.

[3] E. K. Plyler and C. Wilbur Peters, J. Research NBS **45,** 6 (1950) RP2159.

[4] Randal, Dennison, Ginsburg, and Weber, Phys. Rev. 52, 160 (1937).

[5] M. Sprockhoff, Neues Jahr Mineral Geol., Beilage Bd. 18, 117–154 (1904).

[6] W. S. Rodney and R. J. Spindler, J. Opt. Soc. Am. 42, 431 (1952).

[7] R. E. Stephens, Earle K. Plyler, W. S. Rodney, and R. J. Spindler, J. Opt. Soc. Am. **43,** 110 (1953).

[8] L. W. Tilton, E. K. Plyler, and R. E. Stephens, J. Research NBS **43,** 81 (1949) RP2008.

[9] E. K. Plyler and Nicola Acquista, J. Research NBS 60, 61 (1952) RP2343.

WASHINGTON, July 9, 1953.

Journal of Research of the National Bureau of Standards Vol. 51, No. 3, September 1953 Research Paper 2441

An Expansion Method for Parabolic Partial Differential Equations[1]

J. W. Green[2]

The aim of this paper is to adapt to certain parabolic partial differential equations an expansion method of solution developed by S. Faedo[3] for hyperbolic equations. In order to make possible a moderately compact presentation, the equations treated are not the most general to which the method is applicable, but are the simplest nontrivial relatives of the heat equation. Similarly, the boundary values and initial conditions are not the most general, but are assumed to be in a canonical form to which others, if sufficiently smooth, can be reduced. The method of solution not only shows the existence of a solution, but describes a definite procedure for approximating it. Some remarks are made on the possibility of estimating the error.

1. Statement of Problem

In the region S, $0 \leq x \leq \pi$, $0 \leq t < \infty$, we seek a solution of the equation

$$L(u) \equiv u_{xx} - u_t - gu = f \tag{1}$$

subject to the initial conditions

$$u(x,0) = u(0,t) = u(\pi,t) = 0. \tag{2}$$

The functions f and g are continuous in S, together with their first two partial derivatives. As a compatibility condition, we require that $f(0,0) = f(\pi,0) = 0$. It is convenient to assume that $g \geq 0$. This is not at all essential, since a substitution of the form $u = e^{\lambda t} v$ transforms (1) into

$$v_{xx} - v_t - (g+\lambda)v = fe^{-\lambda t}. \tag{1'}$$

The new coefficient $g+\lambda$ can be made positive in as large a part of S as desired, and this is sufficient for our purposes.

This method can be applied to more general equations in which u_t has a variable positive coefficient and the u_x term is present. However, the equation selected is of sufficient generality to illustrate the method and results and yet not make the computations unpleasantly complicated. In case $g \equiv$ constant, the method reduces to the method of expanding in eigenfunctions.

2. The Moment Method[4]

We seek an approximation to u in the form[5,6]

$$u_n(x,t) = \sum_k C_{n,k}(t) \sin kx, \tag{3}$$

subject to

$$\int \{L(u_n) - f\} \sin jx\,dx = 0, \qquad j = 1,2, \ldots, n, \tag{4}$$

where

$$C_{n,k}(0) = 0. \tag{5}$$

Equation (4) amounts to

$$-j^2 C_{n,j}(t) - C'_{n,j}(t) - \sum_k C_{n,k}(t) b_{k,j}(t) - a_j(t) = 0, \tag{6}$$

where

$$b_{k,j}(t) = \frac{2}{\pi} \int g(x,t) \sin jx \sin kx\,dx,$$

$$a_j(t) = \frac{2}{\pi} \int f(x,t) \sin jx\,dx.$$

The functions $C_{n,j}(t)$ are thus determined by a system of n simultaneous first-order linear differential equations. These equations are already in canonical form, that is, the derivatives are solved for in terms of the other quantities, and so they have a unique solution satisfying (5). Thus the functions $u_n(x,t)$ are determined in unique fashion.

We intend to show that the sequence $u_n(x,t)$ converges to a solution of (1). The method proceeds by showing that the u_n and certain of their derivatives are uniformly equicontinuous. Recall that the functions f of a family are uniformly equicontinuous in a region, provided that ϵ is given greater than 0, there is a $\delta > 0$ such that $|f(p) - f(q)| < \epsilon$ for any f of the family and any two points p and q of the region whose distance does not exceed δ. Now, Ascoli's theorem asserts that out of a uniformly bounded and equicontinuous sequence of functions a uniformly continuous subsequence can be selected. Therefore, by selecting subsequences of subsequences a sufficient number of times, we shall arrive at a subsequence of the u_n which converges uniformly, together with sufficiently many of its derivatives to allow us to make the existence proof. This latter is effected by using a Green's function and showing that the u_n, for $n \to \infty$, come

[1] The preparation of this paper was sponsored (in part) by the Office of Naval Research.

[2] University of California and National Bureau of Standards.

[3] S. Faedo, Un nuovo metodo per l'analisi esistenziale e quantitativa dei problemi di propagazioni. Annali della Scuola Normale Superiore di Pisa, [III], 1, Fasc. I-IV (1947).

[4] Or Galerkin's method. See, I. S. Sokolnikoff, Mathematical theory of elasticity (McGraw-Hill Book Co., Inc., New York, N. Y., 1946).

[5] As on p. 37 of the reference given in footnote 3, after the existence of the solution has been proved, one can show that the system $\{\sin kx\}$ can be replaced by other suitable orthonormal systems.

[6] Σ means $\sum_1^n$ and $\int$ means $\int_0^\pi$.

successively closer to satisfying an integral equation corresponding to (1), and thus that the limit function does satisfy such an equation.

To prove equicontinuity of our sequences, we make use of a criterion of Tonelli [7] as follows: A class of continuous functions $v(x,t)$ in the region $S_T: 0 \le x \le \pi$, $0 \le t \le T$, is uniformly equicontinuous in this region if (a) for each $\bar{x}$ and $\bar{t}$, $v(\bar{x},t)$ and $v(x,\bar{t})$ are absolutely continuous functions of t and x, respectively, (b) the partial derivatives v_x and v_t are summable in S_T, (c) there exists a constant c such that $\int v_x^2 dx < c$ and $\int v_t^2 dx < c$ for all members of the family. Furthermore any accumulation function of a class satisfying (a), (b), and (c) also satisfies (a) and (b).

Now the functions u_n and those partial derivatives in which we are interested are easily seen to be continuous and to satisfy (a) and (b), and the burden of the proof of equicontinuity falls on obtaining inequalities of the form in (c). This is done by making use of devices similar to those frequently employed to show uniqueness, and to recall them, we shall first prove a uniqueness theorem.

3. Uniqueness

Suppose that two solutions of the system (1) (2) exist, all derivatives appearing in (1) being continuous in S. Their difference v will satisfy (1), (2) with f replaced by zero. Thus $L(v)=0$ and so

$$\int L(v) v\, dx = \int \{ v_{xx} - v_t - g v \} v\, dx = 0. \tag{7}$$

Now

$$\int v_t v\, dx = \int \tfrac{1}{2} \frac{d}{dt} v^2 dx = \tfrac{1}{2} \frac{d}{dt} \int v^2 dx,$$

and

$$\int v_{xx} v\, dx = v_x v \Big|_0^\pi - \int v_x^2 dx = - \int v_x^2 dx.$$

If we put $K(t) = \int v^2 dx$, (7) becomes

$$\tfrac{1}{2} K'(t) = - \int (v_x^2 + g v^2)\, dx \le 0,$$

since $g \ge 0$. Since by (2), $K(0)=0$, we see that $K(t) \le 0$. But K is by its nature nonnegative and $K \equiv 0$, which implies that $v \equiv 0$ and that the two solutions are identical.

Theorem 0. There is at most one function, continuous together with all derivatives appearing in (1) which satisfies the system (1), (2).

4. Certain Bounds

This section is devoted to obtaining the inequalities required to carry out the program outlined in section 3.

4.1. *Lemma. Let $K(x)$ be a nonnegative function satisfying for $x \ge 0$ the inequality $K'(x) \le \alpha \sqrt{K(x)}$, where $\alpha \ge 0$. Then for $x > 0$, $\sqrt{K(x)} \le \sqrt{K(0)} + (\alpha/2)x$.*

Suppose that for some positive x_0, $\sqrt{K(x_0)} > \sqrt{K(0)} + (\alpha/2)x_0$. Then there exists x_1 such that $\sqrt{K(x_1)} = \sqrt{K(0)} + (\alpha/2)x_1$, but $\sqrt{K(x)} > \sqrt{K(0)} + (\alpha/2)x$ for $x_1 < x \le x_0$. In particular, $K(x) > 0$ in $x_1 < x < x_0$ and so in that interval

$$\frac{K'(x)}{\sqrt{K(x)}} \le \alpha.$$

Integrating from x_1 to x_0, we have

$$\sqrt{K(x_0)} - \sqrt{K(x_1)} \le (\alpha/2)\,(x_0 - x_1),$$

or

$$\sqrt{K(x_0)} \le \sqrt{K(x_1)} + (\alpha/2)\,(x_0 - x_1) = \sqrt{K(0)} + (\alpha/2)x_0,$$

a contradiction. The lemma is proved.

Corollary. Let $K(x)$ be a nonnegative function satisfying for $x \ge 0$ the inequality

$$K'(x) \le \alpha(x) \sqrt{K(x)}, \tag{8}$$

where $\alpha(x)$ is nonnegative and nondecreasing. Then for $x \ge 0$,

$$\sqrt{K(x)} \le \sqrt{K(0)} + \tfrac{1}{2} x \alpha(x). \tag{9}$$

Consider any $x_0 > 0$. For $x \le x_0$, $K'(x) \le \alpha(x_0)\sqrt{K(x)}$. By the preceeding lemma, $\sqrt{K(x)} \le \sqrt{K(0)} + \tfrac{1}{2}\alpha(x_0)x$. Setting $x = x_0$ and noting that x_0 is arbitrary, we get the stated result.

4.2. *The bound* [8] *for $\int u_x^2 dx$.* Let each of the equations (4) be multiplied by $C_{n,j}(t)$ and the results summed. There comes out the equation

$$\int \{ u_{xx} - u_t - g u - f \} u\, dx = 0. \tag{10}$$

Since

$$\int u_{xx} u\, dx = - \int u_x^2 dx \text{ and } \int u_t u\, dx = \tfrac{1}{2} \frac{d}{dt} \int u^2 dx,$$

(10) may be written

$$\tfrac{1}{2} \frac{d}{dt} \int u^2 dx = - \int (u_x^2 + g u^2) dx - \int f u\, dx \le \int |f u|\, dx. \tag{11}$$

Set $\int u^2(x,t)\, dx = K(x)$. From (11) and Schwarz's inequality,

$$\tfrac{1}{2} K'(x) \le \int |f u|\, dx \le \sqrt{\int f^2 dx} \cdot \sqrt{\int u^2 dx}. \tag{12}$$

Set

$$\max_{\tau \le t} \sqrt{\int f^2(x,\tau)\, dx} = F(t). \tag{13}$$

Then (12) gives $K'(t) \le 2F(t)\sqrt{K(t)}$. From the corollary of 4.1 we deduce that $\sqrt{K(t)} \le \sqrt{K(0)} + tF(t)$. Now $K(0) = \int u^2(x,0)\, dx = 0$, and so $\sqrt{K(t)} \le tF(t)$.

[7] Tonelli, L'estremo assoluto degli integrali doppi, Annali della Scuola Normale di Pisa (1933).

[8] In section 4 we shall frequently omit the subscript n from u_n. Wherever u appears in section 4, it will mean u_n.

Theorem 1.

$$\int u_n^2(x,t)dx \le t^2F^2(t), \tag{14}$$

where F is given by (13).

4.3. *The bound for* $\int u_{nt}^2 dx$. Let the equations (4) be differentiated with respect to t, multiplied by $C'_{n,t}(t)$, and added. There results from this

$$\int \{u_{xxt} - u_{tt} - gu_t - g_t u - f_t\} u_t dx = 0. \tag{15}$$

Again,

$$\int u_{xxt}u_t dx = -\int u_{xt}^2 dx \text{ and } \int u_{tt}u_t dt = \tfrac{1}{2}\frac{d}{dt}\int u_t^2 dx,$$

so putting $K(t) = \int u_t^2 dx$, we get

$$\begin{aligned} \tfrac{1}{2}K'(t) &= -\int (u_{xt}^2 + gu_t^2)dx - \int (g_t u + f_t)u_t dx \qquad (16)\\ &\le \int (|g_t u| + |f_t|)|u_t|dx \\ &\le \sqrt{\int (|g_t u| + |f_t|)^2 dx \cdot K(t)}. \end{aligned}$$

We define

$$\max_{\tau \le t} |g_t(x,t)| = G_1(t), \tag{17}$$

and

$$\max_{\tau \le t} \sqrt{\int f_t^2(x,\tau)\,dx} = F_1(t). \tag{18}$$

Then

$$\begin{aligned} \int (|g_t u| + |f_t|)^2 dx &\le \int (G_1^2(t)u^2 + 2G_1(t)|uf_t| + f_t^2)dx \\ &\le G_1^2(t)\int u^2 dx + 2G_1(t)\sqrt{\int u^2 dx \int f_t^2 dx} + \int f_t^2 dx \\ &\le G_1^2(t)t^2F^2(t) + 2G_1(t)tF(t)F_1(t) + F_1^2(t) = H^2(t), \end{aligned}$$

this last equation being a definition of $H(t)$.

From (16) we have $K'(t) \le 2H(t)\sqrt{K(t)}$, and by 4.1,

$$\sqrt{K(t)} \le \sqrt{K(0)} + tH(t). \tag{19}$$

Now

$$\begin{aligned} K(0) &= \int u_t^2(x,0) = \int (\sum C'_{n,k}(0)\sin kx)^2 dx \\ &= \frac{\pi}{2}\sum C'^2_{n,k}(0) = \frac{2}{\pi}\sum (\int f(x,0)\sin kx\,dx)^2 \\ &\le \int f^2(x,0)dx \end{aligned}$$

by Bessel's inequality. Thus $K(0) \le F^2(0)$, and from (19) we conclude that $\sqrt{K(t)} \le F(0) + tH(t)$.

Theorem 2.

$$\int u_{nt}^2(x,t)dx \le (F(0) + tH(t))^2 = A^2(t), \tag{20}$$

where F is given by (13),

$$H^2(t) = G_1^2(t)t^2F^2(t) + 2G_1(t)tF(t)F_1(t) + F_1^2(t), \tag{21}$$

and G_1 and F_1 are given by (17) *and* (18).

4.4. *The bound of* $\int u_x^2 dx$. Equation 10 may be written

$$\int \{-u_x^2 - uu_t - gu^2 - fu\}dx = 0,$$

or

$$\begin{aligned} \int u_x^2 dx &= -\int \{gu^2 + uu_t + fu\}dx \le \int (|uu_t| + |fu|)dx \\ &\le \sqrt{\int u^2 dx \cdot \int u_t^2 dx} + \sqrt{\int u^2 dx \cdot \int f^2 dx} \\ &\le \sqrt{t^2F^2(t)A^2(t)} + \sqrt{t^2F^2(t)F^2(t)} \\ &= tF(t)(A(t) + F(t)). \end{aligned}$$

Theorem 3.

$$\int u_x^2(x,t)dx \le tF(t)(A(t) + F(t)) = B(t), \tag{22}$$

where A is given by (20).

4.5 *The bound of* $\int u_{xtt}^2(x,t)dx$. We differentiate (4) twice with respect to t, multiply by $C''_{n,t}(t)$ and sum, to get

$$\int \{u_{xxtt} - u_{ttt} - gu_{tt} - 2g_t u_t - g_{tt}u - f_{tt}\}u_{tt} = 0. \tag{23}$$

As before, we write

$$\int u_{xxtt}u_{tt}dx = -\int u_{xtt}^2 dx,$$

$$\int u_{ttt}u_{tt}dx = \tfrac{1}{2}\frac{d}{dt}\int u_{tt}^2 dx,$$

and (23) becomes, on setting $K(t) = \int u_{tt}^2 dx$,

$$\begin{aligned} \tfrac{1}{2}K'(t) &= -\int \{u_{xtt}^2 + gu_{tt}^2\}dx - \int \{2g_t u_t + g_{tt}u + f_{tt}\}u_{tt}dx \\ &\le \int \{|2g_t u_t| + |g_{tt}u| + |f_{tt}|\}|u_{tt}|dx. \end{aligned}$$

It is clear that by the use of Schwarz's inequality we can obtain an inequality of the form

$$K'(t) \le J(t)\sqrt{K(t)}, \tag{24}$$

where $J(t)$ is an increasing and continuous function expressible in terms of G_1, F, F_1, and the similar functions G_2 and F_2 corresponding to $g_{tt}f_{tt}$.

We estimate $K(0)$ as follows. Differentiate (4) with respect to t and put $t=0$, to obtain

$$\begin{aligned} \int u_{tt}(x,0)\sin jx dx = \int \{&u_{xxt}(x,0) - gu_t(x,0) \\ &- f_t(x,0)\}\sin jx dx. \end{aligned} \tag{25}$$

for $j = 1, 2, \ldots, n$. Now $u_{tt}(x,0)$ is a linear combination of $\sin jx$, $j = 1, 2, \ldots n$, and by (25) its first n Fourier coefficients are the same as those of $u_{xxt}(x,0) - gu_t(x,0) - f_t(x,0)$. Thus by Bessel's inequality,

$$\int u_{tt}^2(x,0)dx \le \int \{u_{xxt}(x,0) - gu_t(x,0) - f_t(x,0)\}^2 dx. \tag{26}$$

If in (4) one puts $t=0$, there results

$$-\int u_t(x,0)\sin jx dx = \int f(x,0)\sin jx dx.$$

Two integrations by parts gives

$$-\int u_{xxt}(x,0)\sin jx\,dx=\int f_{xx}(x,0)\sin jx\,dx,$$

and since $u_{xxt}(x,0)$ is a linear combination of $\sin jx$, $j=1, 2, \ldots, n$, we see as above,

$$\int u_{xxt}^2(x,0)dx\leq\int f_{xx}^2(x,0)dx. \tag{27}$$

By using Schwarz's inequality, (27), and the bounds previously obtained, the right hand number of (25) can be dominated by a continuous function depending only on f and g and their derivatives. That is, $K(0)$ is bounded uniformly in n, and from (24) it follows that the same is true of $K(t)$.

Theorem 4. *There exists a continuous function $C(t)$, determined by f,g and their derivatives, such that*

$$\int u_{xtt}^2(x,t)dx\leq C(t). \tag{28}$$

4.6. *The bound for* $\int u_{xt}^2dx$. From eq (15) we have on replacing $\int u_{xxt}u_t dx$ by $-\int u_{xt}^2dx$,

$$\int u_{xt}^2dx=\int\{u_{tt}+gu_t+g_tu+f_t\}u_t dx.$$

Because of the bounds previously obtained, it is clear that we have the theorem:

Theorem 5. *There exists a continuous function $D(t)$, expressible in terms of f and g and their derivatives such that*

$$\int u_{xt}^2(x,t)dx\leq D(t). \tag{29}$$

4.7. *The bound for* $\int u_{xx}^2dx$. If equations (4) be multiplied by $j^2\sin jx$ and summed, we have

$$\int u_{xx}^2dx=\int\{u_t+gu+f\}u_{xx}dx$$

$$\leq\sqrt{\int\{u_t+gu+f\}^2dx}\sqrt{\int u_{xx}^2dx}.$$

Now from the previous bounds we can find a continuous function $E(t)$ which depends only on f,g and their derivatives, such that

$$\int\{u_t+gu+f\}^2dx\leq E(t). \tag{30}$$

Thus we have the theorem:

Theorem 6. *There exists a continuous function $E(t)$ independent of n such that*

$$\int u_{xx}^2(x,t)dx\leq E(t). \tag{31}$$

4.8. *An integral inequality.* Consider the Green's function $G(x,\xi)$ relative to the equation $y''+\lambda y=0$ $=y(0)=y(\pi)$. Specifically

$$G(x,\xi)=\begin{cases}\dfrac{x(\pi-\xi)}{\pi} & x\leq\xi,\\[2ex] \dfrac{\xi(\pi-x)}{\pi} & x\geq\xi,\end{cases}$$

and its uniformly convergent Fourier expansion is

$$G(x,\xi)=-\frac{2}{\pi}\sum_1^\infty\frac{\sin jx\sin j\xi}{j^2}. \tag{32}$$

For brevity, set

$$u_t+gu+f=\Phi(u). \tag{33}$$

then

$$u_{xx}-\Phi(u)=L(u)-f. \tag{34}$$

Multiply (34) by $G(x,\xi)$ and integrate with respect to x to obtain

$$-u(\xi,t)-\int\Phi(u)G(x,\xi)dx=\int\{L(u)-f\}G(x,\xi)dx. \tag{35}$$

Now

$$\int\{L(u)-f\}G(x,\xi)dx$$

$$=-\frac{2}{\pi}\sum_1^n\frac{\sin j\xi}{j^2}\int\{L(u)-f\}\sin jxdx$$

$$=-\frac{2}{\pi}\sum_{n+1}^\infty\frac{\sin j\xi}{j^2}\{L(u)-f\}\sin jxdx,$$

because of (4). Now $L(u)-f=u_{xx}-\Phi(u)$, and

$u_{xx}=-\sum_1^n C_{n,j}(t)j^2\sin jx$; hence

$$\int u_{xx}\sin jxdx=0$$

for $j>n$, giving

$$\int\{L(u)-f\}G(x,\xi)dx=-\frac{2}{\pi}\sum_{n+1}^\infty\frac{\sin j\xi}{j^2}\int\Phi(u)\sin jxdx.$$

By Schwarz's inequality,

$$\left|\int\{L(u)-f\}G(x,\xi)dx\right|$$

$$\leq\frac{2}{\pi}\sqrt{\sum_{n+1}^\infty\frac{1}{j^4}}\cdot\sqrt{\sum_{n+1}^\infty(\int\Phi(u)\sin jxdx)^2}. \tag{36}$$

Now

$$\sum_{n+1}^\infty\frac{1}{j^4}\leq\frac{1}{3n^3}$$

and

$$\sum_{n+1}^\infty(\int\Phi(u)\sin jxdx)^2$$

$$\leq\sum_1^\infty(\int\Phi(u)\sin jxdx)^2\leq\frac{\pi}{2}\int\Phi^2(u)dx.$$

By (30), $\int\Phi^2(u)dx\leq E(t)$, and so from (36) we can conclude

$$\left|\int\{L(u)-f\}G(x,\xi)dx\right|\leq\frac{2}{\pi}\sqrt{\frac{1}{3n^3}}\cdot\sqrt{\frac{\pi}{2}E(t)}.$$

Referring back to (35) we have a theorem:

Theorem 7.

$$|-u_n(\xi,t)-\int\Phi(u_n)G(x,\xi)dx|\leq\sqrt{\frac{2E(t)}{3\pi n^3}}. \tag{37}$$

5. Existence Theorem

Recall now the discussion of equicontinuity and the criterion of Tonelli given at the end of section 2. Because of the inequalities contained in theorems 1 through 6, we see that the functions u_n, u_{nx}, and u_{nt} are uniformly equicontinuous. Thus by Ascoli's theorem, we can pick out, by a suitable diagonal process, a subsequence $\{v_m\}$ of $\{u_n\}$ such that

$$v_m(x,t)\to u(x,t),$$

$$v_{mx}(x,t)\to v(x,t),$$

$$v_{mt}(x,t)\to w(x,t),$$

the approach being uniform in each case. Because of this uniformity, one sees that $v=\partial u/\partial x$ and $w=\partial u/\partial t$. The derivatives u_{xx}, u_{xt}, u_{tt} exist almost everywhere and are summable. We consider the expression

$$-v_m(\xi,t)-\int\Phi(v_m)G(x,\xi)dx. \tag{38}$$

Since $v_m=u_{n_m}$, theorem (7) tells us that the expression (38) tends to zero as $m\to\infty$. Also $\Phi(v_m)\to\phi(u)$ uniformly, and G is bounded, so we have

$$\lim_{m\to\infty}\{-v_m(\xi,t)-\int\Phi(v_m)G(x,\xi)d\xi\}$$
$$=-u(\xi,t)-\int\Phi(u)G(x,\xi)dx=0.$$

The integral $\int\Phi(u)G(x,\xi)dx$ has a second derivative with respect to x, namely, $-\Phi(u)=-u_t-gu-f$. Hence u_{xx} exists, is continuous, and satisfies

$$-u_{xx}(\xi,t)+\Phi(u)=0, \tag{39}$$

which is identical with (1). Since u obviously satisfies (2), it is a solution of the system (1), (2) in the region S_T. But T is arbitrary, and a solution u of (1), (2) exists in all S.

We have shown that a subsequence of u_n converges to the solution u, together with first order derivatives. Actually the entire sequence u_n so converges. If this were not the case, there would be a subsequence u_{n_j} such that, for instance, $\lim_{n_j\to\infty}u_{n_j}\neq u$ at some point x,t. From the sequence u_{n_j} we could pick another subsequence in the manner of this section, such that this subsequence has for limit a solution v of the problem. By the uniqueness theorem, $u=v$, and so $\lim u_{n_j}(x,t)=u(x,t)$, a contradiction. Thus we have

Theorem 8. *The sequence $u_n(x,t)$ has for uniform limit in any S_T the unique function $u(x,t)$ satisfying* (1) *and* (2). *Furthermore, $u_{nx}\to u_x$ and $u_{nt}\to u_t$ uniformly in S_T.*

6. Convergence in Mean of u_{nxx}

The solution $u(x,t)$ of the system (1), (2) has a Fourier series

$$u(x,t)=\sum_1^\infty\lambda_j(t)\sin jx,$$

which may be differentiated twice with respect to x, and the resulting series converges in the mean to u_{xx}. Set

$$v_n=\sum_1^n\lambda_j(t)\sin jx. \tag{40}$$

If (4) are multiplied by $-j^2(C_{n,j}(t)-\lambda_j(t))$ and summed, we get

$$\int\{L(u_n)-f\}\frac{\partial^2}{\partial x^2}(u_n-v_n)dx=0. \tag{41}$$

Since $L(u)=f$, we may write (41) as

$$\int\{L(u_n-v_n)-L(u-v_n)\}\frac{\partial^2}{\partial x^2}(u_n-v_n)dx=0. \tag{42}$$

Recalling that

$$L(u)=u_{xx}-u_t-gu-f+f=u_{xx}-\Phi(u)+f,$$

we write (42) in the form

$$\int\left\{\frac{\partial^2}{\partial x^2}(u_n-v_n)\right\}^2dx$$
$$=\int\{-\Phi(u_n-v_n)+f-L(u-v_n)\}\frac{\partial^2}{\partial x^2}(u_n-v_n)\,dx,$$

and Schwarz's inequality gives

$$\sqrt{\int\left\{\frac{\partial^2}{\partial x^2}(u_n-v_n)\right\}^2dx}$$
$$\leq\sqrt{\int\{-\Phi(u_n-v_n)+f-L(u-v_n)\}^2dx}. \tag{43}$$

Now, $-\Phi(u_n-v_n)+f=-(u_n-v_n)_t-g(u_n-v_n)\to0$ uniformly, and $L(v-v_n)$ tends to zero in the mean; thus the right hand member of (43) tends to zero and so

$$\int\left\{\frac{\partial^2}{\partial x^2}(u_n-v_n)\right\}^2dx\to0.$$

From this and an appropriate triangular inequality it follows that

$$\int\left\{\frac{\partial^2}{\partial x^2}(u_n-u)\right\}^2dx\to0.$$

Theorem 9. *The second derivatives u_{nxx} of the approximating functions tend in the mean* to u_{xx}.

It is too much to expect that $u_{nxx}\to u_{xx}$ uniformly, or even pointwise. For example, $u_{nxx}(0,t)\equiv0$, while $u_{xx}(0,t)=f(0,t)$, and this latter does not need to vanish identically.

7. Estimating the Error

From theorem 9 it is easy to prove that $L(u_n)\to L(u)$ in the mean. Set $L(u_n)=f_n$. Then

$$L(u_n-u)=L(u_n)-L(u)=f_n-f\xrightarrow{\text{l.m.}}0.$$

Using the method of 4.2, we prove that

$$\int (u_n-u)^2dx \le t^2F_n^{*2}(t),$$

where

$$F_n^*(t)=\max_{\tau\le t}\sqrt{\int\{f(x,\tau)-f_n(x,\tau)\}^2dx}. \tag{44}$$

Theorem 10. *The mean square error satisfies the inequality*

$$\int (u_n-u)^2dx \le t^2F_n^{*2}(t), \tag{45}$$

where $F_n^*(t)$ *is given by* (44), *and* $F_n^*(t)\to 0$ *as* $n\to\infty$.

Theorem 10 unfortunately gives information only about the mean square of the error instead of about the error at a point, which would be desirable. This latter will be mentioned below. Apart from this, however, theorem 10 gives a rather curious sort of information about the m.s.e. It does not give an a priori estimate of this error; that is, we cannot say that after n steps the error will have a certain bound, because we do not know how rapidly F_n tends to zero. On the other hand, we do seem to know more than the mere fact that the m.s.e. tends to zero. We know that if we take n sufficiently large, the m.s.e. will be small and we shall know it to be small. What we do not know is when we shall know it!

In section 5 it was mentioned that u_{xt} is a summable function. Thus from $L(u)=f$, it follows that u_{xxt} is summable. From the equation $L(u_n-u)=f_n-f$, we obtain, using the methods of sections 4.3 and 4.4, the inequality analogous to (22),

$$\int\{(u_n-u)_x\}^2dx \le tF_n^*(t)(A_n^*(t)+F_n^*(t))=G_n^{*(t)},$$

where F_n^* and A_n^* are given by (13) and (20), except that f_n-f is used insted of f in their definitions. Now we are unable to say much about the factor A_n^* since it contains terms of the form $\int\{f_{nt}-f_t\}^2dx$; that is, depends on u_{xxt} and u_{nxxt}. However, it appears quite likely in many cases that A_n^* will remain bounded as $n\to\infty$. In any case the inequality

$$\int\{(u_n-u)_x\}^2dx \le G_n^*(t)$$

is a valid one, and in a given computation $G_n^*(t)$ can actually be computed. Setting $\Delta_n(x,t)=u_n-u$, we have from Schwarz's inequality

$$|\Delta_n(x,t)|=\int_0^x \Delta_{nx}(s,t)\,ds \le \sqrt{x\int_0^x\{\Delta_{nx}(s,t)\}^2ds} \tag{46}$$

$$\le\sqrt{x\int\{\Delta_{nx}(s,t)\}^2ds}\le\sqrt{xG_n(t)}.$$

In an analogous fashion we obtain by integrating from π instead of from zero,

$$\Delta_n(x,t)\le\sqrt{(\pi-x)G_n^*(t)}. \tag{47}$$

From (46) and (47) it follows that

$$\Delta_n(x,t)\le\sqrt{\frac{2}{\pi}x(\pi-x)G_n^*(t)}.$$

Theorem 11.

$$|u_n(x,t)-u(x,t)|\le\sqrt{\frac{2}{\pi}x(\pi-x)G_n^*(t)}, \tag{48}$$

where

$$G_n^*(t)=tF_n^*(t)\{A_n^*(t)+F_n^*(t)\},$$

$$F_n^*(t)=\max_{\tau\le t}\sqrt{\int\{f_n-f\}^2dx},$$

$$A_n^*(t)-F_n^*(0)-tH_n^*(t),$$

$$\{H_n^*(t)\}^2=G_1(t)t^2\{F_n^*(t)\}^2+2G_1(t)tF_n^*(t)+F_{1n}^*(t)+\{F_{1n}^*(t)\}^2,$$

$$F_{1n}^*(t)=\max_{\tau\le t}\sqrt{\int\{f_{nt}(x,\tau)-f_t(x,\tau)\}^2dx}.$$

For any stage n of the solution, the function $G_n^*(t)$ can be explicitly calculated. If the A_n^* do remain bounded, then $G_n^*\to 0$, and we will get a useful estimate of the error.

Los Angeles, April 24, 1952.

Journal of Research of the National Bureau of Standards Vol. 51, No. 3, September 1953 Research Paper 2442

Characteristics of Internal Solitary Waves[1]

Garbis H. Keulegan

This is an application of the method of approximations initiated by Boussinesq to the disturbances of the interface points for waves of permanent form and the internal solitary wave. The system considered is a layer of liquid on another layer of greater density, the liquids of the layers being initially at rest and of constant total depth. The form of the wave is established. The dependence of wave velocity on wave height, on density differences and on layer thickness is determined.

1. Introduction

In investigations on the model laws of density currents, a project now being carried out at the National Hydraulics Laboratory, need arose for the consideration of the genesis and the damping of internal waves at the interface between layers of fresh and saline waters. Among the many possible modes of such disturbances, one may consider for the sake of simplicity the behavior of a single intumescence and of nearly sinusoidal progressive waves.

It has been our purpose to deal with these two types of internal wave motions experimentally. The experimental studies of solitary waves have been completed. As a natural guide in the study of the data, resort has been made to a theoretical analysis. The present paper gives the basis and the result of this analysis. Relations are here obtained giving the dependence of the velocity of wave propagation on wave heights, the form of the solitary wave, and the expressions for the velocity vector on the upper and the lower layers. Consideration of the experimental data, however, is reserved for a future occasion.

After putting forth the basic conditions for the analysis, the question of internal waves of infinitesimal height and negligible interfacial surface curvature is taken up in the first approximate solution. In the second approximate solution the characteristics of solitary waves are revealed. In general, there are seen to be some similarities between ordinary surface solitary waves and internal solitary waves. No attempt is made to extend the approximations to a third-order analysis as no special demand is made by experimental evidence for this.

2. Mathematical Formulation

A layer of lighter liquid of thickness H' and of density ρ' rests on a layer of a denser liquid of thickness H and of density ρ. The upper liquid at its free surface is exposed to air and the lower liquid rests on a rigid horizontal bed. Both liquids are initially at rest. The displacement of the interface with respect to its initial undisturbed position is denoted by h; the displacement of the free surface with respect to the level of the undisturbed free surface is denoted by h' (see fig. 1). Taking the origin, O, of rectangular axes at the undisturbed interface, the axis of x is drawn horizontally. The axis of z is drawn vertically and the positive branch points upwards. The velocity components along these axes are denoted by u, w, and u', w', the primed symbols referring to particle velocities in the upper liquid.

It will be assumed that the disturbanees are produced in liquids initially at rest, so that the consequent flow is irrotational and admits the velocity potentials ϕ and ϕ'. The vorticity that is naturally present at the interface will be ignored. Since the type of disturbance visualized is translational, that is, the particle velocities in vertical planes normal to the direction of wave motion are nearly constant for each layer, it is appropriate to introduce the expressions of the velocity potentials

$$\phi=\left(\cos z\,\frac{\partial}{\partial x}\right)\phi_0+\left(\sin z\,\frac{\partial}{\partial x}\right)\theta_0 \qquad (1)$$

for the lower layer, and

$$\phi'=\left(\cos z\,\frac{\partial}{\partial x}\right)\phi_0'+\left(\sin z\,\frac{\partial}{\partial x}\right)\theta_0' \qquad (2)$$

for the upper layer. Here, ϕ_0, θ_0, ϕ_0', and θ_0' are functions of x and t alone.

Altogether there are six unknowns, h, h', ϕ_0, ϕ_0', θ_0, and θ_0', which are determined on the basis of the kinematic and dynamic conditions at the various boundaries. The pressure is atmospheric at the free surface. At the interface the pressure is continuous. A particle in the free surface remains in this surface. The particles in the upper surface of the lower liquid at the interface remain in this surface. Finally, the normal particle velocities vanish at the horizontal bottom.

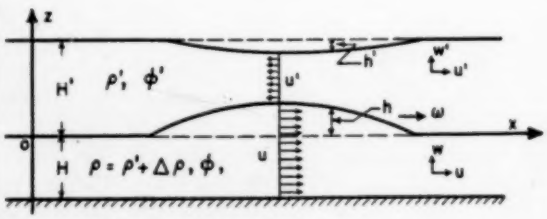

FIGURE 1. *Notation diagram.*

[1] The preparation of this paper was sponsored in part by the Office of Naval Research.

The mathematical formulation of the dynamic boundary conditions requires that expressions be given for the pressures at all points in the two layers. Assuming that the atmoshperic pressure is reduced to zero,

$$\frac{p}{\rho}=\frac{\partial\phi}{\partial t}-gz-\frac{1}{2}(u^2+w^2)+\frac{\rho'}{\rho}gH' \tag{3}$$

for the lower liquid, and

$$\frac{p'}{\rho'}=\frac{\partial\phi'}{\partial t}-gz-\frac{1}{2}(u'^2+w'^2)+gH' \tag{4}$$

for the upper liquid. Translating now the statements of the boundary conditions above into mathematical relations, neglecting w^2 with respect to u^2, and w'^2 with respect to u'^2, they are

$$\frac{\partial\phi'}{\partial t}-gh'-\frac{1}{2}u'^2=0, \qquad z=H'+h', \tag{5}$$

$$w'-\frac{\partial h}{\partial t}-u'\frac{\partial h'}{\partial x}=0, \qquad z=H'+h', \tag{6}$$

$$\rho'\left(\frac{\partial\phi'}{\partial t}-gh-\frac{1}{2}u'^2\right)=\rho\left(\frac{\partial\phi}{\partial t}-gh-\frac{1}{2}u^2\right), \qquad z=h, \tag{7}$$

$$w-\frac{\partial h}{\partial t}-u\frac{\partial h}{\partial x}=0, \qquad z=h, \tag{8}$$

$$w'-\frac{\partial h}{\partial t}-u'\frac{\partial h}{\partial x}=0, \qquad z=H, \tag{9}$$

and

$$w=0, \qquad z=h. \tag{10}$$

3. Internal Waves of Infinitesimal Height

The functions θ_0 and θ_0' may be expressed in terms of ϕ_0 and ϕ_0', respectively, after noting the kinematic boundary conditions at the bottom and at the free surface. From eq 1, keeping only the first three terms,

$$\phi=\phi_0+z\frac{\partial\theta_0}{\partial x}-\frac{z^2}{2}\frac{\partial^2\phi_0}{\partial x^2}, \tag{11}$$

and therefore

$$\frac{\partial\phi}{\partial z}=\frac{\partial\theta_0}{\partial x}-z\frac{\partial^2\phi_0}{\partial x^2}. \tag{12}$$

The latter in view of eq 10 requires that

$$\frac{\partial\theta_0}{\partial x}=-H\frac{\partial^2\phi_0}{\partial x^2}. \tag{13}$$

Hence,

$$\phi=\phi_0-\left(Hz+\frac{z^2}{2}\right)\frac{\partial^2\phi_0}{\partial x^2}, \tag{14}$$

and therefore

$$\frac{\partial\phi}{\partial z}=-(H+z)\frac{\partial^2\phi_0}{\partial x^2}. \tag{15}$$

Similarly, from eq 2,

$$\phi'=\phi_0'+z\frac{\partial\theta_0}{\partial x}-\frac{z^2}{2}\frac{\partial^2\phi_0'}{\partial x^2}, \tag{16}$$

hence

$$\frac{\partial\phi'}{\partial z}=\frac{\partial\theta_0'}{\partial x}-z\frac{\partial^2\phi_0'}{\partial x^2}. \tag{17}$$

Taking the kinematic boundary condition of the upper surface, eq 6, and neglecting the product term which is a small quantity,

$$\frac{\partial\theta_0'}{\partial x}-(H'+h')\frac{\partial^2\phi_0'}{\partial x^2}=-\frac{\partial h'}{\partial t}. \tag{18}$$

And as h' may be neglected in comparison with H',

$$\frac{\partial\theta_0'}{\partial x}=-\frac{\partial h'}{\partial t}+H'\frac{\partial^2\phi_0'}{\partial x^1}, \tag{19}$$

hence

$$\phi'=\phi_0'-z\frac{\partial h'}{\partial t}+\left(zH'-\frac{z^2}{2}\right)\frac{\partial^2\phi_0}{\partial x^2}, \tag{20}$$

and therefore

$$\frac{\partial\phi'}{\partial x}=-\frac{\partial h'}{\partial t}+(H'-z)\frac{\partial^2\phi_0'}{\partial x^2}. \tag{21}$$

For the points at the interface, that is $z=h$, one may write from eq 14 and 15, neglecting the terms involving z and its square,

$$\frac{\partial\phi}{\partial t}=\frac{\partial\phi_0}{\partial t} \tag{22}$$

and

$$\frac{\partial\phi}{\partial z}=-w=-H\frac{\partial^2\phi_0}{\partial x^2}. \tag{23}$$

From eq 20 and 21

$$\frac{\partial\phi'}{\partial t}=\frac{\partial\phi_0'}{\partial t} \tag{24}$$

and

$$\frac{\partial\phi'}{\partial z}=-w'=-\frac{\partial h'}{\partial t}+H'\frac{\partial^2\phi_0}{\partial x^2}. \tag{25}$$

These imply that wave height h is small in comparison with H or H' and also that the curvature of the wave surface is small.

Taking next the boundary conditions, eq 5, 7, 8, and 9, neglecting in them terms consisting of squares

or of products, and using the relations from eq 22 to 25, inclusive,

$$\frac{\partial \phi_0'}{\partial t} = gh', \tag{26}$$

$$\rho' \left(\frac{\partial \phi_0'}{\partial t} - gh \right) = \rho \left(\frac{\partial \phi_0}{\partial t} - gh \right), \tag{27}$$

$$H \frac{\partial^2 \phi_0}{\partial x^2} = \frac{\partial h}{\partial t}, \tag{28}$$

$$-H \frac{\partial^2 \phi_0}{\partial x^2} = -\frac{\partial h'}{\partial t} + H' \frac{\partial^2 \phi_0'}{\partial x^2}. \tag{29}$$

Rearranging the terms in eq 27 and then differentiating twice with respect to t, we have

$$\frac{\partial^3 \phi_0'}{\partial t^3} = \frac{\rho}{\rho'} \frac{\partial^3 \phi_0}{\partial t^3} - \frac{\rho - \rho'}{\rho'} g \frac{\partial^2 h}{\partial t^2}. \tag{30}$$

Differentiating eq 27 twice with respect to x,

$$\frac{\partial^3 \phi_0'}{\partial t \partial x^2} = \frac{\rho}{\rho'} \frac{\partial^3 \phi_0}{\partial t \partial x^2} - \frac{\rho - \rho'}{\rho} g \frac{\partial^2 h}{\partial x^2}. \tag{31}$$

Multiplying eq 29 by g, introducing the value of h' from eq 26, and differentiating the result with respect to t

$$-gH \frac{\partial^3 \phi_0}{\partial x^2 \partial t} - gH' \frac{\partial^3 \phi_0'}{\partial x^2 \partial t} = -\frac{\partial^3 \phi_0'}{\partial t^3}.$$

This reduces, after eliminating ϕ_0' by means of eq 30 and 31, to

$$-gH \frac{\partial^3 \phi_0}{\partial x^2 \partial t} - gH' \frac{\rho}{\rho'} \frac{\partial^3 \phi_0}{\partial x^2 \partial t} + g^2 H' \frac{(\rho - \rho')}{\rho} \frac{\partial^2 h}{\partial x^2} = -\frac{\rho}{\rho'} \frac{\partial^3 \phi}{\partial t^3} + \frac{\rho - \rho'}{\rho'} g \frac{\partial^2 h}{\partial t^2}.$$

Differentiating the latter with respect to t, and then eliminating h by means of eq 28, there results, finally,

$$\frac{\partial^4 \phi_0}{\partial t^4} - g(H + H') \frac{\partial^4 \phi_0}{\partial x^2 \partial t^2} + g^2 H' H \frac{\rho - \rho'}{\rho} \frac{\partial^4 \phi_0}{\partial x^4} = 0, \tag{32}$$

which is the differential equation of wave motion in a liquid system consisting of two strata of different densities for small disturbances.

Putting $\rho - \rho' = \Delta\rho$,

$$\omega_1^2 \omega_2^2 = g^2 H' H \frac{\Delta\rho}{\rho}, \tag{33}$$

and

$$\omega_1^2 + \omega_2^2 = g(H + H'), \tag{34}$$

the wave equation, eq 32, may be rewritten

$$\left(\frac{\partial^2}{\partial t^2} - \omega_1^2 \frac{\partial^2}{\partial x^2} \right) \left(\frac{\partial^2}{\partial t^2} - \omega_2^2 \frac{\partial^2}{\partial x^2} \right) \phi_0 = 0. \tag{35}$$

Two types of waves are possible. In one the waves have the velocity of propagation $\pm\omega_1$; in the other, the velocity $\pm\omega_2$. The plus sign refers to waves moving in the direction of x negative and the minus sign, in the opposite direction. Furthermore, these waves, of infinitesimal wave height and of negligible surface curvature, travel without distortion of form.

The discrete values of the velocities may be shown from eq 34, neglecting the higher powers of the density differences, to be

$$\omega_1^2 = g(H + H') \left(1 - \frac{H'H}{(H + H')^2} \frac{\Delta\rho}{\rho} \right) \tag{36}$$

and

$$\omega_2^2 = \frac{gH'H}{H + H'} \frac{\Delta\rho}{\rho} \left(1 + \frac{H'H}{(H + H')^2} \frac{\Delta\rho}{\rho} \right). \tag{37}$$

Of these, the second refers to disturbances of the interface, that is, to internal waves. The first refers to ordinary waves; in this expression one notices the effect of the nonhomogeneity of fluid on the velocity of propagation of the ordinary waves. Nonhomogeneity reduces the value of the velocity of propagation. For a given relative density difference the reduction is greatest when the layers are of equal depth. For the purposes of the present work, the secondary effects of the relative density differences will be ignored. Accordingly the velocity of propagation of internal waves of infinitesimal height, replacing subscript 2 by 0, will be given as

$$\omega_0^2 = \frac{gH'H}{H + H'} \frac{\Delta\rho}{\rho}. \tag{38}$$

The next question to be considered is in regard to the particle velocities in the two layers. One commences the analysis with the lower layer. As was noted above, the internal waves of infinitesimal height progress without change of form. This fact is equivalent to the equality of the operators

$$\frac{\partial}{\partial t} = \mp \omega \frac{\partial}{\partial x}. \tag{39}$$

The negative sign is chosen for waves moving in the direction of x positive and the positive sign for waves moving in the direction of x negative. For the subsequent analysis it will be assumed that the internal waves move in the direction of x positive, and thus

$$\frac{\partial}{\partial t} = -\omega \frac{\partial}{\partial x}. \tag{40}$$

One now naturally selects that kinematic condition of the interface stating that a particle of the lower liquid once on the interface remains on the interface. This condition is given by eq 28, which now may be written as

$$H \frac{\partial^2 \phi_0}{\partial x^2} = -\omega \frac{\partial h}{\partial x},$$

and, as in terms of the potential, the particle velocity u_0 is

$$u_0 = -\frac{\partial \phi_0}{\partial x}, \tag{41}$$

we have

$$H \frac{\partial u_0}{\partial x} = \omega \frac{\partial h}{\partial x}.$$

Integrating the latter equation with respect to x and observing that u_0 vanishes when h vanishes, then

$$u_0 = \omega \frac{h}{H}. \tag{42}$$

Accordingly, particle velocities in the lower layer are proportional to the velocity of wave propagation and vary with the wave-element height of the internal wave. When these heights are positive, that is when the wave elements are elevated, particle motion in the lower layer is in the direction of wave motion.

In terms of the velocity potential the particle velocity in the upper layer is

$$u_0' = -\frac{\partial \phi_0'}{\partial x}. \tag{43}$$

To obtain the values of u_0' one now considers the other kinematic boundary condition of the interface. The reference is to eq 29, which when treated in an analogous manner yields

$$H' u_0' + H u_0 = \omega h'. \tag{44}$$

Now, when in eq 26 the partial differentiation with respect to t is replaced by the partial differentiation with respect to x, the result is

$$\omega u_0' = g h'. \tag{45}$$

Eliminating h between eq 44 and 45, and introducing the value of ω from eq 38, one obtains the relation

$$H' u_0' \left(1 - \frac{\Delta \rho}{\rho} \frac{H}{H+H'}\right) + H u_0 = 0, \tag{46}$$

and this connects the particle velocities in the two layers. As the term containing the relative density difference is small, it will be neglected, and therefore

$$\frac{u_0'}{u_0} = -\frac{H}{H'}. \tag{47}$$

Thus the motion of the particles in the upper layer is oppositely directed to the motion of the particles in the lower layer.

It will be instructive to show to what extent the internal waves do affect the free surface. This will be better understood if the ratio h'/h is investigated. The combinations of the expressions in eq 42 and 45 gives

$$\frac{h'}{h} = \frac{\omega^2}{gH} \frac{u_0'}{u_0},$$

which, in view of eq 38 and 39, reduces to

$$\frac{h'}{h} = -\frac{\Delta \rho}{\rho} \frac{H}{H+H'}. \tag{48}$$

The interpretation is that the displacement of the surface is directed oppositely to that of the interface. Furthermore, the disturbances of the free surface are very much reduced in comparison with the displacements of the internal waves.

Finally, the question of the energy of internal waves of infinitesimal heights may be considered. The energy of waves is in one part potential and in another part kinetic. Evaluating the potential energy with respect to the undisturbed configuration of the two layers, the appropriate expression is

$$E_\rho = g \frac{\Delta \rho}{2} \int_0^\lambda h^2 dx + g \frac{\rho'}{2} \int_0^\lambda h'^2 dx,$$

where λ is the effective wave length, that is the length along which h^2 is measurable. Expressing h' in terms of h through eq 48,

$$E_\rho = g \frac{\Delta \rho}{2} \left[1 + \frac{\Delta \rho}{\rho} \left(\frac{H}{H+H'}\right)^2\right] \int_0^\lambda h^2 dx. \tag{49}$$

The kinetic part of the energy in terms of the particle velocities in the two layers is

$$E_k = \frac{\rho'}{2} \int_0^\lambda u_0'^2 H' dx + \frac{\rho}{2} \int_0^\lambda u_0^2 H dx.$$

Expressing u_0' in terms of u_0 with the use of eq 46, expressing u_0 in terms of h and ω with the use of eq 42, and introducing the more exact values of ω from eq 37, the final value of kinetic energy is

$$E_k = g \frac{\Delta \rho}{2} \left[1 + \frac{\Delta \rho}{\rho} \left(\frac{H}{H+H'}\right)^2\right] \int_0^\lambda h^2 dx. \tag{50}$$

Comparison of the expressions for the two energies shows that, in internal waves of infinitesimal wave height when the upper surface is free, the potential and kinetic energies are of like value. When the relative density-difference term is ignored the energy of internal waves is simply

$$E = g \Delta \rho \int_0^\lambda h^2 dx. \tag{51}$$

The form of the internal waves together with the difference of the density of the two layers is sufficient for the evaluation of the energy.

Some of these properties of internal waves of large wave length and of infinitesimal wave height are well known. A short derivation of these results, for example, by the method of Lord Rayleigh is given by Thorade [1].

4. The Internal Solitary Wave

In general when the wave-element heights of the internal waves are finite, a deformation of the wave surface occurs during the travel of the waves even when the two liquids are assumed to be perfect and ideal. The extent of the deformation depends on the height h and on the surface curvature $\partial^2 h/\partial x^2$. The corresponding mode of the deformation in the ordinary translation waves, as first discussed by Boussinesq, is well known [2, 3]. A similar theory can be worked out also in the cases of internal waves, and this theory could form a basis for the study of internal waves which travel without deformation. A second procedure is to assume the existence of internal solitary waves, positive or negative, which travel long distances without deformation in the absence of viscosity. These intumescences will be referred to as internal solitary waves, and the analysis to be followed below will determine the form of the waves.

Ordinarily in establishing the character of the progressive waves of the permanent type resort is made to an artifice [4]. By superposing on the flow a current of the magnitude equaling the velocity of propagation of the wave and moving in the direction opposite to that of the wave, the system is reduced to a steady state. Another method, and this will be used here, is that the time differentiations will be changed into space differentiations for the wave traveling in the direction of x positive using

$$\frac{\partial}{\partial t}=-\omega\frac{\partial}{\partial x}, \tag{40a}$$

where ω is the velocity of progression of the wave of permanent type. In the present case ω is the velocity of progression of the solitary wave.

The expression for the vector potential in the lower layer to the second approximation, is, from eq 1,

$$\phi=\phi_0+z\frac{\partial\theta_0}{\partial x}-\frac{z^2}{2}\frac{\partial^2\phi_0}{\partial x^2}-\frac{z^3}{6}\frac{\partial^3\theta}{\partial x^3}. \tag{52}$$

Evaluating the last term on the right-hand side, since it is the term of smallest value, from the first approximative value,

$$\frac{\partial\theta}{\partial x}=-H\frac{\partial^2\phi_0}{\partial x^2}, \tag{13a}$$

the vector potential now is

$$\phi=\phi_0+z\frac{\partial\theta_0}{\partial x}-\frac{z^2}{2}\frac{\partial^2\phi_0}{\partial x^2}+\frac{Hz^3}{6}\frac{\partial^4\phi_0}{\partial x^4},$$

and, therefore,

$$\frac{\partial\phi}{\partial z}=\frac{\partial\theta_0}{\partial x}-z\frac{\partial^2\phi_0}{\partial x^2}+\frac{Hz^2}{2}\frac{\partial^4\phi_0}{\partial x^4}.$$

In view of the bottom kinematic boundary condition, eq 10,

$$\frac{\partial\theta_0}{\partial x}=-H\frac{\partial^2\phi_0}{\partial x^2}-\frac{H^3}{2}\frac{\partial^4\phi_0}{\partial x^4}, \tag{53}$$

which than is the second approximative value of $\partial\theta_0/\partial x$. Thus, the resulting form of the vector potential is

$$\phi=\phi_0-Hz\frac{\partial^2\phi_0}{\partial x^2}-\frac{H^3z}{2}\frac{\partial^4\phi_0}{\partial x^4}-\frac{z^2}{2}\frac{\partial^2\phi_0}{\partial x^2}+\frac{Hz^3}{6}\frac{\partial^4\phi_0}{\partial x^4}, \tag{54}$$

and, therefore,

$$\frac{\partial\phi}{\partial z}=-H\frac{\partial^2\phi_0}{\partial x^2}-z\frac{\partial^2\phi_0}{\partial x^2}-\frac{H^3}{2}\frac{\partial^4\phi_0}{\partial x^4}+\frac{Hz^2}{2}\frac{\partial^4\phi_0}{\partial x^4}. \tag{55}$$

This is the expression for the velocity potential in the lower layer to the second approximation involving the single unknown function ϕ_0. When the height of the internal solitary wave is smaller than the depth H of the lower layer, the expression for the vertical component of the particle velocities at the interface may be simplified by neglecting z^2 in eq 55. Mathematically the basis of the approximation is

$$\frac{h^2}{2}\frac{\partial^4\phi_0}{\partial x^4}\ll H\frac{\partial^2\phi_0}{\partial x^2}. \tag{56}$$

Thus, neglecting z^2,

$$\frac{\partial\phi}{\partial x}=-H\frac{\partial^2\phi_0}{\partial x^2}-z\frac{\partial^2\phi_0}{\partial x^2}-\frac{H^3}{2}\frac{\partial^4\phi_0}{\partial x^4}. \tag{57}$$

Now, the last two terms on the right-hand side being the smallest in value, substitutions may be made for them from the first approximative values,

$$\left.\begin{aligned}\frac{\partial\phi_0}{\partial x}&=-u_0=-\omega_0\frac{h}{H},\\ \frac{\partial^2\phi_0}{\partial x^2}&=-\frac{\omega_0}{H}\frac{\partial h}{\partial x},\\ \frac{\partial^3\phi_0}{\partial x^3}&=-\frac{\omega_0}{H}\frac{\partial^2 h}{\partial x^2},\\ \frac{\partial^4\phi_0}{\partial x^4}&=-\frac{\omega_0}{H}\frac{\partial^3 h}{\partial x^3}.\end{aligned}\right\} \tag{58}$$

Introducing these in eq 55 and putting $z=h$, the vertical component of the particle velocity at the interface, sign reversed, is

$$\frac{\partial\phi}{\partial z}=-H\frac{\partial^2\phi_0}{\partial x^2}+\frac{\omega_0^2}{H}\frac{\partial h}{\partial x}+\frac{\omega_0 H^2}{2}\frac{\partial^3 h}{\partial x^3},\qquad z=h. \tag{59}$$

Similarly the expression for the vector potential in the upper liquid, from eq 1, is

$$\phi=\phi_0'+z\frac{\partial\theta_0'}{\partial x}-\frac{z^2}{2}\frac{\partial^2\phi_0'}{\partial x^2}-\frac{z^3}{\partial}\frac{\partial^3\theta_0'}{\partial x^3}. \tag{60}$$

The last term on the right-hand side being the smallest term, the value of θ_0' may be taken from the first approximation,

$$\frac{\partial \theta_0'}{\partial x} = -\frac{\partial h'}{\partial t} + H' \frac{\partial^2 \phi_0'}{\partial x^2}. \tag{19a}$$

It is permissible at this time to affect a small modification in the analysis, and this consists of neglecting the term $\partial h'/\partial t$. The assumption implies that

$$-\frac{\partial h'}{\partial t} \ll H' \frac{\partial^2 \phi_0'}{\partial x},$$

and may be verified as follows. In view of eq 40a,

$$-\frac{\partial h'}{\partial t} = \omega_0 \frac{\partial h}{\partial x}.$$

Also, in view of eq 43, 45, and 38,

$$H' \frac{\partial^2 \phi_0'}{\partial x^2} = -H' \frac{\partial u_0'}{\partial x} = \frac{gH'}{\omega_0} \frac{\partial h'}{\partial x} = \frac{\omega_0 (H+H')}{H} \frac{\rho}{\Delta \rho} \frac{\partial h'}{\partial x}.$$

Thus, since

$$\Delta \rho H \ll (H+H')\rho.$$

it is permissible to neglect $\partial h'/\partial t$ and write for the first approximative value of $\partial \theta'/\partial x$

$$\frac{\partial \theta'}{\partial x} = H' \frac{\partial^2 \phi_0'}{\partial x^2}. \tag{19b}$$

Introducing this is eq 55,

$$\phi' = \phi_0' + z \frac{\partial \theta_0}{\partial x} - \frac{z^2}{2} \frac{\partial^2 \phi_0'}{\partial x^2} - \frac{z^3 H'}{6} \frac{\partial^4 \phi_0'}{\partial x^4}, \tag{61}$$

and, therefore,

$$\frac{\partial \phi'}{\partial z} = \frac{\partial \theta_0'}{\partial x} - z \frac{\partial^2 \phi_0'}{\partial x^2} - \frac{z^2 H'}{2} \frac{\partial^4 \phi_0'}{\partial x^4}. \tag{62}$$

Since $\partial h'/\partial t$ may be neglected and also $u' \partial h'/\partial t$ which is still smaller, the kinematic boundary condition for the upper surface, eq 6 reduces to

$$w' = \frac{\partial \phi'}{\partial z} = 0, \qquad z = H' + h', \tag{63}$$

and this requires that

$$\frac{\partial \theta_0'}{\partial x} = H' \frac{\partial^2 \phi_0'}{\partial x^2} + \frac{H'^3}{2} \frac{\partial^4 \phi_0'}{\partial x^4}, \tag{64}$$

which is the second approximative value of $\partial \theta_0'/\partial x$. Substituting in eq 61,

$$\phi' = \phi_0' + zH' \frac{\partial^2 \phi_0'}{\partial x^2} - \frac{z^2}{2} \frac{\partial^2 \phi_0'}{\partial x^2} + \frac{2H'^3}{2} \frac{\partial^4 \phi_0'}{\partial x^4} - \frac{z^3 H'}{6} \frac{\partial^4 \phi_0'}{\partial x^4} \tag{65}$$

and

$$\frac{\partial \phi'}{\partial z} = H' \frac{\partial^2 \phi_0'}{\partial x^2} - z \frac{\partial^2 \phi_0'}{\partial x^2} + \frac{H'^3}{2} \frac{\partial^4 \phi_0'}{\partial x^4} - \frac{z^2 H'}{2} \frac{\partial^4 \phi_0'}{\partial x^4}. \tag{66}$$

When the latter expression is applied to the region close to the interface, h^2 being smaller than H'^2, the term involving z^2 may be neglected. Thus,

$$\frac{\partial \phi'}{\partial z} = H' \frac{\partial^2 \phi_0'}{\partial x^2} - z \frac{\partial^2 \phi_0'}{\partial x^2} + \frac{H'^3}{2} \frac{\partial^4 \phi_0'}{\partial x^4}. \tag{67}$$

Now the last two terms on the right-hand side being the smallest in value, substitution may be made for them from the first approximate values

$$\left.\begin{aligned} \frac{\partial \phi_0'}{\partial x} &= -u_0' = \omega_0 \frac{h}{H'}, \\ \frac{\partial^2 \phi_0'}{\partial x^2} &= \frac{\omega_0}{H'} \frac{\partial h}{\partial x}, \\ \frac{\partial^3 \phi_0'}{\partial x^3} &= \frac{\omega_0}{H'} \frac{\partial^2 h}{\partial x^2}, \\ \frac{\partial^4 \phi_0'}{\partial x^4} &= \frac{\omega_0}{H'} \frac{\partial^3 h}{\partial x^3}. \end{aligned}\right\} \tag{68}$$

Hence,

$$\frac{\partial \phi'}{\partial z} = H' \frac{\partial^2 \phi_0'}{\partial x^2} - \frac{\omega_0^2}{h'} \frac{\partial h}{\partial x} + \frac{\omega_0 h'}{2} \frac{\partial^3 h}{\partial x^3}, \qquad z = h. \tag{69}$$

Consider next the two kinematic boundary conditions for the interface given by eq 8 and 9. These may be written, in view of the rule of eq 40a,

$$w = -\frac{\partial \phi}{\partial z} = -\omega \frac{\partial h}{\partial x} + u \frac{\partial h}{\partial x}, \qquad z = h, \tag{70}$$

$$w' = -\frac{\partial \phi'}{\partial z} = -\omega \frac{\partial h}{\partial x} + u' \frac{\partial h}{\partial x}, \qquad z = h, \tag{71}$$

The last terms on the right-hand sides of these two equations being the smallest, the values of u and u' in them may be taken from the first approximate values

$$u = \omega_0 \frac{h}{H} \quad \text{and} \quad u' = -\omega_0 \frac{h}{H}.$$

Thus,

$$w = -\frac{\partial \phi}{\partial z} = -\omega \frac{\partial h}{\partial x} + \frac{\omega_0 h}{H} \frac{\partial h}{\partial x}, \qquad z = h, \tag{72}$$

and

$$w' = -\frac{\partial \phi'}{\partial z} = -\omega \frac{\partial h}{\partial x} - \frac{\omega_0 h}{H} \frac{\partial h}{\partial x}, \qquad z = h. \tag{73}$$

Substituting in eq 72 the value of w from eq 59,

and in eq 73 the value of w' from eq 69, the kinematic boundary conditions reduce to

$$H\frac{\partial^2\phi_0}{\partial x^2}=-\omega\frac{\partial h}{\partial x}+2\frac{\omega_0 h}{H}\frac{\partial h}{\partial x}+\frac{\omega_0 H^2}{2}\frac{\partial^3 h}{\partial x^3}, \quad (74)$$

and

$$-H'\frac{\partial^2\phi_0'}{\partial x^2}=-\omega\frac{\partial h}{\partial x}-2\frac{\omega_0 h}{H'}\frac{\partial h}{\partial x}+\frac{\omega_0 H'^2}{2}\frac{\partial^3 h}{\partial x^3}. \quad (75)$$

Multiplying eq 74 by ρ/H, integrating with respect to x, and putting the constant of integration equal to zero since there is no disturbance at infinity, one obtains

$$\rho\frac{\partial\phi_0}{\partial x}=-\rho\omega\frac{h}{H}+\rho\omega_0\left(\frac{h}{H}\right)^2+\rho\frac{\omega_0 H}{2}\frac{\partial^2 h}{\partial x^2}. \quad (76)$$

Multiplying eq 75 by ρ'/H', integrating with respect to x, and again putting the constant of integration equal to zero,

$$-\rho'\frac{\partial\phi_0'}{\partial x}=-\rho'\omega\frac{h}{H'}-\rho'\omega_0\left(\frac{h}{H'}\right)^2+\rho'\frac{\omega_0 H'}{2}\frac{\partial^2 h}{\partial x^2}. \quad (77)$$

Adding eq 76 and 77,

$$-\rho'\frac{\partial\phi_0'}{\partial x}+\rho\frac{\partial\phi_0}{\partial x}=-\omega\left[\frac{\rho'}{H'}+\frac{\rho}{H}\right]h+\omega_0\left[\frac{\rho}{H^2}-\frac{\rho'}{H'^2}\right]h^2+\frac{\omega_0}{2}[\rho'H'+\rho H]\frac{\partial^2 h}{\partial x^2}. \quad (78)$$

The dynamic condition for the interface given by eq 7 may be written in the form

$$\rho'\frac{\partial\phi'}{\partial t}-\rho\frac{\partial\phi}{\partial t}=\rho' gh-\rho gh+\frac{\rho' u'^2}{2}-\frac{\rho u^2}{2}. \quad (79)$$

The last two terms on the right-hand side are small quantities and these may be evaluated by the first approximative values of the particle velocities $u'=-\omega_0 h/H'$ and $u=\omega_0 h/H$.

Hence,

$$\rho'\frac{\partial\phi'}{\partial t}-\rho\frac{\partial\phi}{\partial t}=(\rho'-\rho)\,gh+\frac{\omega_0^2}{2}\left[\rho'\left(\frac{h}{H'}\right)^2-\rho\left(\frac{h}{H}\right)^2\right]. \quad (80)$$

In view of the rule given by eq 40a,

$$-\rho'\omega\frac{\partial\phi'}{\partial x}+\rho\omega\frac{\partial\phi}{\partial x}=-(\rho-\rho')gh+\frac{\omega_0^2}{2}\left[\rho'\left(\frac{h}{H'}\right)^2-\rho\left(\frac{h}{H}\right)^2\right]. \quad (81)$$

Expressing the value of the density difference $\rho-\rho'=\Delta\rho$ in terms of ω_0^2, using eq 38, and dividing by ω,

$$-\rho'\frac{\partial\phi'}{\partial x}+\rho\frac{\partial\phi}{\partial x}=-\frac{\rho\omega_0^2}{\omega}\left[\frac{1}{H'}+\frac{1}{H}\right]h+\frac{\omega_0^2}{2\omega}\left[\rho'\left(\frac{h}{H'}\right)^2-\rho\left(\frac{h}{H}\right)^2\right]. \quad (82)$$

Keeping only the first two terms of the right-hand members of eq 54 and 65,

$$\frac{\partial\phi}{\partial x}=\frac{\partial\phi_0}{\partial x}-Hh\frac{\partial^3\phi_0}{\partial x^3}, \qquad z=h,$$

and

$$\frac{\partial\phi'}{\partial x}=\frac{\partial\phi_0'}{\partial x}-H'h\frac{\partial^3\phi_0'}{\partial x^3}, \qquad z=h.$$

In view of the approximative values from eq 58 and eq 68,

$$\frac{\partial\phi}{\partial x}=\frac{\partial\phi_0}{\partial x}+\omega_0 h\frac{\partial^2 h}{\partial x^2}, \qquad z=h,$$

$$\frac{\partial\phi'}{\partial x}=\frac{\partial\phi_0'}{\partial x}+\omega_0 h\frac{\partial^2 h}{\partial x^2}, \qquad z=h.$$

Thus, if $(\omega_0 h)\,\partial^2 h/\partial x^2$ is neglected, eq 82 reduces to

$$-\rho'\frac{\partial\phi_0'}{\partial x}+\rho\frac{\partial\phi_0}{\partial x}=-\rho\frac{\omega_0^2}{\omega}\left[\frac{1}{H'}+\frac{1}{H}\right]h+\frac{\omega_0^2}{2\omega}\left[\rho'\left(\frac{h}{H'}\right)^2-\rho\left(\frac{h}{H}\right)^2\right], \qquad z=h \quad (83)$$

Equating the right-hand members of eq 78 and 82, since the left-hand members are the same quantities, and collecting the terms,

$$\left[\omega\left(\frac{\rho'}{H'}+\frac{\rho}{H}\right)-\rho\frac{\omega_0^2}{\omega}\left(\frac{1}{H'}+\frac{1}{H}\right)\right]h+\left[\frac{\omega_0^2}{2\omega}\left(\frac{\rho'}{H'^2}-\frac{\rho}{H^2}\right)+\omega_0\left(\frac{\rho'}{H'^2}-\frac{\rho}{H^2}\right)\right]h^2-\frac{\omega_0}{2}[\rho'H'+\rho H]\frac{\partial^2 h}{\partial x^2}=0. \quad (84)$$

If we divide by $\omega\rho$ and ignore the terms containing $\Delta\rho/\rho$, the final result is

$$\left[\left(\frac{\omega}{\omega_0}\right)^2-1\right]\left[\frac{1}{H'}+\frac{1}{H}\right]h-\frac{3}{2}\left[-\frac{1}{H'^2}+\frac{1}{H^2}\right]h^2-\frac{1}{2}[H'+H]\frac{\partial^2 h}{\partial x^2}=0.$$

This simplifies, after dividing by $(H'+H)/HH'$, to

$$\left[\left(\frac{\omega}{\omega_0}\right)^2-1\right]h-\frac{3}{2}\left[\frac{H'-H}{H'H}\right]h^2-\frac{1}{2}[H'H]\frac{\partial^2 h}{\partial x^2}=0. \quad (85)$$

Multiplying by $\partial h/\partial x$, integrating once with respect to x, and putting the constant of integration equal to zero since all disturbances vanish at infinity, we obtain

$$\left(\frac{\omega^2}{\omega_0^2}-1\right)h^2-\left(\frac{H'-H}{H'H}\right)h^3-\frac{1}{2}H'H\left(\frac{\partial h}{\partial x}\right)^2=0. \quad (86)$$

Let the crest height of the wave be h_1. As this is a maximum, $\partial h/\partial x$ vanishes at this point. Hence

$$\left(\frac{\omega^2}{\omega_0^2}-1\right)h_1^2-\left(\frac{H'-H}{H'H}\right)h_1^3=0,$$

or

$$\frac{\omega^2}{\omega_0^2}-1=\frac{H'-H}{H'H}h_1, \quad (87)$$

or

$$\omega=\omega_0\sqrt{1+\left(\frac{H'-H}{H'H}\right)h_1}. \quad (88)$$

This is the law of velocity of propagation of an internal solitary wave. The magnitude of ω_0, the velocity of propagation when the wave is exceedingly small, is given in eq 38. Substituting in eq 86 from eq 88,

$$h_1h^2-h^3-\frac{1}{2}\frac{H'^2H^2}{H'-H}\left(\frac{\partial h}{\partial x}\right)^2=0,$$

and the solution of the equation is

$$h=h_1\sec^2\mathrm{h}\alpha\left(\frac{x}{H}-\frac{\omega t}{H}\right), \quad (89)$$

where

$$\alpha=\sqrt{\frac{1}{2}\left(\frac{H'-H}{H'}\right)\frac{h_1}{H}}. \quad (90)$$

This gives the form of internal solitary waves.

Examination of eq 86 reveals that the relation of the thickness of the two layers has an important bearing on the formation of internal solitary waves. When the depth of the upper layer is greater than the depth of the lower layer, $H'>H$, the internal solitary wave is of positive type, that is, h is positive. When the depth of the lower layer is greater than the depth of the upper layer, the internal solitary wave is of negative height, that is, h is negative everywhere. When the two layers are of the same depth and the difference of the densities is very small, the formation of a solitary wave is excluded by this analysis.

The consideration of a fairly large number of experiments tending to verify the above theoretical results, first in regard to the dependence of velocity of propagation on wave height, and second in regard to the form of internal solitary waves, will be reserved for another occasion.

5. References

[1] H. Thorade, Probleme der Wasserwellen, p. 94 (Henri Grand, Hamburg, 1931.)

[2] J. Boussinesq, Theorie des ondes et des remous qui se propagent le long d'un canal rectangulaire horizontal, en communiquant au liquide contenu dans ce canal de vitesses sensiblement pareilles de la surface au fond, Liouville's J. Math. **17,** 55 (1872).

[3] Garbis H. Keulegan and George W. Patterson, Mathematical theory of irrotational translation waves, J. Research NBS **24,** 47 (1940) RP1272.

[4] Lord Rayleigh, On waves, Phil. Mag. [5] **1,** 257 (1876). (Scientific papers 1, p. 251).

Washington, July 3, 1953.

Journal of Research of the National Bureau of Standards Vol. 51, No. 3, September 1953 Research Paper 2443

Becker Value of Manila Rope by Photoelectric Reflectometry

Sanford B. Newman, Harry K. Hammond, III, and Helen F. Riddell

Becker value, or reflectance under specified conditions, has been used for more than 20 years as an index of fiber quality in the purchase of manila cordage. The accepted method for determining Becker value requires a visual reflectometer. Previous attempts to use photoelectric reflectometers were unsuccessful because the instruments lacked sensitivity, attributable in part to the low transmittance of the chosen filter combination. Properly selected filters used with a sensitive reflectometer permit photoelectric determinations to be made with greater speed and precision than visual determinations. The results obtained photoelectrically agree well with the averages of visual determinations.

1. Introduction

Manila fiber (abacá) is one of the important raw materials or cordage. Rope made from this fiber was consumed at an annual rate of over 50,000 tons in 1939 [1] [1].[2] The Federal specification for manila rope [2] contains requirements for strength, weight, and other physical characteristics. Opinion in the industry, however, holds that serviceability is related to color, the dark grades of fiber being less serviceable than the lighter [3]. Becker and Appel, at the request of the Cordage Institute and the Federal Specification Board, investigated the color characteristics of manila rope fiber and in 1933 reported a quantitative visual method of evaluation [3, 4]. One result of their investigation was the establishment of the "Becker value" of manila rope, defined as 100 times the ratio of the reflectance of a suitably prepared sample of fiber to that of a standard magnesium oxide layer for monochromatic light of approximately 500 mμ. Fiber and standard were equally illuminated at 45° with CIE (Commission Internationale de l'Éclairage) standard source A and viewed perpendicularly. Measurements were made with a Martens (visual) photometer with a Wratten filter No. 75 over the eyepiece.

Despite the lack of data on correlation of color with serviceability, measurements of Becker value continue to be made and appear to have facilitated the purchase of satisfactory manila cordage. With the passage of time, considerable confidence has been placed in the efficacy of Becker value measurements, and they will probably continue to be used in cordage specifications for some time.

Since the method was first described, Becker value has been determined by means of a reflectometer utilizing a Martens (visual) photometer. The procedure requires four pairs of observations, or settings, with the visual photometer, averaged to obtain one determination. As with all visual photometers, the results are dependent on the skill and experience of the observer. Furthermore, the Martens photometer scale is graduated in degrees so that Becker values cannot be obtained directly from readings of the photometer. A precise direct-reading photometer would be more desirable. Thus there arose the desire to replace the visual apparatus for determining Becker value with photoelectric equipment. Therefore, a photoelectric reflectometer [3] was adapted to meet the requirements for Becker value measurement.

2. Instrumentation

The optical arrangement of the photoelectric reflectometer chosen for use in determining Becker value is shown schematically in figure 1. The filter system first tried consisted of (1) a Barnes luminosity filter [5] to correct the response of the photocell to

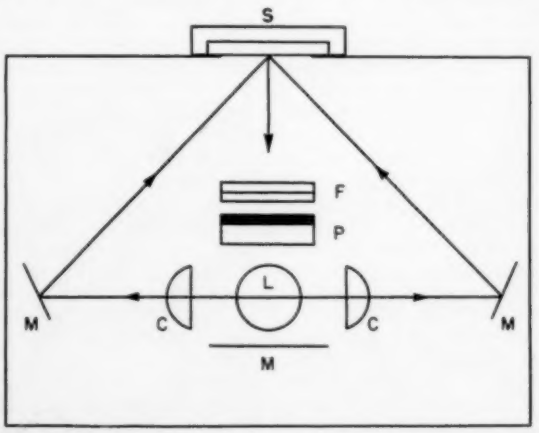

FIGURE 1. *Schematic diagram of photoelectric reflectometer*

S, Cell containing cut fiber; F, filters; P, photocell; M, mirrors; C, condenser lenses; L, light source.

[1] More recent data have not been released.

[2] Figures in brackets indicate the literature references at the end of this paper.

[3] This is the photometric unit with 45°0° exposure head designed by Hunter [Gardner Laboratory, Bethesda, Md.].

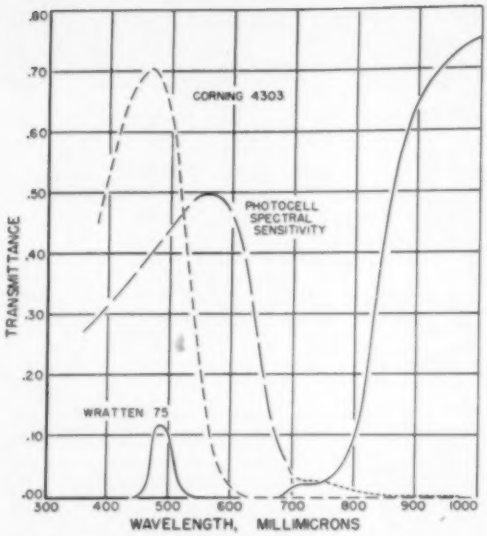

FIGURE 2. *Spectral characteristics of filters and photocell used in the photoelectric reflectometer.*

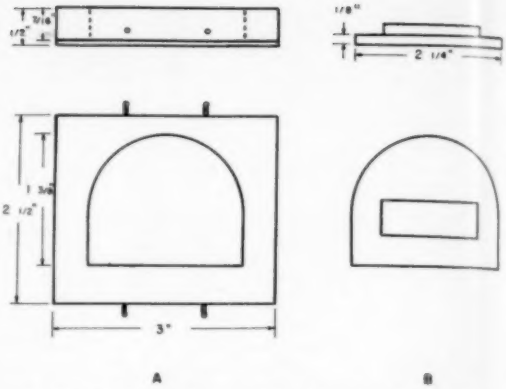

FIGURE 3. *Plastic specimen cell used in photoelectric determinations.*

A, Body of cell; B, back of cell. The back is held in place by the tension of rubber bands which are looped over the protruding studs in A and contact the back on the rectangular raised portion.

that of the CIE standard observer, and (2) a Wratten filter No. 75 to obtain essentially monochromatic light at 500 mμ, as required for the measurement of Becker value. Although nominally duplicating the spectral response of the visual method, this combination produced reflectometer readings considerably higher than those obtained visually. Substitution of a Hunter (bluer) luminosity filter [6] for the Barnes filter produced somewhat better agreement between the visual and photoelectric values. Investigation of the spectral characteristics of the source-filter-photocell combination revealed that infrared radiation was responsible for the high reflectance values obtained with the photoelectric reflectometer. Figure 2 shows the spectral response of a barrier-layer type photocell and the spectral transmittance of the Wratten filter 75. The Barnes and Hunter luminosity filters also transmitted some infrared radiation. To eliminate the infrared component and to obtain maximum sensitivity at 500 mμ, the luminosity filter was removed and a Corning glass 4303 was used to absorb the red and infrared radiation. This glass in combination with the Wratten filter 75 gave quite satisfactory results, as will be shown later.

The specimen holder ordinarily used with the Martens photometer provides too small an area of sample to permit the use of the entire illuminating beam of the photoelectric reflectometer. The specimen cell shown in figure 3 was constructed to permit large area illumination of the sample in the photoelectric reflectometer and still permit measurement in the visual instrument. The cell is constructed of methyl methacrylate. This material is easily worked with ordinary laboratory tools, and the plastic provides a good, durable substitute for the "water white" cover glass, which often is not readily available. The plastic cover is softer than glass and will abrade with use, but replacement is easily accomplished. An electrostatic charge, induced by cleaning or filling the cell, can be removed with a gas flame or high relative humidity, as is done with conventional cells. Differential orientation of the fiber caused by a charged cell is readily detected photoelectrically by observing the instrument galvanometer while rotating the cell in its own plane. Specimen heating by the light source is much reduced with the photoelectric instrument as the light source draws about 20 watts as compared to 1,000 watts for the source in the visual instrument.

As with nearly all reflectometry, the primary reflectance standard for Becker value measurements is a freshly prepared layer of magnesium oxide. Working standards of porcelain enamel, however, are much easier to use. For greatest accuracy with visual or photoelectric reflectometers, a working standard should have spectral characteristics similar to those of the specimens being measured. Becker reported the spectral reflectance of fiber from 25 samples of 1-in. manila rope from 13 manufacturers [3] and the spectral reflectance of the Philippine Island Government standards [4]. The reflectance at 500mμ ranged from 20 to 60 percent. The spectral reflectances increased nearly linearly from 450 to 550mμ at the rate of approximately 0.15 percent per millimicron. A pale-yellow enamel working standard with a factor of 55.0, as related to 100 for MgO, was used in most of this work.

3. Observations and Results

Becker values were determined on several dozen samples of rope that had been submitted for test for conformance with the Federal specification [2]. The rope was prepared for test as described in the standard procedure, except that a rotary knife was used for cutting the fiber into the short lengths required. The knife was driven slowly, and no detectable scorching of the fiber occurred. Reflectance measurements were made visually and photoelectrically without disturbing the contents of the cells. In figure 4 the values obtained visually are plotted against those obtained photoelectrically. The relationship between the two sets of values is practically linear. Consequently, a straight line was fitted (broken line in fig. 4), using the method of least squares, and considering the precision of the photoelectric values as appreciably better than that of the Martens values. The equation for this line is

$$y=1.21+0.97x,$$

where x is the photoelectric value and y the Martens value.

Statistical analysis of the data shows that the departure from a zero-intercept unit-slope relation is not attributable entirely to random fluctuation. From a practical viewpoint, however, these departures are unimportant. The minimum Becker values permitted by the Federal specification [2] are 40 for rope over 2 in. in circumference, and 43 for rope 2 in. in circumference and under. In the Becker value range 35 to 55, the range of practical importance, the greatest discrepancy between the two methods is only 0.3.

A statistical analysis has been made of 25 determinations of Becker value by one operator using one Martens photometer. From this analysis the conclusion was drawn that a single determination of Becker value by the visual method is unlikely to be in error by more than one unit. Comparison of data from different laboratories [7], however, indicates that as many as four determinations may be necessary for this precision. Observers of unequal experience show considerable variation of Becker value on the same specimen, and even experienced observers show a range of about 1.5 for 25 observations on the same sample.

Photoelectric determinations, on the other hand, are not influenced by the operator. It is estimated that instrument variations amount to as much as a few tenths of unit of Becker value.

In conclusion, it may be stated that the photoelectric method is considerably more precise than the visual method and that the two methods show a systematic variation of not more than 0.3 unit over the extreme range of interest.

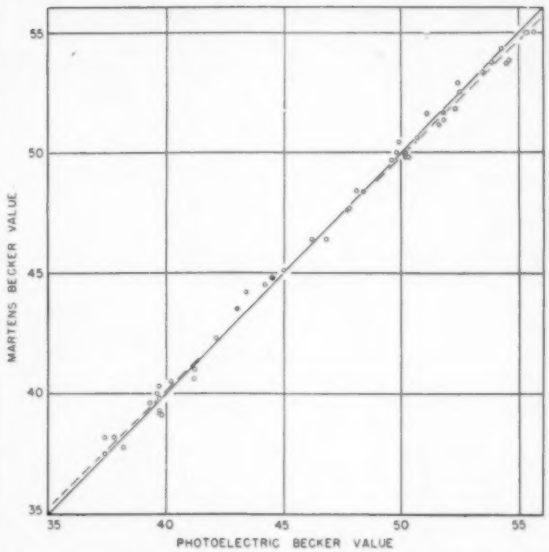

FIGURE 4. *Photoelectric Becker values plotted against visual values.*

Broken line represents the least-square line.

The authors acknowledge the assistance of John Mandel in analyzing the data.

4. References

[1] Mathews' textile fibers, 5th ed., edited by Herbert Mauersberger (John Wiley & Sons, New York, N. Y., 1947).

[2] Federal Standard stock catalog, sec. IV, part 5, Federal Specification T–R–601a for Rope; Manila, (Nov. 26, 1935) and Amendment 2 (Dec. 10, 1943).

[3] G. Becker and W. D. Appel, Evaluation of manila-rope fiber for color, BS J. Research **11,** 811 (1933) RP627.

[4] G. Becker, Spectral reflectance of the Philippine Island Government Standards for abaca fiber, BS J. Research **11,** 823 (1933) RP628.

[5] B. T. Barnes, A four-filter photoelectric colorimeter, J. Opt. Soc. Am. **29,** 448 (1939).

[6] R. S. Hunter, Photoelectric tristimulus colorimetry with three filters, NBS Circular 429 (1942).

[7] G. Becker, Measurement of reflectance for interlaboratory comparison, letter report to the Cordage Institute (1940).

WASHINGTON, July 10, 1953.

Journal of Research of the National Bureau of Standards Vol. 51, No. 3, September 1953 Research Paper 2444

Dielectric Relaxation in a Styrene-Acrylonitrile Copolymer During and After its Polymerization[1,2]

Paul Ehrlich[3] and Nicholas J. De Lollis

Dielectric relaxation in plasticized copolymers of styrene and acrylonitrile is studied during their formation as well as in the fully polymerized copolymers by measurements of dielectric constant and loss factor at several frequencies from 100 c/s to 100 kc/s. In the polymerizing mixture, there occur, at an early stage of the reaction, sigmoid decreases in the dielectric constant at each frequency, accompanied by maxima in the loss factor, when these variables are plotted as a function of reaction time. These changes are interpreted as resulting from the relaxation of the nitrile groups. The electrical properties of the fully polymerized copolymer, as it goes through its glass transition, are in semiquantitative agreement with those of the polymerizing mixture at the stage of the reaction referred to, demonstrating the occurrence of similar phenomena in each case.

1. Introduction

Only isolated studies on the variation of electrical properties throughout a polymerization reaction have been reported. Lazarev and Raschketaev [1][4] have noted a dependence of d-c conductivity, dielectric constant, and dielectric loss on the degree of polymerization of the product resulting from the heat treatment of drying oils. Majury and Melville [2] have drawn certain conclusions about the nonstationary state in vinyl-type polymerizations from the observation of very small and very rapidly occurring changes in dielectric constant observed in the early stages of the reaction. This paper reports on a direct study of changes in dielectric constant and dielectric loss occurring throughout the polymerization of a polar casting resin. The measurements were carried out while the reaction mixture was polymerizing and cross-linking from a viscous solution containing mostly monomer to the fully cured polymer, which was a hard solid.

According to the Debye concept of dipolar relaxation [3] the contribution of dipole relaxation to the dielectric constant, $\epsilon'(\omega)-\epsilon_\infty$, is given by

$$\epsilon'(\omega)-\epsilon_\infty=(\epsilon_s-\epsilon_\infty)/1+\omega^2\tau^2,$$

and the loss factor, ϵ'', resulting from this process is given by

$$\epsilon''(\omega)=(\epsilon_s-\epsilon_\infty)\omega\tau/1+\omega^2\tau^2.$$

The loss factor thus goes through a maximum at a frequency f_{max}, such that

$$\tau=1/2\pi f_{max}. \quad (1)$$

Furthermore, the Debye theory predicts for a dilute suspension of dipolar spheres in a nonpolar solvent that

$$\tau=4\pi\eta a^3/kT, \quad (2)$$

where ϵ_s and ϵ_∞ are the static and infinite frequency values of the dielectric constant, respectively, $\epsilon'(\omega)$ is the frequency dependent value of the dielectric constant, $\epsilon''(\omega)$ is the loss factor ($\epsilon''=\epsilon'$ tan δ), tan δ is the loss angle tangent or dissipation factor, f is the frequency in cycles per second, $\omega=2\pi f$, τ is the relaxation time for dipole relaxation, η is the viscosity, a is the radius of the spheres, k is the Boltzmann constant, and T the absolute temperature.

Relation (2) has generally been found invalid, because in most systems investigated, values of the viscosity calculated from it differed from those observed, sometimes by orders of magnitude. The quantity η has therefore often been represented as an "internal viscosity," a concept lacking quantitative definition in terms of measurable variables. In alternate treatments, applicable to systems with sharply specified energy states [4], the hydrodynamic theory is abandoned and a thermodynamic one is substituted.

In the case at hand, it will be found useful to retain the hydrodynamic concept in a qualitative sense. This predicts a dependence of the relaxation time, and, therefore, of the frequency region in which dipolar losses occur, on viscosity and temperature. The usual way of studying the effect of these variables is, of course, by determining the effect of temperature on the dielectric properties of the solid polymer [5]. The hydrodynamic concept, however, suggests that similar effects might be observed by changing the viscosity at constant temperature. This picture, as we shall see, does indeed furnish a qualitative interpretation of the dielectric changes occurring during the polymerization reaction. In fact, the agreement between corresponding changes occurring in the fully polymerized polymer as a function of temperature and those occurring in the polymerizing mixture as a function of reaction time will be seen to be semiquantitative.

[1] Sponsored by the Department of the Army, Office of the Chief of Ordnance.
[2] Presented in part before the American Physical Society, Durham, N. C., March 26-28, 1953.
[3] Present address, Department of Chemistry, Harvard University, Cambridge, Mass.
[4] Figures in brackets indicate the literature references at the end of this paper.

2. Materials and Methods

2.1. Materials

The primary ingredients of the casting resin were commercial grades of styrene, polystyrene, divinylbenzene, and hydrogenated terphenyl plasticizer. Of these the sytrene and the plasticizer were used without further purification, whereas the acrylonitrile (AN) was redistilled once, removing most, but not all, of the inhibitor. To insure a reasonable shelf life and a good curing rate of the stock solution, the composition of which will be described presently, the polystyrene used was a 50–50 mixture of polymers with weight-average-molecular weights of 160,000 (manufacturer's data) and 840,000, as determined by light-scattering measurements. The divinylbenzene preparation (DVB) was stated by the manufacturer to contain 40 percent of divinylbenzene, most of which was the meta isomer. The other ingredients in this product were mainly diethylbenzene and ethyl vinylbenzene. The inhibitor was removed from it by passing it through activated alumina.

The minor ingredients of the resin were purified commercial benzoyl peroxide, a cobalt catalyst (cobalt naphthenate) containing 6 percent of cobalt, which was used without further purification and Promoter A.[5]

2.2. Methods

The systems studied, except the ones containing no DVB, were made up from a stock solution of the following composition by weight: Styrene, 50 parts; polystyrene, 30 parts; hydrogenated terphenyl, 13 parts; AN, 5 parts; DVB solution, 2 parts.[6] Systems termed 6-percent and 11-percent DVB were made up by adding 4 g and 10 g of the DVB solution, respectively, to 100 g of the stock solution; the system with the nominal AN content of 10 percent was made up by adding an additional 5 g of AN to 100 g of the stock solution. The system termed 0-percent DVB was made up separately and differed from the stock solution in that the 2 g of DVB solution were replaced by an equal weight of styrene.[7] Prior to each experiment, 0.4 percent of benzoyl peroxide, 0.04 percent of promoter A, and 0.15 percent of cobalt catalyst were added to the other ingredients to start the polymerization, and the viscous solution was poured into the cylindrical sample holder, which was kept at 50°±0.5° C by circulating water from a thermostat through its jacket. The samples were kept at 50° C for about 35 hr and were subsequently cured for 14 hr at 100° C. The 50° cure, during which the electrical measurements were carried out, took place in a room in which the humidity was controlled to not exceed 50 percent, and the sample holder was kept stoppered during that period.

Also, to make possible a determination of the dielectric properties of the fully polymerized resin as a function of temperature, the polymerizing mixtures were poured into forms somewhat larger than the required samples and were cured in a desiccator at the same temperatures and for the same lengths of time as the samples investigated during their polymerization.

Measurements of dielectric constant and dielectric loss were made throughout the polymerization in two two-terminal sample holders designed for liquids and consisting of stainless-steel concentric cylinders separated by a ¼-in. gap. These sample holders were calibrated with benzene. Their interelectrode and residual capacitances were approximately 7 and 2 $\mu\mu f$, respectively. Although this equipment should be inherently capable of dielectric-constant determinations accurate to several tenths of 1 percent, some of the measurements probably resulted in values that were as much as 5 percent low, as discussed later. Loss tangents could be determined with an accuracy of $\pm 3\times 10^{-4}$, resulting in loss-factor accuracies of $\pm 9\times 10^{-4}$ at a dielectric constant of 3.0. The same variables, as well as the d-c conductivity, were also measured as a function of temperature for the fully cured samples prepared in disk form. These measurements were made on a high-temperature two-terminal sample holder for solids housed in an air thermostat [6]. The estimated accuracy of the dielectric-constant determination on this sample holder is believed to be within 1 percent; that of the loss tangent was $\pm 2\times 10^{-4}$, resulting in loss-factor accuracies of $\pm 6\times 10^{-4}$ at a dielectric constant of 3.0. The d-c conductivity measurements were made with the help of a d-c micro-microampere amplifier connected directly to the high-temperature sample holder, capable of measuring currents of 2×10^{-11} amp. The samples prepared for these measurements had been machined to give disks 1½ in. in diameter and 3/16 in. thick, with surfaces flat and parallel within 0.0005 in. Secondary electrodes had been applied to these samples by spraying them with a commercial silver paint.

All measurements of dielectric constant and loss were carried out on the same model of a commercial a-c bridge. Two different bridges, but of the same make, were used with the cylindrical and the high-temperature sample holders, which, because of a replacement of a capacitor in one of them, gave capacitance readings of different accuracies, i. e., to ± 0.005 and ± 0.001 $\mu\mu f$, respectively. The signal was generated by a beat frequency oscillator, capable of a 10-v rms output. For detection of the signal a preamplifier and a cathode-ray oscilloscope

[5] This material is a 10-percent solution of β-hydroxy ethyl tetrahydroquinoline in hydrogenated terphenyl and is covered in a pending patent application by Max M. Lee.

[6] A casting resin made from a reaction mixture of this composition has been developed at NBS and termed AN-5 casting resin. (M. M. Lee and E. L. Hebb, unpublished experiments.)

[7] It was later found that aging of the stock solution may have had a slight effect on the experimental results. A fresh solution, and one which had stood at room temperature for several months, underwent electrical changes during polymerization in satisfactory agreement with one another, as far as the magnitudes of the electrical variables were concerned. However, the plots of these variables as a function of time were somewhat displaced toward shorter times in the case of the old solution, presumably because of a small amount of progressive polymerization. This variation is of no importance, as far as most of the experimental results presented in section 3 are concerned, because we shall not be concerned with kinetic questions, for the most part. In the one case where a qualitative examination of kinetic factors was made (effect of peroxide concentration) care was taken to perform all the runs less than 1 month apart and to keep the stock solution under refrigeration.

were used in conjunction with the cylindrical sample holder and a preamplifier with a null-detector in conjunction with the high-temperature sample holder.

Nitrogen analyses were performed by a micro-Kjeldahl method. These gave the acrylonitrile concentration in the cured polymer. Separate analyses were performed for each sample investigated in the cylindrical sample holder, because small differences in acrylonitrile content were to be expected due to evaporation during handling and during the polymerization. In the case of the specimens prepared for the high-temperature sample holder, only 1 sample with a nominal acrylonitrile content of 5 percent and 1 of 10 percent were analyzed, because all these samples were cured in 1 batch and in the same desiccator, and because differences in acrylonitrile content between them may be assumed to result only from differences in acrylonitrile content in the polymerizing mixture, which can be calculated from the percentage composition.

3. Results and Discussion

3.1. Electrical Behavior During the Polymerization Process

Figure 1 illustrates the electrical behavior of a typical polymerizing mixture as a function of time at several frequencies. The initial loss factor, especially at the lower frequencies, was very high and decreased rapidly with time. The frequency dependence of these initially high losses suggested the presence of considerable d-c conductivity, and this was borne out in a d-c conductivity measurement of a sample of acrylonitrile, which gave a value of approximately 2.5×10^{-7} mho/cm. This conductivity was much too high to be attributable to the acrylonitrile itself, and could be reduced roughly by a factor of 50 if a careful fractional distillation process was carried out. This was not done in the experiments cited because the a-c losses attributable to the d-c conductivity decreased rapidly with time and vanished in the fully cured resin. The small amount of cobalt catalyst in the polymerizing mixture, because of its ionic nature, also contributed to the previously noted upswing of the loss curves toward the zero time axis. After these ionic losses had substantially disappeared, a second rise took place in the loss factor at all frequencies, accompanied by a decrease in the dielectric constant. This loss appeared and went through its maximum, first at the highest frequency and last at the lowest frequency, and is attributed to dipole orientation associated with a relaxation time, τ. The loss factor must therefore go through a maximum at a frequency f_{max} given by eq (1). In terms of the qualitative hydrodynamic concept, the "internal viscosity", and therefore the relaxation time, will increase with the extent of the reaction. This explains the observed shift of the loss maximum from high to low frequencies as the polymerization procedes. The gel point occurs shortly after the 70,000-c/s loss factor starts on its pronounced rise. The loss factor shows no discontinuity at the gel point. The curves of figure 1 bear a superficial resemblance to the Debye dispersion curves modified for a distribution of relaxation times [7, 8, 9] if the time axis is imagined replaced by a log frequency axis. This results from the fact that the rate of change of dielectric constant with time must be correlated with the magnitude of the out-of-phase component of the complex dielectric constant, i. e., the loss factor. Figure 1 also presents points from another run made with a fresher stock solution. The reproducibility is satisfactory as far as the shape of the curves is concerned; their displacement with respect to one another is probably caused by some progressive polymerization in the older solution, as discussed in section 2. A slight variation in the acrylonitrile content of the two samples may also have contributed to the shift.

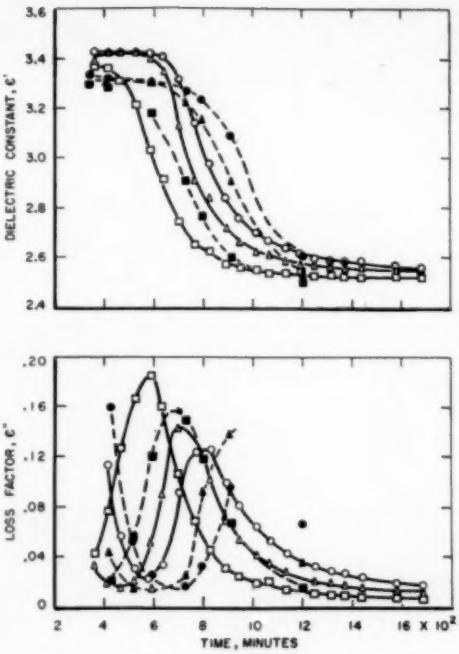

FIGURE 1. *Dielectric constant and loss factor at 50° C as a function of time after initiation of polymerization for a sample containing 4.9 percent of AN and 2 percent of DVB solution.*

○, 100c/s; △, 1,000c/s; □, 70,000 c/s. Filled in symbols and dashed curves refer to an alternate run made with a polymerizing mixture of the same nominal composition for which an AN analysis was not available.

To a first approximation, the magnitudes of the loss-factor maxima at any frequency are proportional to the concentration of acrylonitrile at a DVB concentration of 2 percent (table 1). The loss is therefore attributed primarily [8] to the orien-

[8] E. B. Baker, R. P. Auty, and G. J. Ritenour, J. Chem. Phys. **21**, 159 (1953) have shown that polystyrene itself exhibits dipolar losses, which presumably result from the asymmetry introduced by the phenyl groups. This loss is inseparable from the one described, but amounts to only a small fraction of it.

TABLE 1. *Magnitude of loss-factor maxima during polymerization at 50° C for various concentrations of AN and of DVB solution.*

Concentration of DVB solution	Concentration of AN	Loss-factor maximum at—				
		100 c/s	300 c/s	1,000 c/s	10,000 c/s	70,000 c/s
wt %	*wt %*					
0	5.7	0.125	.....	0.185	0.211	0.230
2	4.9	.125	0.133	.142	.188	.186
2	10.9	.257	.296	.287	.328	.335
6	4.4	.094	.104	.107	.122	.137
11	4.2	.052	.060	.059	.070	.085

tation of the CN dipoles. A similar dependence of the magnitudes of the loss-factor maxima on the acrylonitrile concentration is found for the high-temperature measurements made on the fully cured polymer discussed later (figs. 4 and 7, table 5).

The peak losses at any frequency decrease as the concentration of cross-linking agent is increased (table 1). A plot of loss factor versus log frequency for various concentrations of DVB shows the maxima to decrease and the curves to become broader as the concentration of DVB is increased (fig. 2).[9] These phenomena can best be described in terms of a broadened distribution of relaxation times resulting from an increasing failure of the CN dipoles to orient independently of one another. This effect is seen to be most pronounced at the highest DVB concentrations.

Table 2 shows the time at which they 70,000-c/s loss peak occurs for various peroxide concentrations. Qualitative observations of the fluidity of the solution and, later, of the rigidity of the gel as a function of time indicated that the polymerization rate was strongly dependent on the peroxide concentration at concentrations below 0.2 percent, but that no such dependence could be readily observed in the range

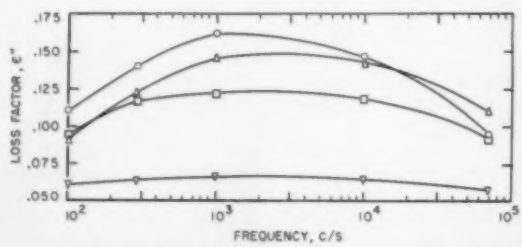

FIGURE 2. *Loss factor during polymerization at 50° C as a function of frequency at the approximate time at which the 1,000-c/s loss-factor maximum occurs for several concentrations of the DVB solution.*

Loss-factor values have been corrected to an AN content of 5.0 percent. ○, 0-percent DVB solution. △, 2-percent DVB solution. □, 6-percent DVB, solution. ▽, 11-percent DVB solution.

[9] In order to make this comparison more significant, the data plotted in this figure have been corrected to the same AN concentration. This is done by making use of the fact that any linear theory of polarization requires proportionality between dipole concentration and dielectric loss at any frequency, subject to the restriction that the distribution of relaxation times is independent of dipole concentration.

TABLE 2. *Time for 70,000-c/s loss factor to reach its maximum as a function of the peroxide concentration; polymerization carried out at 50° C*

Concentrations of AN and of DVB solution are 4.9 and 2 percent, respectively

Peroxide concentration	Time
wt. %	*min*
0.1	>4080
.2	730
.4	645

TABLE 3. *Effect of an additional 60-hour cure at 100° C on the electrical properties at 24° C of a sample containing 4.9 percent of AN and 2 percent of DVB solution*

Frequency	Standard cure		Prolonged cure	
	Dielectric constant	Loss factor	Dielectric constant	Loss factor
c/s				
100	2.54	0.0026	2.52	.....
300	2.54	.0030	2.51	0.0020
1,000	2.54	.0030	2.51	.0018
10,000	2.53	.0028	2.51	.0028
70,000	2.53	.0016	2.51	.0020

from 0.2 to 0.4 percent. This indicates that the time at which the loss peak occurs at any one frequency, under conditions where the structure of the polymer and the reaction mechanism may be assumed to be identical, is a convenient measure of the reaction rate.

After approximately 35 hr at 50° C, followed by a 14-hr cure at 100° C, this being the standard cure condition, the dielectric constant and loss at all frequencies had become essentially constant. Table 3 shows the effect of an additional 60-hr cure at 100° C. There is no significant change in the values of the loss factor during that period. The new values of the dielectric constant are slightly lower, but this is probably caused by shrinkage of the sample. The conclusion seems warranted that the electrical properties of the sample did not change significantly after the initial cure. This conclusion is not surprising, as, in terms of the qualitative picture presented here, a nonpolar plasticizer and small amounts of unpolymerized monomer would be expected to affect the electrical properties in a similar manner, i. e., primarily by reducing the "internal viscosity." It has been shown by Fuoss [10] that the effect of the plasticizer is most pronounced at very low concentrations. In the presence of relatively high plasticizer concentrations (13 percent in this case) small amounts of unpolymerized monomer should therefore have no significant effect on the electrical properties, which, in systems like the one discussed here, should not be expected to provide a sensitive criterion for completeness of cure.

Table 4 provides data comparing the properties of a sample cured as described and measured in the cylindrical cell for liquids with the average computed

TABLE 4. *Comparison of electrical properties of two samples of identical composition, cured in cylindrical cell and disk form, respectively*

Sample A[1]			Sample B[2]		
24° C					
Frequency	Dielectric constant	Loss factor	Frequency	Dielectric constant	Loss factor
c/s			c/s		
100	2.54	0.0026	100	2.65	0.0062
1,000	2.54	.0030	1,000	2.64	.0038
10,000	2.53	.0028	10,000	2.64	.0041
70,000	2.53	.0016	100,000	2.63	.0038
80° C					
100	2.80	0.105	100	2.83	0.089
1,000	2.67	.078	1,000	2.73	.055
10,000	2.60	.032	10,000	2.64	.033
70,000	2.58	.019	100,000	2.59	.025

[1] Cured in the cylindrical cell. (Same sample used in table 3.)
[2] Average computed from 2 samples cast and cured in disk form and measured on the high-temperature holder. The AN concentration of this sample was reduced to that of sample A.

for two fully-cured disks of identical composition (complete data are presented in fig. 4) measured on a high-temperature sample holder. Data for this comparison had been made available by taking several of the samples polymerized in the cylinderical cell through part of the temperature range covered by the high-temperature sample holder and by interpolating (fig. 4) from values obtained on that sample holder to make the comparison at 80° C. In accounting for discrepancies between the two sets of values, the following factors should be kept in mind: Shrinkage of the sample during polymerization in the cylinderical cell, curing conditions that could not be made exactly identical (e. g., different surface areas and different rates of evaporation), different geometries and different electrical arrangements of the sample holders, and different rates of attainment of temperature equilibrium throughout electrodes and sample. Shrinkage during polymerization probably accounts for the lower dielectric-constant values obtained in the cylinderical cell. Surface conductance at the lower frequencies, and a small effective series resistance due to the secondary silver electrodes at the higher frequencies, together with the difference in curing conditions could account for the somewhat higher loss-factor values obtained on the high-temperature sample holder at room temperature. The discrepancies between the loss-factor values obtained at 80° C are probably due to imperfect temperature equilibrium, because in this region the loss factor changes rapidly with temperature. The most rapid change takes place at precisely the frequency (1,000 c/s) at which the discrepancy is largest. In view of these considerations, one may conclude that the samples prepared by the two methods were closely similar in their electrical response. It should be kept in mind that studies of dielectric properties as a function of temperature are as yet relatively rare and that questions of the reproducibility of such measurements at elevated temperatures, even when carried out on the same sample holder, have been left virtually unexplored.

3.2. Electrical Behavior of the Fully Cured Resin

When the electrical properties of the fully cured resin are investigated as a function of temperature, a familiar behavior is found [5]. At any frequency there is a sharp rise in dielectric constant with temperature, a maximum is reached, followed by a slow decrease. Paralleling this, there is a rise in loss factor, a maximum occurs, and by the time the dielectric constant has gone through a maximum, the loss factor is small again. It is also a familiar fact that the rise in dielectric constant and loss factor shifts to higher temperatures as the frequency is raised. This is consistent with eq (1) and the qualitative hydrodynamic concept, which predicts a decrease of the relaxation time with temperature, keeping in mind that τ represents an average value introduced because we are dealing with a distribution of relaxation times. The behavior described is illustrated in figures 3, 4, 5, 6, and 7. Figure 4

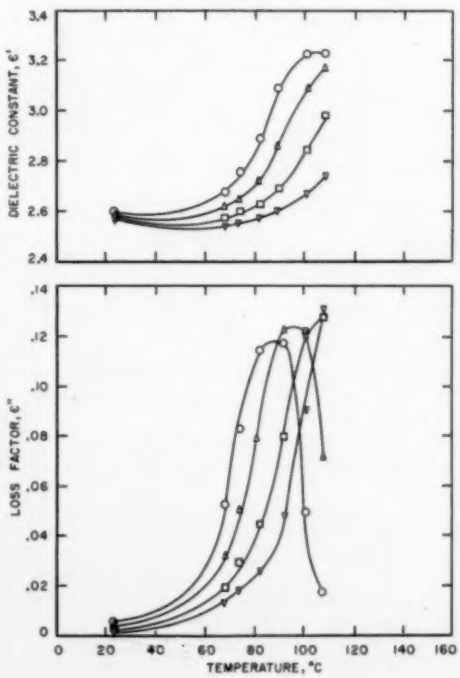

FIGURE 3. *Dielectric constant and loss factor of the fully cured resin as a function of temperature for a sample containing 0 percent of the DVB solution.*

AN content is 5.6 percent. ○, 100 c/s, △, 1,000 c/s; □, 10,000 c/s; ▽, 100,000 c/s.

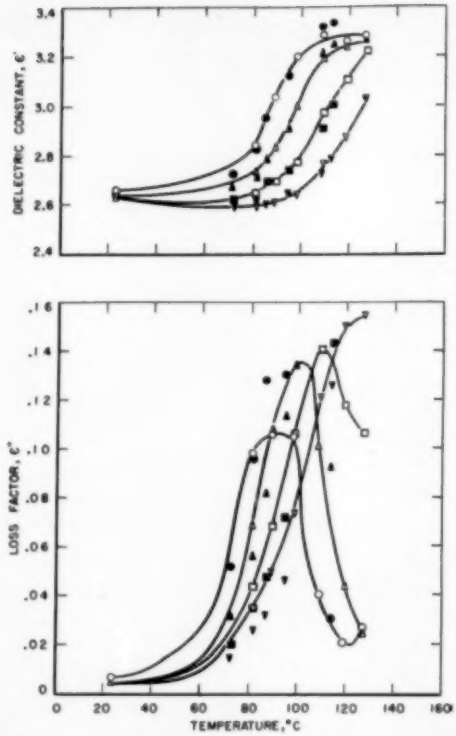

FIGURE 4. *Dielectric constant and loss factor of the fully cured resin as a function of temperature for a sample containing 2 percent of the DVB solution.*

AN content is 5.6 percent. ○, 100 c/s; △, 1,000 c/s; □, 10,000 c/s; ▽, 100,000 c/s. Filled in symbols refer to an alternate sample.

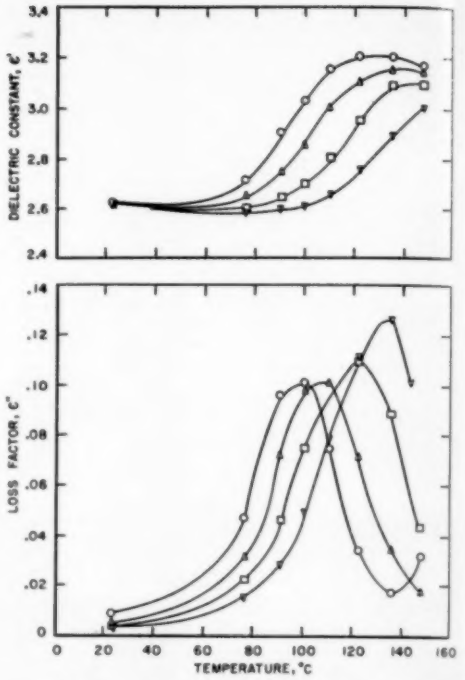

FIGURE 5. *Dielectric constant and loss factor of the fully cured resin as a function of temperature for a sample containing 6 percent of the DVB solution.*

AN content is 5.3 percent. ○, 100 c/s; △, 1,000 c/s; □, 10,000 c/s; ▽, 100,000 c/s.

includes points from a duplicate run. As the 2 samples from which the 2 runs were made were prepared under identical conditions, the discrepancies between them are probably largely attributable to imperfect temperature equilibrium. The initial small decrease in dielectric constant at the higher frequencies would appear to indicate that in this region the disordering effect of temperature overshadows the dipole alinement.

Figure 8 shows the loss factors as a function of frequency for several concentrations of DVB at approximately the temperature at which the 1,000-c/s loss factors go through their maxima. We note here a parallel with the behavior of the resins during their polymerization at the times at which the 1,000-c/s loss factors go through their maxima in those systems (fig. 2). In both cases we find that the losses generally become less and the loss factor versus log frequency curves become broader as the concentration of DVB is increased. The interpretation in both cases is the same, although for the fully cured polymer the effect only becomes definitely established at the highest concentrations of DVB. We also note that the magnitudes of the losses in both cases are similar. This can be seen best by comparing the loss maxima for each DVB concentration and for each frequency, that is, by picking the proper time for the polymerization studies and the proper temperature for the high-temperature studies on the fully cured polymers (table 5). This observation can be rationalized by the supposition that the losses depend essentially on the average dipole relaxation time, that changes in this relaxation time can be brought about by variation of temperature or by changes in the "internal viscosity" occurring during the polymerization at constant temperature, and that the distribution of relaxation times is not greatly different in the systems compared. Because average molecular weights and molecular-weight distributions during and after complete polymerization are different, this would also mean that the relaxation distribution function is essentially independent of these variables throughout the range considered. It is worth noting that these systems of equivalent electrical response are rather different in their macroscopic mechanical appearance—the polymerizing systems can be described best as gels, the fully polymerized systems as rubbers.

The temperature of the loss-factor maximum at any frequency increases with the concentration of DVB. This is related to the observation that the

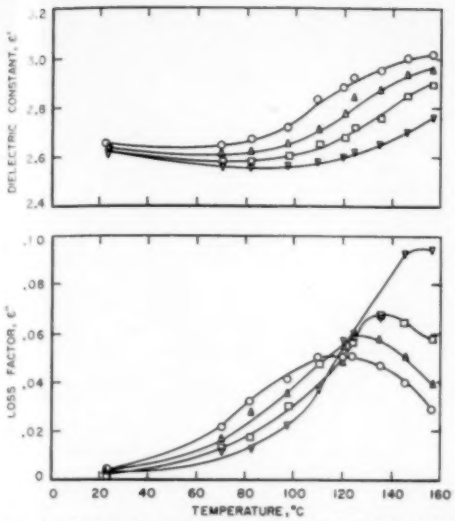

FIGURE 6. *Dielectric constant and loss factor of the fully cured resin as a function of temperature for a sample containing 11 percent of the DVB solution.*

AN content is 5.1 percent. ○, 100 c/s; △, 1,000 c/s; □, 10,000 c/s; ▽, 100,000 c/s.

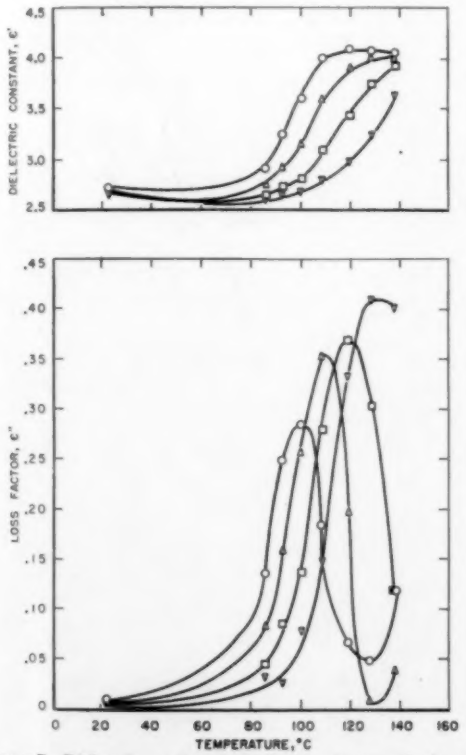

FIGURE 7. *Dielectric constant and loss factor of the fully cured resin as a function of temperature for a sample containing 2 percent of the DVB solution.*

AN content is 11.6 percent. ○, 100 c/s; △, 1,000 c/s; □, 10,000 c/s; ▽, 100,000 c/s.

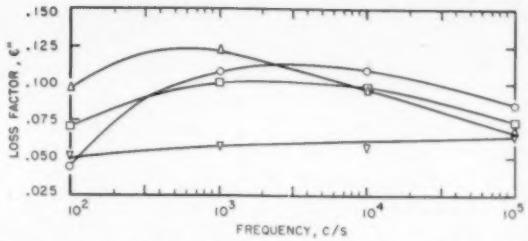

FIGURE 8. *Loss factor of the fully cured resin as a function of frequency at the approximate temperature at which the 1,000-c/s loss-factor maximum occurs for several concentrations of the DVB solution.*

Loss factor values are corrected to an AN content of 5.0 percent. ○, 0-percent DVB solution; △, 2-percent DVB solution; □, 6-percent DVB solution; ▽, 11-percent DVB solution.

TABLE 5. *Comparison of loss-factor maxima reduced to AN contents of 5 or 10 percent of polymerizing systems at 50° C and of fully polymerized systems at elevated temperatures*

Polymerizing systems					
AN	DVB	100 c/s	1,000 c/s	10,000 c/s	70,000 c/s
Percent	*Percent*				
5	0	----------	0. 162	0. 185	0. 203
5	2	0. 127	. 145	. 192	. 190
5	6	. 107	. 122	. 139	. 156
5	11	. 062	. 067	. 079	. 097
10	2	. 236	. 263	. 301	. 307

Fully cured polymers [1]					
AN	DVB	100 c/s	1,000 c/s	10,000 c/s	100,000 c/s
Percent	*Percent*				
5	0	0. 104 (87° C)	0. 111 (95° C)	0. 114 (108° C)	----------
5	2	0. 099 (92° C)	0. 125 (101° C)	0. 130 (109° C)	0. 144 (127° C)
5	6	0. 095 (100° C)	0. 096 (109° C)	0. 104 (122° C)	0. 120 (132° C)
5	11	0. 050 (115° C)	0. 058 (128° C)	0. 067 (136° C)	0. 091 (154° C)
10	2	0. 245 (100° C)	0. 304 (109° C)	0. 319 (119° C)	0. 355 (132° C)

These data were obtained by interpolation from figures 3, 4, 5, 6, and 7.

loss maxima occur in the temperature range in which the samples undergo the change from glass-like to rubber-like behavior [11, 12], and that this transition occurs at higher temperatures the higher the concentration of DVB.

At the higher temperatures the samples exhibit some d-c conductivity (table 6), which could be due to a small amount of pyrolysis or to a freeing of ionic impurities in the polymerizing mixture. Ionic conductance in phase with the applied field gives rise to an equivalent a-c loss factor equal to $18\times10^{11}\ G/f$, where G is the d-c conductivity. When this quantity is subtracted from the measured a-c loss factor, the remainder should be representative of the dipolar loss alone. A calculation shows that after this subtraction is made, the a-c loss factor still increases with temperature, after having gone through a minimum, and, although this may mean that a second dipolar loss mechanism has come into play, an alternate explanation is that the ionic

TABLE 6. *Direct-current conductivities of fully cured resins as a function of temperature*

0 percent of DVB solution, 5.6 percent of AN		2 percent of DVB solution, 5.4 percent of AN		6 percent of DVB solution, 5.3 percent of AN		11 percent of DVB solution, 5.1 percent of AN		2 percent of DVB solution, 11.6 percent of AN	
Temp	d-c conductivity	Temp	d-c conductivity	Temp	d-c conductivity	Temp	d-c conductivity	Temp	d-c conductivity
° C	*Mho/cm*	° C	*Mho/cm*	° C	*Mho/cm*	° C	*Mho/cm*	° C	*Mho/cm*
23 to 108	$<5\times10^{-15}$	23 to 98	$<5\times10^{-15}$	23 to 110	$<5\times10^{-15}$	23 to 120	$<5\times10^{-15}$	128	4×10^{-13}
.....	.....	109	2×10^{-14}	122	3×10^{-14}	124	2×10^{-14}	138	13×10^{-13}
.....	.....	119	6×10^{-14}	135	15×10^{-14}	135	7×10^{-14}	.....	.....
.....	.....	127	15×10^{-14}	.....	.....	146	20×10^{-14}	.....	.....
.....	.....	.....	.....	.....	.....	157	60×10^{-14}	.....	.....

conductance has an out-of-phase component, giving a larger a-c loss than that which would be expected from a pure ionic in-phase mechanism [13].

By application of the theory of absolute reaction rates to dielectric relaxation [14], one obtains

$$1/\tau = kT/he^{\Delta S/R}e^{-\Delta H/RT}, \qquad (3)$$

where k is the Boltzmann constant, h is Planck's constant, and ΔS and ΔH are entropy and heat of activation, respectively. Calculations of ΔS and ΔH were performed for all samples for which sufficient data were available (all except the sample containing no cross-linking agent). As an additional check, a run was made with another sample containing 2 percent of the DVB solution, and measurements were made at closer frequency intervals (table 7). Figure 9 shows the plots of log f_{max} versus $1/T$ for all these systems made from the data in figures 4, 5, 6, 7 and table 7. These plots give, within the experimental error, parallel lines, and the heat of activation averages 63,000 cal/mole. For the entropies of activation, values of 122, 115, and 107 (cal/mole)/deg are obtained for the samples containing 2, 6, and 11 percent of the DVB solution, respectively, and the normal amount of acrylonitrile, whereas a value of 115 (cal/mole)/deg is obtained for the sample with the high AN content. The systems investigated therefore show the high values of both heat and entropy of activation commonly observed for dipolar relaxation in high polymers [11].

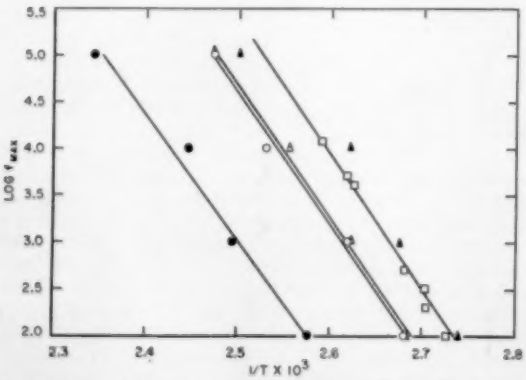

FIGURE 9. *Log f_{max} as a function of reciprocal absolute temperature for the samples whose behavior is illustrated in figures 3 to 7.*

▲, □, 2 different samples with 2-percent DVB solution; ○, 6-percent DVB solution; ●, 11-percent DVB solution; ▲, □, ○, ●, approximately 5-percent AN; △, 2-percent DVB, 11-percent AN.

TABLE 7. *Detailed high-temperature data for a sample containing 5.4 percent of AN and 2 percent of DVB solution*

Frequency	Dielectric constant	Loss factor	Frequency	Dielectric constant	Loss factor
94° C			108° C		
c/s			c/s		
10^2	3.053	0.131	10^2	3.242	0.056
2×10^2	2.987	.133	2×10^2	3.213	.076
5×10^2	2.917	.131	5×10^2	3.171	.110
10^3	2.827	.115	10^3	3.084	.125
2×10^3	2.706	.0985	2×10^3	3.014	.137
5×10^3	2.719	.086	5×10^3	2.927	.140
10^4	2.667	.073	10^4	2.837	.125
2×10^4	2.639	.062	2×10^4	2.772	.119
5×10^4	2.606	.0525	5×10^4	2.708	.114
10^5	2.573	.047	10^5	2.649	.093
97° C			113° C		
10^2	3.105	0.125	10^2	3.242	0.0308
2×10^2	3.039	.134	2×10^2	3.237	.0423
5×10^2	2.959	.142	5×10^2	3.214	.060
10^3	2.867	.132	10^3	3.160	.094
2×10^3	2.801	.119	2×10^3	3.108	.113
5×10^3	2.738	.104	5×10^3	3.031	.138
10^4	2.677	.089	10^4	2.918	.143
2×10^4	2.634	.074	2×10^4	2.861	.140
5×10^4	2.599	.064	5×10^4	2.789	.138
10^5	2.564	.055	10^5	2.707	.126

It has been shown that distributions of relaxation times can be calculated from dielectric dispersion [9, 15, 16] and that dielectric losses can be calculated from dielectric-constant data without introducing any assumptions concerning the form of the distribution function [15]. We have for a linear dielectric of very small d-c conductivity:

$$\epsilon'(\omega)-\epsilon_\infty=\int_0^\infty \frac{y(\tau)d\tau}{1+\omega^2\tau^2}=\int_{-\infty}^{+\infty}\frac{Y(\ln\tau)d\ln\tau}{1+\omega^2\tau^2}, \qquad (4)$$

$$\epsilon''(\omega)=\int_0^\infty \frac{y(\tau)\omega\tau d\tau}{1+\omega^2\tau^2}=\int_{-\infty}^{+\infty}\frac{\omega\tau Y(\ln\tau)d\ln\tau}{1+\omega^2\tau^2}; \qquad (5)$$

and, if the dispersion is not too sharp, we have to a very good approximation [15]:

$$Y(\ln 1/\omega)=-\frac{d\epsilon'}{d\ln\omega}, \qquad (6)$$

where $y(\tau)$ is the distribution of electrical relaxation

times [10] and $Y(\ln \tau)d \ln \tau = y(\tau)d\tau$. Often it is of interest to obtain the function Y from the imaginary part as well. This has been attempted for the analogous mechanical case [17, 18]. The same treatment applied to the electrical case would result in

$$Y(\ln 1/\omega) = -\epsilon'' \frac{d \log (\epsilon''/\omega)}{d \log \omega}. \tag{7}$$

As has been pointed out [15], the use of the approximation resulting in (7), when used in the calculation of ϵ'' from ϵ', leads to values that are 30 to 40 percent too small. The reason for this discrepancy is that, whereas the approximation made in the calculation of (6), namely,

$$\frac{1}{1+\omega^2\tau^2} = \begin{cases} 1 & 0 < \tau < 1/\omega \\ 0 & 1/\omega < \tau < \infty \end{cases} \tag{8}$$

is excellent, the approximation which results in (7), namely,

$$\frac{\omega\tau}{1+\omega^2\tau^2} = \begin{cases} \omega\tau & 0 < \tau < 1/\omega \\ 0 & 1/\omega < \tau < \infty \end{cases} \tag{9}$$

if poor, because we are interested in the integrals of these expressions (fig. 10). It is clear, therefore, that we cannot obtain Y with the aid of approximation (9). We can, however, define a function Y', given by

$$\epsilon'' = \int_{-\infty}^{\ln 1/\omega} \omega\tau Y'(\ln \tau) d \ln \tau. \tag{10}$$

It is this function Y', not Y, that is equal to the right-hand side of (7) which must, therefore, be replaced by

$$Y'(\ln 1/\omega) = -\epsilon'' \frac{d \log (\epsilon''/\omega)}{d \log \omega}. \tag{11}$$

We can now calculate Y' in terms of Y from eq (5) and (10), obtaining

$$\int_{-\infty}^{+\infty} \frac{\omega\tau Y(\ln \tau) d \ln \tau}{1+\omega^2\tau^2} = \int_{-\infty}^{\ln 1/\omega} \omega\tau Y'(\ln \tau) d \ln \tau. \tag{12}$$

Since, in most practical cases, the variation of Y and Y' is small in the region in which the integral has a significant value, we can write instead of (12)

$$Y(\ln \tau) \int_{-\infty}^{+\infty} \frac{\omega\tau}{1+\omega^2\tau^2} d \ln \tau = Y'(\ln \tau) \int_{-\infty}^{\ln 1/\omega} \omega\tau d \ln \tau. \tag{13}$$

Making use of the symmetry of the integral on the left, and transforming, we obtain

$$2Y(\ln \tau) \int_0^{1/\omega} \frac{\omega}{1+\omega^2\tau^2} d\tau = Y'(\ln \tau) \int_0^{1/\omega} \omega d\tau. \tag{14}$$

[10] Properly speaking, this is a distribution of relative permittivities.

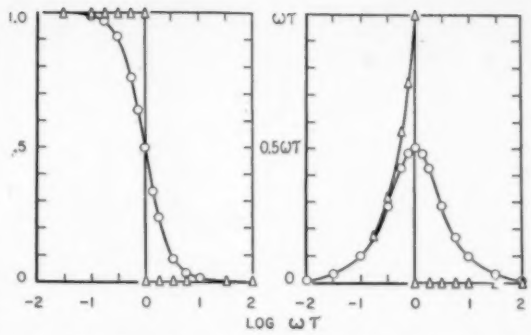

FIGURE 10. *Plot of exact expressions and of approximations required for correlations between real and imaginary parts of the dielectric constant plotted as a function of log* $\omega\tau$.

On the left, $1/(1+\omega^2\tau^2)$ and approximation (8); on the right, $\omega\tau/(1+\omega^2\tau^2)$ and approximation (9). ○, exact expressions; △, approximations.

Hence

$$\pi/2\ Y(\ln \tau) = Y'(\ln \tau) \tag{15}$$

i. e., the two functions are simply related through a constant over their entire spectrum, and by (6), (11), and (15)

$$Y(\ln \tau) = -1/2.303 \frac{d\epsilon'}{d \log f} = -2/\pi\ \epsilon' \frac{d \log \epsilon''/f}{d \log f}. \tag{16}$$

The appearance of the factor $2/\pi$ immediately explains the discrepancy between the observed and calculated values of ϵ'' noted previously [15], since the use of approximation (9) is equivalent to the neglect of the difference between Y and Y'.[11] For materials whose losses are essentially frequency independent (12) reduces to

$$Y(\ln \tau) = -1/2.303 \frac{d\epsilon'}{d \log f} = 2/\pi\ \epsilon''. \tag{17}$$

The identical relation has been derived by Gevers and Du Pre, using a somewhat different argument [19]. Equation (17) provides a very convenient first approximation connecting dielectric dispersion and loss. Table 8 gives a comparison of values of the loss factor as observed and as calculated by the procedure previously described [15], i. e., through use of eq (6), followed by (5). It also presents values of $Y(\ln \tau)$ calculated from real and imaginary parts of the dielectric constant through the use of eq (16). The reasonable agreement of the two sets of ϵ'' and Y values demonstrates the self-consistency of the approximations outlined, which is fully adequate in view of the inaccuracies entailed by the graphical operations.

For the analogous mechanical case, successful calculations of dynamical properties at various temperatures have been made from measurements at a

[11] Ferry et al. [17], who use approximation (9), noted that in some of their results the use of an empirical constant "a" equal to 0.77 occurring in the place of $2/\pi$ in an equation analogous to (16) harmonized distribution functions calculated from real and imaginary parts of the modulus.

TABLE 8. *Electrical properties of a sample containing 5.4 percent of AN and 2 percent of DVB solution at 94° C*

Frequency	ϵ'	ϵ'' (observed)	ϵ'' (calculated)	Y (from ϵ')	Y (from ϵ'')
c/s					
10^5	3.053	0.131	.....	0.078	0.079
2×10^5	2.987	.133	.....	.088	.084
5×10^5	2.917	.131	.....	.103	.089
10^6	2.827	.115	0.124	.100	.087
2×10^6	2.766	.099	.109	.073	.074
5×10^6	2.719	.086	.092	.058	.065
10^7	2.667	.073	.080	.049	.055
2×10^7	2.639	.062	.....	.041	.047
5×10^7	2.606	.0525	.....	.039	.040
10^8	2.573	.049	.....	.033	.036

different temperature, using the assumption that the distribution of relaxation times did not change with temperature [20]. Although some success has been reported for the electrical case also [16], similar calculations of ϵ' and ϵ'' as a function of temperature, from data obtained at a different temperature, do not give sufficiently accurate results when applied to the data cited here. The reason seems to be that the distribution functions are not independent of temperature. As it is not possible to calculate distribution functions with an accuracy of better than 5 to 10 percent by the method outlined, we may cite the observed increase in the loss-factor maxima at the higher temperatures (table 5) as evidence that these functions sharpen with temperature. Since $\epsilon_0-\epsilon_\infty$ is proportional to $\int_{-\infty}^{+\infty}\epsilon''d\ \ln f$, and since ϵ_0 decreases with temperature while ϵ_∞ is essentially temperature independent over a small temperature range, an increase in the loss-factor maximum with temperature must be connected with a sharpening of the distribution function with temperature.[12] Such a sharpening has been concluded to occur for polymers in general by several investigators, both on the basis of experimental data and on theoretical grounds [9, 11, 12].

Because of the analogous effects on the relaxation time of temperature changes in the case of the cured polymer and of "internal viscosity" changes in the case of the growing polymer, it is interesting to note that the loss-factor maxima during the polymerization increase with frequency (table 1).

4. Summary

1. The marked changes in dielectric constant and in dielectric loss observed during the polymerization of the polar casting resins described are attributable primarily to the dipolar relaxation of the nitrile groups present.

2. As seen by its electrical effects, the hardening of the reaction mixture at a certain stage of the polymerization is quite similar to the glass-phase transition occurring when the temperature of the fully cured rubber-like polymer is lowered—the dipolar relaxations occurring in the above two transitions result in loss factors that agree semiquantitatively, and a similar broadening of the relaxation distribution functions take place upon addition of cross-links in each case.

3. In the polymerizing systems discussed, electrical measurements can be used as an indicator of reaction rate in a qualitative way. However, such questions as completeness of cure cannot be decided in this manner because all significant electrical changes occur at a relatively early stage of the reaction.

4. A scheme is described whereby distributions of electrical relaxation times can be calculated with comparable accuracy from real and imaginary parts of the complex dielectric constant.

The authors express thanks to Max M. Lee for many helpful suggestions, to Emma Lee Hebb for preparing the polymerizing mixtures, to A. H. Scott for loan of the high-temperature equipment, to M. Wales and L. Williams for performing the molecular weight determination of one of the polystyrenes, to Rolf Paulson for performing the nitrogen analyses, and to A. Glasgow and his group for purifying some of the acrylonitrile.

5. References

[1] A. Lazarev and I. Raschketaev, Tech. Phys. USSR **31,** 366 (1936).
[2] T. G. Majury and H. W. Melville, Proc. Roy. Soc. [A] **205,** 496 (1951).
[3] P. Debye, Polar molecules (Dover Publishers, New York, N. Y.).
[4] J. D. Hoffman and C. P. Smyth, J. Am. Chem. Soc. **72,** 171 (1950).
[5] R. M. Fuoss, The chemistry of large molecules, ch. VI (Interscience Publishers, New York, N. Y., 1943). This work lists many references to the original literature.
[6] A. H. Scott and P. Ehrlich, Annual Report of Conference on Electrical Insulation (1953).
[7] K. W. Wagner, Ann. Physik. **40,** 817 (1913).
[8] W. A. Yager, Physics **7,** 434 (1936).
[9] R. M. Fuoss and J. G. Kirkwood, J. Am. Chem. Soc. **63,** 385 (1941).
[10] R. M. Fuoss, J. Am. Chem. Soc. **63,** 378 (1941).
[11] W. Kauzmann, Rev. Modern Phys. **14,** 12 (1942).
[12] R. F. Tuckett, Trans. Faraday Soc. **40,** 448 (1944).
[13] D. J. Mead and R. M. Fuoss, J. Am. Chem. Soc. **67,** 1566 (1945).
[14] S. Glasstone, K. J. Laidler, and H. Eyring, The theory of rate processes, ch. IX (McGraw-Hill Book Co. New York, N. Y., 1941).
[15] P. Ehrlich, J. Research NBS **50,** 19 (1953) RP2382.
[16] J. D. Ferry and E. R. Fitzgerald, J. Colloid Sci. **8,** 224 (1953).
[17] J. D. Ferry, W. M. Sawyer, G. V. Browning, and A. H. Groth, J. Appl. Phys. **21,** 513 (1950).
[18] F. Schwarzl, Physica **17,** 923 (1951).
[19] M. Gevers and F. K. Du Pre, Trans. Faraday Soc. **42A** 53 (1946).
[20] J. D. Ferry, J. Am. Chem. Soc. **72,** 3746 (1950).

WASHINGTON, July 23, 1953.

[12] This argument assumes that the resultant dipole moment of the polymer molecule is independent of temperature.

Journal of Research of the National Bureau of Standards Vol. 51, No. 3, September 1953 Research Paper 2445

Study of Degradation of Polystyrene, Using Ultraviolet Spectrophotometry

Mary Jane Reiney, Max Tryon, and B. G. Achhammer

The role of ultraviolet radiant energy and effect of presence of monomer on degradation of polystyrene were studied by means of ultaviolet absorption techniques. It was found that exposure of pure polystyrene to ultraviolet radiant energy resulted in increased absorption in the ultraviolet region of 280 to 400 millimicrons, which advanced progressively as exposure time increased. The presence of monomer increased the rate of degradation without altering the general type of absorption. A post-radiation effect was noted in both the purified polymer and polymer containing monomer styrene. Again, the presence of monomer increased the rate of progress of the post-radiation effect. Possible mechanisms are postulated for the ultraviolet degradation, and the concept of entrapped free radicals is considered as a possible explanation for the post-radiation effect observed.

1. Introduction

It has been shown by infrared spectrophotometric measurements that carbonyl and hydroxyl groups are formed in polystyrene on exposure to ultraviolet radiant energy in the presence of oxygen [1, 2].[1] The volatile products given off and measured by mass spectrometry and the changes in solubility and oxygen content on exposure of polystyrene to heat and/or ultraviolet radiant energy in vacuum and in oxygen have also been reported [3]. This report presents the changes in the ultraviolet spectrum of polystyrene as a result of exposure to ultraviolet radiant energy in air. A mechanism is suggested to describe possible chemical changes in the polymer that could be responsible for the variation of the ultraviolet spectrum of polystyrene, both on exposure of the polymer to ultraviolet radiant energy and on subsequent storage in the absence of light.

2. Materials and Methods

The polystyrene samples used in this study are described in table 1. All samples were prepared by the Dow Chemical Co. Samples A and E1 are commercial resins; they do not contain any compounding ingredients and were used as received. Samples W, X, and Y were prepared by polymerizing purified monomer without catalyst or solvent in a nitrogen atmosphere.

TABLE 1. *Description of samples of polystyrene*

Sample	Approximate molecular weight	Polymerization temperature
		° C
A	[a] 308,000	
E1	[a] 299,000	
W	[b] 500,000	60
X	[b] 237,000	120
Y	[b] 110,000	180

[a] Weight average obtained by light scattering.
[b] Number average obtained from osmotic pressure.

The spectrophotometric measurements on these samples as received are designated by the sample letters alone. The measurements made after partial purification of the samples by a "frozen benzene technique" [2] are designated by the sample letters followed by P. Sample X was also subjected to purification by solution in methyl ethyl ketone and precipitation with isopropanol three times; the samples from the first, second, and third precipitations are designated X1, X2, and X3, respectively.

The technique for preparation of the samples in film form of various thicknesses has been described previously [2]. Casting of the thicker films on a surface of regenerated cellulose, instead of directly on glass, facilitated their removal because wetting the opposite side of the cellulose with water swelled the cellulose and broke the bond between it and the polystyrene film.

Exposure of the films to ultraviolet radiant energy was accomplished by placing the films in holders on a revolving table 6 in. from an S–1 sunlamp. The exposure was done in air, and the temperature at the table was 60° C. This sunlamp equipment is described in method No. 6021 of Federal Specification L–P–406a [4].

A Beckman model DU spectrophotometer with ultraviolet accessories was used for all the transmission measurements.[2] For solution work, silica cells of 1.000-cm path length were used.

3. Effect of Film Thickness on Transmittance

In the same manner that the concentration of a solution for a given light path length will dictate the spectrum of polystyrene obtained, the thickness of films of the polymer will be the controlling factor in determining its absorption spectrum. The effect of film thickness on the spectrum of polystyrene films of sample XP is shown in figure 1.

Films of thickness equivalent to that of curve E of figure 1 were selected for the present study because they are thick enough to be mechanically stable;

[1] Figures in brackets indicate the literature references at the end of this paper.

[2] The various spectral transmission and absorption terms used in this paper are based on the terminology recommended by Kasson S. Gibson in NBS Circular 484, Spectrophotometry (200 to 1,000 millimicrons) (Sept. 15, 1949).

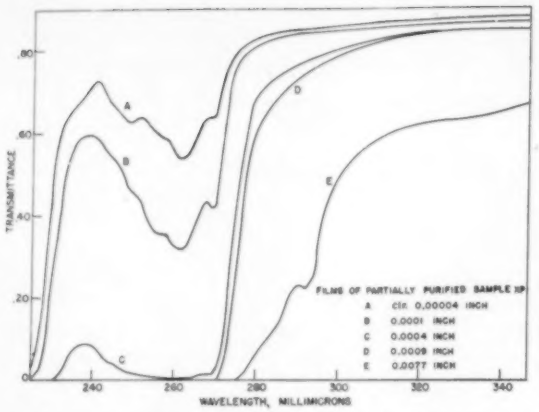

FIGURE 1. *Effect of film thickness on the ultraviolet transmittance of polystyrene.*

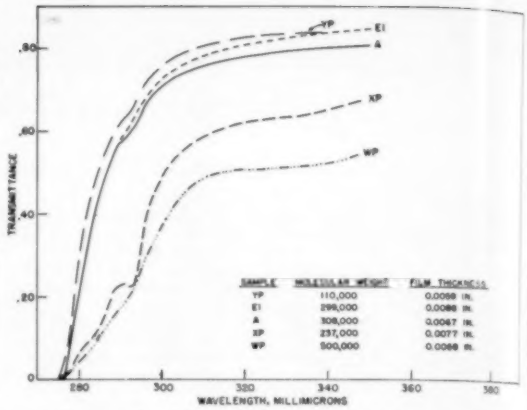

FIGURE 2. *Ultraviolet transmittance of partially purified polystyrenes.*

they are not too thick to show the shape of the absorption curve in the region 275 to 350 mμ where the greatest differences between the polymers studied were obtained; and their strong absorptance [3] below 270 mμ is relatively unimportant to this study. Smakula [5] states that the absorptance of polystyrene at about 260 mμ is due to the phenyl residues. These would not be expected to change appreciably on degradation of the polymer. Furthermore, monomer styrene, which has been suggested as playing an important part in the discoloration phase of the degradation of the polymer [1], is known to absorb in the ultraviolet at 291.5 mμ. The fact that the absorption band at 291.5 mμ is present in curve E indicates that the purification of the sample was not complete and that some monomer remained in the sample.

4. Transmittance of Undegraded Polymers

Figure 2 presents the spectra of films of the various polymer samples studied. It is thought that the differing spectra cannot be ascribed to the moderate thickness variations of the films. This is substantiated by the measurements made on solutions of 18 g/liter concentration of WP, XP, and YP in benzene, which are presented in figure 3. The solution spectra of these three samples bear out the relationship shown by the spectra of these samples in film form.

Moreover, the variation in the spectra cannot be ascribed to the molecular weight differences of the samples. McGovern and coworkers [6] found that the same spectrum was obtained at wavelengths of 282 and 291 mμ, regardless of the molecular weight of the polystyrene. Meehan [7] showed that the specific extinction coefficient, referred to weight concentration of polystyrene, at 260 mμ is independent of molecular weight. Newall [8] measured five polystyrene samples and observed that neither molecular weight nor variables of the polymerization reaction

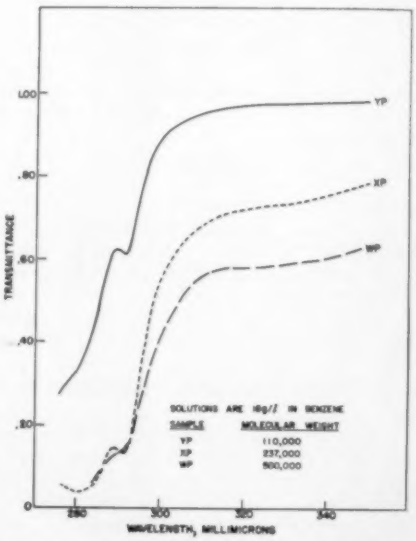

FIGURE 3. *Ultraviolet transmittance of partially purified polystyrenes.*

affected the spectrum of polystyrene at the shorter wavelengths.

The spectrum of polystyrene, however, is a function of the purity of the sample. Sample X was carefully purified by repeated solution in methyl ethyl ketone and precipitation with isopropanol. The X3 curve in figure 4 represents the pure polymer, and the other spectra denote varying degrees of contamination retained by the polymer. The X polymer shows marked regions of absorptance not characteristic of pure polystyrene. Figure 5 combines the spectra of 18 g/liter solutions of X3 and X with those of the unpurified polymers W and Y. The difference in purity of the polymers W, X, and Y is clearly shown,

[3] Absorptance is defined as "1−Transmittance."

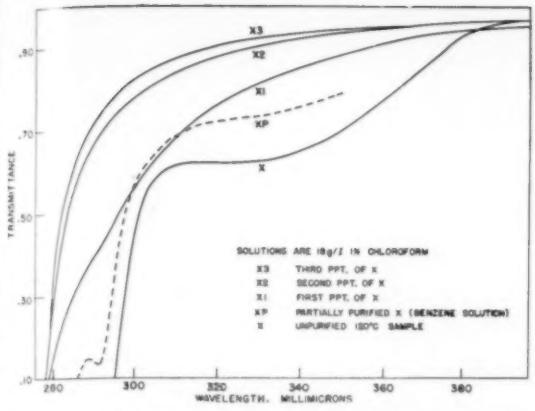

FIGURE 4. *Ultraviolet transmittance of polystyrene of varying degree of purity.*

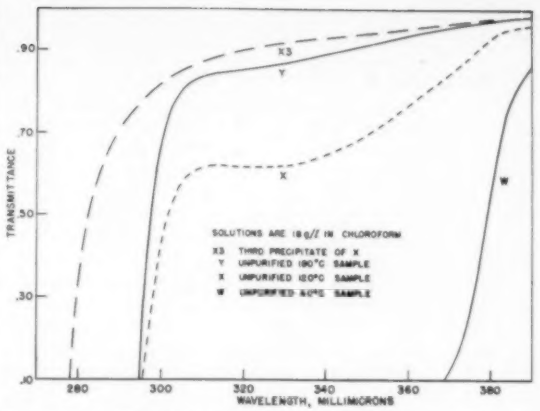

FIGURE 5. *Ultraviolet transmittance of polystyrenes of varying degree of purity.*

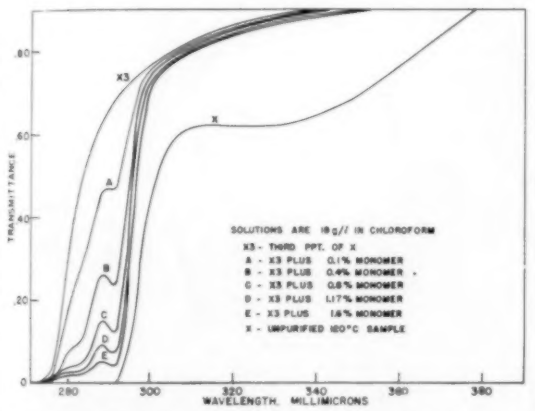

FIGURE 6. *Effect of monomer and impurities on the ultraviolet transmittance of polystyrene.*

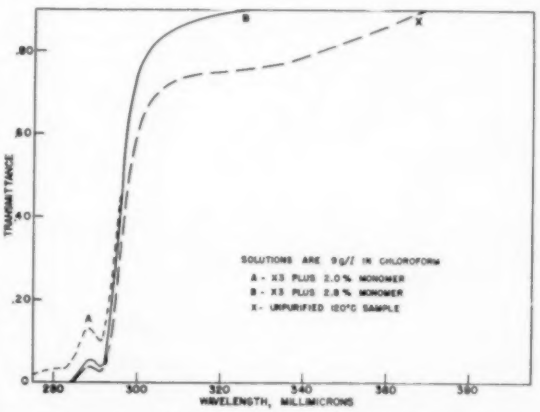

FIGURE 7. *Effect of monomer and impurities on the ultraviolet transmittance of polystyrene.*

particularly the considerable contamination in the W polymer. It is reasonable, therefore, that an identical purification procedure applied to each polymer might not produce samples of the same degree of purity, thus leading to the differing spectra exhibited by the samples WP, XP, and YP in figure 3.

5. Effect of Styrene Monomer on Polymer Spectra

In order to determine the part that residual monomer contributes to the contamination of the unpurified polymer, styrene was added to solutions of pure polystyrene (precipitate X3 of sample X). Solutions containing approximately 0.1, 0.4, 0.8, 1.17, 1.6, 2.0, 2.8, 5.0, and 7.35 percent of styrene were prepared. Figure 6 shows the curve of the pure polymer, those of the first five solutions in the monomer-addition series and that of the unpurified polymer, all at 18 g/liter concentration. The effect of increasing monomer content is clearly shown. There is also an absorption band from 310 to 385 mμ in the unpurified sample. That this band cannot be attributed to monomer contamination is evident from the spectra in figure 7 made with solutions of 9 g/liter concentration. Even when the 292 mμ monomer band of X is approximately duplicated by the addition of 2.8 percent of monomer to X3 there is still no indication of the 310 to 385 mμ band of X present in the spectrum of the latter solution. Changes in absorptance in the 310- to 385-mμ wavelength region were noted on exposure of the films to ultraviolet radiant energy, and a more detailed investigation of this region is described in section 8.

This failure of residual monomer to account for the long-wavelength contamination of the unpurified

polymers is further shown by examination of figure 8. The pure polymer solution containing 7.35 percent of added monomer shows a spectrum comparable to that of W only below approximately 295 mμ. The presence of monomer causes no appreciable change in the spectrum of the pure polymer at wavelengths longer than 300 mμ. This figure shows the two monomer absorption bands at approximately 282 and 291.5 mμ more clearly than any of the preceding figures and illustrates that monomer is responsible for the decreased transmittance [4] of W below 295 mμ.

Figure 9 presents the spectra of three solutions of styrene monomer alone in chloroform. The absorption bands at 282 and 291.5 mμ are shown, as well as the intense band at 248 mμ; but even when the spectrum of a very concentrated solution is considered (curve C), there is no indication of an absorption band at longer wavelengths. The absorption bands shown are due to the presence of the double bond in conjugation with the benzene ring and form the very characteristic spectrum that is distinguishable from that of saturated derivatives and from that of unsaturated compounds without the double bond in conjugation with the benzene ring [9]. This pattern of absorptance displayed by the monomer permits quantitative determination of styrene in polystyrene spectrophotometrically [6, 8] as well as the determination of monomer styrene in ethylbenzene [10].

6. Effect of Monomer on Polystyrene Degradation

To study the effect of styrene monomer on the degradation of polystyrene, two films were prepared. One was cast from a benzene solution of sample X3 and the other from a benzene solution of sample X3 to which 2 percent of monomer was added. The films were made by the same procedure and measured 0.0066 and 0.0068 in. thick, respectively. They were exposed to ultraviolet radiant energy from an S–1 sunlamp at 60° C in air. Ultraviolet transmission measurements of these films at intervals during their exposure give an insight into the degradation of the pure polymer and polymer contaminated with monomer but not with other impurities. Figure 10 shows the effect of exposure to S–1 radiant energy on the transmittance of the pure film in the ultraviolet region of the spectrum, and figure 11 shows similar information for the film prepared from the solution to which monomer was added. A progressive general increase in absorptance is noted in each case but is initially more severe for the film containing monomer. The 20- and 50-hr spectra of figure 11 bear a resemblance to the partially purified XP film spectrum noted previously. Both films yellowed very slightly as they were exposed, the monomer-containing film slightly more so than the pure film.

[4] "Transmittance," T, is defined as the ratio of the radiant energy leaving the sample to the incident radiant energy; $100T$=percentage transmittance.

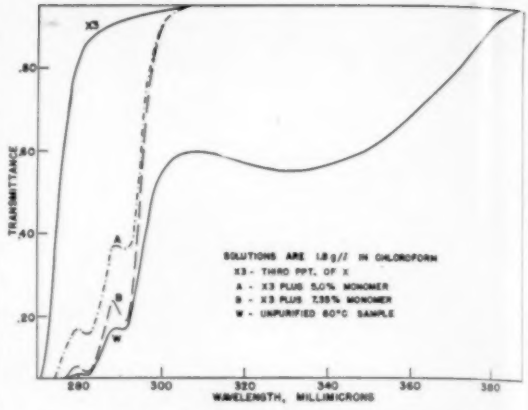

FIGURE 8. *Effect of monomer and impurities on the ultraviolet transmittance of polystyrenes.*

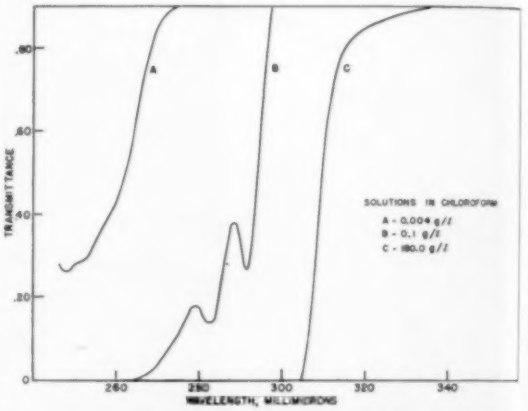

FIGURE 9. *Ultraviolet transmittance of styrene monomer.*

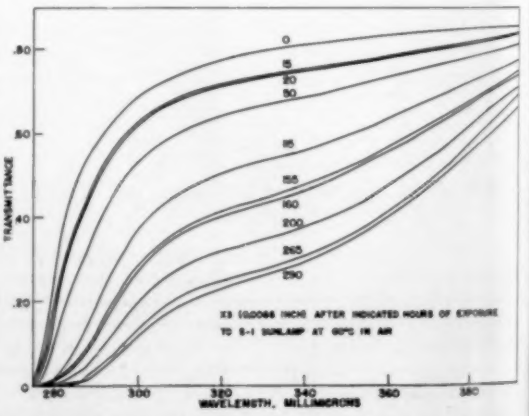

FIGURE 10. *Effect of radiant energy on the ultraviolet transmittance of pure polystyrene film.*

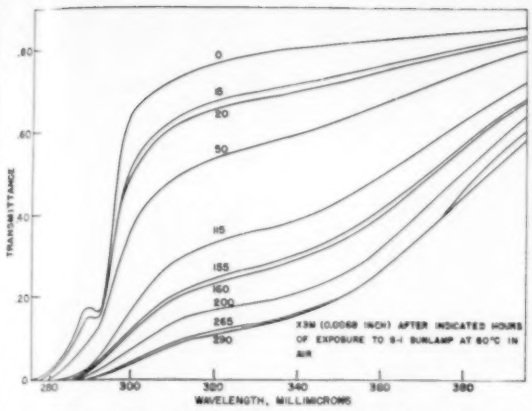

FIGURE 11. *Effect of radiant energy on the ultraviolet transmittance of pure polystyrene film plus monomer.*

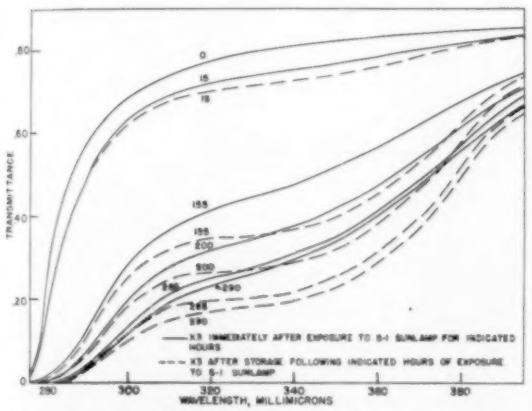
TRANSMITTANCE
WAVELENGTH, MILLIMICRONS
X3 IMMEDIATELY AFTER EXPOSURE TO S-1 SUNLAMP FOR INDICATED HOURS
X3 AFTER STORAGE FOLLOWING INDICATED HOURS OF EXPOSURE TO S-1 SUNLAMP

FIGURE 12. *Effect of radiant energy and subsequent storage on the ultraviolet transmittance of pure polystyrene film.*

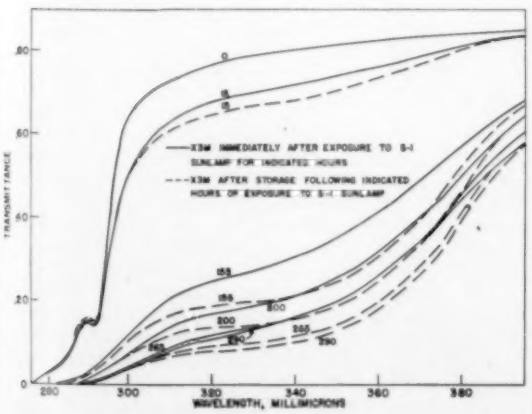
TRANSMITTANCE
WAVELENGTH, MILLIMICRONS
X3M IMMEDIATELY AFTER EXPOSURE TO S-1 SUNLAMP FOR INDICATED HOURS
X3M AFTER STORAGE FOLLOWING INDICATED HOURS OF EXPOSURE TO S-1 SUNLAMP

FIGURE 13. *Effect of radiant energy and subsequent storage on the ultraviolet transmittance of pure polystyrene film plus monomer.*

7. Post-radiation Changes in Polystyrene Degradation

In the course of the degradation studies, a post-radiation effect was observed. The first indication of this effect was noted when, following the 15-hr S–1 sunlamp exposure, the films were stored in the dark at room conditions in air for 99 hr and their transmittance measured before further exposure. The resulting spectra showed a noticeable increase in absorptance when compared to the spectra measured directly after exposure to radiant energy. The 20- and 25-hr total S–1 exposures followed the pattern of the 15-hr exposure. After 155 hr of total S–1 sunlamp exposure, the films were stored for 13 days, and a very large change in absorptance was apparent when the spectra were measured. The films were then exposed to an additional 5 hr of radiant energy from an S–1 sunlamp, to give a total of 160 hr of exposure, and their spectra remeasured. The increased absorptance apparent after storage was eliminated, and the 160-hr spectra fell in line with the spectra measured immediately upon completion of the 155 hr of exposure. This effect was checked by storing the films for 13-day periods following the 200-, 265-, and 290-hr total exposure times and was found to be real. Figures 12 and 13 present the spectra of the films measured just before and after storage periods. The dashed lines represent the measurements made following the storage periods.

Upon completion of the 290-hr S–1 sunlamp exposure, the spectra of the films were measured at intervals during the ensuing storage of the films in order to determine the length of time necessary for the development of the increased absorptance. When the corrected absorbance, A_c,[5] at a particular wavelength is plotted versus the hours of storage following the 290-hr exposure to ultraviolet radiant energy, a curve is obtained for each film which shows that most of the increased absorbance develops in the first 75 hr of storage. Figure 14 is such a plot for numerous wavelengths. From this figure it is seen that the slopes of the curves are very slight at greater than 75 hr of storage and also that a greater and more rapid change occurs at any particular wavelength on storing the monomer-containing film than on storing the pure film.

From this information, it is clear that the first storage-period measurement, which was made after 99 hr of storage following the 15 hr of exposure to ultraviolet radiant energy, is representative of the maximum increase of absorbance due to storage following that S–1 exposure. Two hours of exposure to ultraviolet radiant energy is sufficient to eliminate the absorption increase due to storage. The 202-hr curves and the 267-hr curves were not presented in figures 10 and 11 because they closely follow the 200- and 265-hr curves, with slightly decreased transmittance. One hour of ultraviolet radiant

[5] A_c represents the absorbance reading of the film at a given wavelength minus the absorbance reading at that wavelength measured on the film prior to all treatment. "Absorbance" is defined as $\log_{10} I_0/I$; also known as optical density

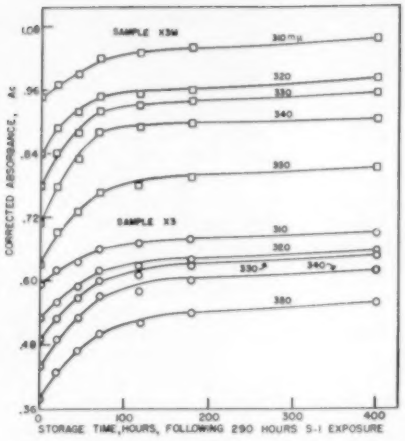

FIGURE 14. *Relation between duration of storage and absorbance of polystyrene films at various wavelengths.*

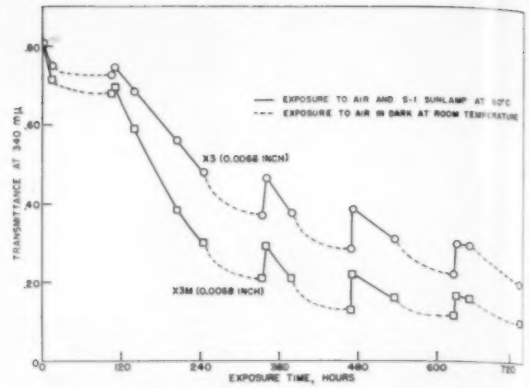
EXPOSURE TO AIR AND S-1 SUNLAMP AT 60°C
EXPOSURE TO AIR IN DARK AT ROOM TEMPERATURE
X3 (0.0068 INCH)
X3M (0.0068 INCH)
TRANSMITTANCE AT 340 mμ
EXPOSURE TIME, HOURS

FIGURE 15. *Effect of exposure to radiant energy and to subsequent storage on the ultraviolet transmittance of polystyrene film at 340 mμ.*

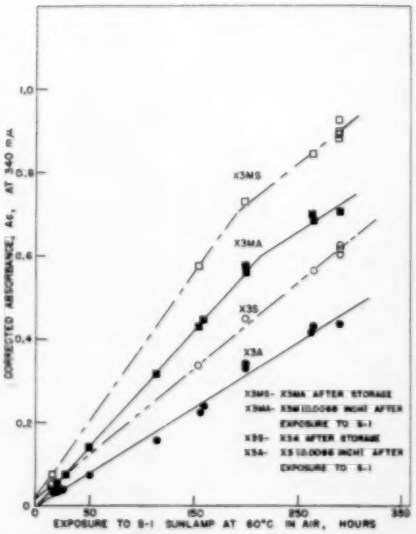
X3MS
X3MA
X3S
X3A
X3MS- X3MA AFTER STORAGE
X3MA- X3M (0.0068 INCH) AFTER EXPOSURE TO S-1
X3S- X3A AFTER STORAGE
X3A- X3 (0.0068 INCH) AFTER EXPOSURE TO S-1
CORRECTED ABSORBANCE, As, AT 340 mμ
EXPOSURE TO S-1 SUNLAMP AT 60°C IN AIR, HOURS

FIGURE 16. *Relations between exposures and absorbance of polystyrene films at 340 mμ.*

energy, however, was shown to be inadequate to cause this effect, for the 266-hr total-exposure curves fell below 267-hr curves and were of a shape more like that of the storage curves.

Because 2 hr of exposure to ultraviolet radiant energy at 60° C in air would return a storage curve to the previous S–1 exposure curve, 2 hr of exposure to 60° C heat in air was administered to the films following the storage after the 290-hr total S–1 exposure to observe the effect of heat alone. Heat did not remove the storage absorption band, and there was no change in the transmittance as a result of the treatment.

A graphical presentation of these data, which depicts the complete pattern of treatment of the films, is shown in figure 15. As representative of the absorption band covering the 310- to 385-mμ wavelength region, transmittance at 340 mμ is plotted versus exposure time in hours; the storage time (90 hr being considered as maximum storage) is included as well as the time of exposure to S–1 sunlamp radiant energy. This graph reveals the stepwise pattern assumed as the transmittance decreased on exposure to ultraviolet radiant energy, decreased at a different rate on storage, increased sharply on exposure to 2 hr of ultraviolet energy to the value attained preceding storage, and decreased on further exposure to ultraviolet energy, etc.

In order that a study of the rates of increased absorbance of both the pure film and the monomer-containing film for both the exposures to ultraviolet energy and the storage treatments following them could be made, plots of the corrected absorbance, A_c, at various wavelengths versus hours of exposure to ultraviolet radiant energy were made. Figure 16 is such a plot for 340-mμ wavelength. The dashed lines are drawn through the readings made after 13 days of storage following the particular exposure to ultraviolet energy. The plots for the pure film are linear but the plots for the monomer-containing film appear to deviate from linear behavior following the 200-hr exposure. With up to 200-hr treatment, the plots for the monomer-containing film have steeper slopes than those for the pure film, but at longer exposures the slopes seem to be equal, the curves being practically parallel to each other.

The slopes of these lines plotted for numerous wavelengths were calculated and gave the rates of increased absorbance with treatments of the films for the various wavelengths. These rates are presented in the first four columns of table 2. In an attempt to estimate the rate of increase of absorbance due to storage alone, the rate due to the exposure to ultraviolet energy was subtracted from the

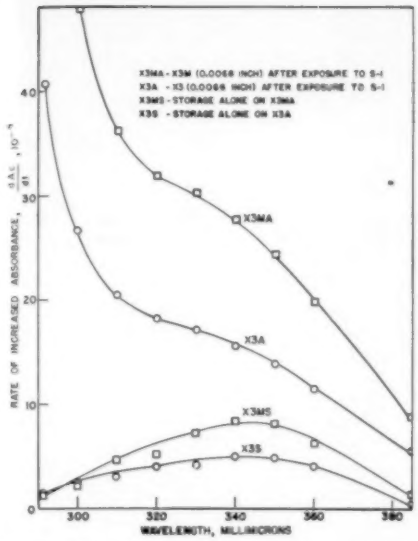
X3MA - X3M (0.0068 INCH) AFTER EXPOSURE TO S-1
X3A - X3 (0.0068 INCH) AFTER EXPOSURE TO S-1
X3MS - STORAGE ALONE ON X3MA
X3S - STORAGE ALONE ON X3A
RATE OF INCREASED ABSORBANCE, $\frac{\Delta A_c}{dt}$, 10^{-3}
X3MA
X3A
X3MS
X3S
WAVELENGTH, MILLIMICRONS

FIGURE 17. *Effect of exposures on absorbance of polystyrene films.*

rate calculated from the measurements made following the storage periods. Columns 5 and 6 of table 2 list these rates of increased absorbance due to storage alone for the various wavelengths.

If the rates of increased absorbance listed in columns 1, 2, 5, and 6 of table 2 are plotted versus wavelength of absorbance (fig. 17), the difference between the absorption curves obtained from films exposed to ultraviolet energy and films subsequently stored in the dark is emphasized. The greatest rate of change in the absorption curves obtained from exposure to ultraviolet energy alone is seen to be at the shorter wavelengths. The maxima in the two lower curves indicate that 340 mμ is the wavelength of greatest rate of change of absorbance on storage of the films.

TABLE 2. *Rates of increased absorbance, dA_c/dt*

Values for pure polystyrene film are based on exposures to radiant energy from an S-1 sunlamp up to 200 hours. Values for pure polystyrene film plus monomer are based on exposures up to 200 hours.

Wavelength plotted	Exposure of film to S-1 sunlamp at 60° C in air		Exposure of film to S-1 sunlamp plus storage in dark		Storage of film in dark	
	Pure	Plus monomer	Pure	Plus monomer	Pure	Plus monomer
	1	2	3	4	5	6
mμ						
300	0.0027	0.0048	0.0029	0.0050	0.0002	0.0002
310	.0020	.0036	.0023	.0041	.0003	.0005
320	.0018	.0032	.0022	.0037	.0004	.0005
330	.0017	.0030	.0021	.0037	.0004	.0007
340	.0015	.0028	.0020	.0036	.0005	.0008
350	.0014	.0024	.0019	.0032	.0005	.0008
360	.0012	.0020	.0016	.0026	.0004	.0006
385	.0005	.0009	.0005	.0010	.0000	.0001

8. Sources of Characteristic Absorption Bands in a Degraded Polystyrene

8.1. Benzaldehyde

It is apparent that exposure to ultraviolet radiant energy leads to the alteration of the polymer so that it absorbs in a characteristic manner, and that subsequent storage leads to further alteration which causes absorptance in a different characteristic manner. It was also noted that the absorption band that developed on storage was similar to the "impurity" band observed in the impure polymers. This similarity is observed by comparing the curve of impure sample X in figure 6 with the curve of pure polymer exposed to 155 hr S-1 plus storage shown in figure 12.

Because infrared spectrophotometric studies of polystyrene films indicated the presence of carbonyl and hydroxyl groups after treatment with ultraviolet radiant energy, and previous mass spectrometric measurements of gaseous products formed on degradation [3] showed some formaldehyde and benzaldehyde, benzaldehyde [6] was examined in the ultraviolet region. It gave the curves shown in figure 18 for 0.1- , 1.0- , and 2.0-g/liter solutions in chloroform. On addition of 1.6 percent of benzaldehyde to an 18-g/liter solution of pure polymer X3 in chloroform, the spectrum obtained (fig. 19) showed a resemblance in shape to the observed curves obtained on storage after exposure of the polystyrene films to ultraviolet energy. However,

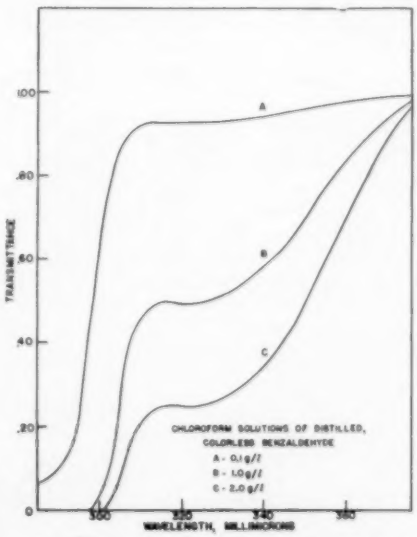

FIGURE 18. *Ultraviolet transmittance of benzaldehyde.*

[6] The benzaldehyde was not purified but contained oxidation products, and was, therefore, considered to be more representative of the material possibly present in the polymer.

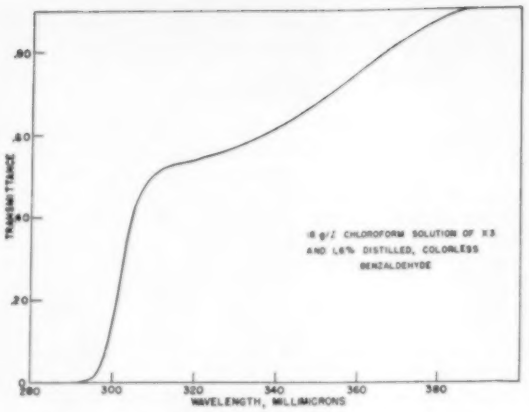

FIGURE 19. *Ultraviolet transmittance of polystyrene contaminated with benzaldehyde.*

the absorptance shown in figure 19 is not as broad and not as intense at 340 mμ as that which develops on storage. Also, there is an intense absorptance below 300 mμ; storage causes little change at these shorter wavelengths (fig. 17). The $K_{291.5}$* of benzaldehyde is 9.67, whereas its K_{320} is 0.3; therefore, the presence of an unreasonably high concentration of benzaldehyde in the sample would be required to give the long wavelength absorption. Hence, it is not plausible to assume that the absorption pattern caused by exposure to ultraviolet energy can be attributed to the presence of benzaldehyde alone.

8.2. Conjugated Carbonyl-Containing Compounds

Other compounds containing a more extended system of conjugation including the carbonyl group were therefore investigated in order that one having an extinction coefficient sufficient to explain either type of absorption might be found. The API RP collection of spectra [11] and the Friedel and Orchin collection [12] show numerous compounds which exhibit absorbance in these regions. Those compounds exhibiting absorption bands similar in shape to those under discussion usually contain one or the other of the following structures:

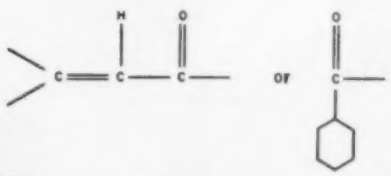

*K=specific extinction coefficient at indicated wavelength in millimicrons=absorbance for a concentration of 1 g/liter.

Some examples are: benzoin, benzophenone, mesityl oxide, methyl vinyl ketone, crotonaldehyde, benzoyl acetone, and *p*-toluyl acetone. However, the extinction coefficients at the desired wavelengths are again quite small. The latter two compounds have appreciable extinction coefficients, but the maxima of the absorption bands are shifted to 310 and 317 mμ, respectively.

While benzaldehyde and its oxidation products [13] do not have high enough extinction coefficients to account for the observed absorbance in the polystyrene films, it is likely that related structures such as those shown below might be present in the system, and their oxidation products might easily have sufficient conjugation to give very large extinction coefficients:

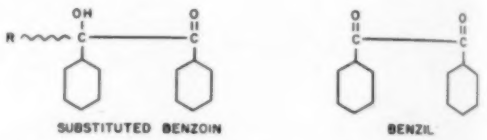

There is also the possibility of a reaction similar to an aldol condensation, once carbonyl is formed:

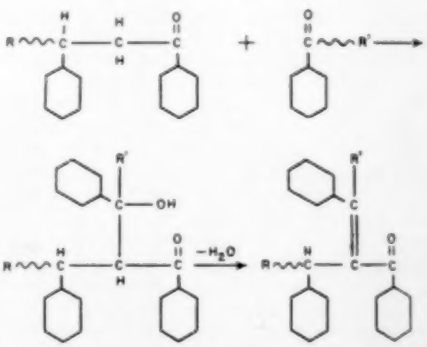

This condensation reaction results in a final product with a high degree of conjugation. Both pure and monomer-containing films may undergo this type of reaction on exposure to ultraviolet radiant energy, once the carbonyl is formed. Monomer styrene has a reactive site for oxidation and reacts to form carbonyl compounds of lower molecular weight, such as formaldehyde and benzaldehyde, thus affording greater mobility for reaction than might be expected from larger carbonyl-containing compounds.

The yellow color evidenced by partially oxidized benzaldehyde is caused by large amounts of a material of a high degree of conjugation in the oxidation products. Yellowing of polystyrene films can be explained in a similar manner if structures like the above are postulated. Infrared studies confirm that carbonyl structures do exist in polystyrene after exposure to ultraviolet radiant energy in air as mentioned previously.

8.3. Stable Free Radical Compounds

It is possible that the absorbance of the film immediately following exposure to ultraviolet radiant energy is the absorbance of a relatively stable free radical whose structure can shift to a higher order of conjugation on storage in the dark, only to be reactivated by ultraviolet radiant energy at a later time. Such possible mechanisms might be of the types:

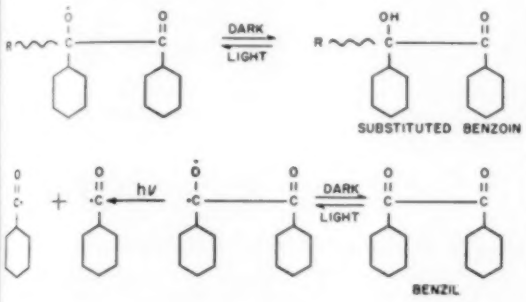

Both compounds would be relatively nonvolatile at the temperatures of the exposure and storage conditions used in this work. Infrared spectra of the films in a post-radiated state were nearly identical with spectra of the films made immediately following an exposure period. Therefore, no change in carbonyl or hydroxyl content between the two states could be so detected; but such a change might be too small to be measurable by this method.

The reaction occurring in the dark is not continuously progressive as is the reaction in ultraviolet radiant energy in the sense that most of the storage degradation products after any one exposure are formed in the first 75 hr of storage and very little more is formed even after as many as 64 days of storage. The reaction in the dark does not seem to affect the rate of degradation by ultraviolet radiant energy, but the reaction in ultraviolet governs the reaction in the dark. In the first place, the reaction in the dark requires a previous S–1 sunlamp exposure for it to occur. Specimens of the pure film and of the monomer-containing film were stored for 4 months in the dark at room temperature with no other treatment, and their ultraviolet transmittance showed no change during that time. Second, the amount of storage product formed at any one time is proportional to the total number of hours of exposure to ultraviolet radiant energy received at that time. Even though an exposure to ultraviolet energy immediately following a storage period seems to counteract the effect of storage, the following storage period shows an increase in the development of storage product over the previous period due to the additional exposure to ultraviolet radiant energy. These facts seem to support the assumption of the formation on exposure to ultraviolet radiant energy of relatively stable free radicals which shift to structures of more conjugation on storage; the latter are, in turn, reactivated and more free radicals formed by further exposure to ultraviolet radiant energy.

These "stable" free radicals probably can exist because the polymer is exposed and measured in the solid state. Evidence for the presence of long-lived free radicals in materials of rigid or crystalline structure is increasing day by day [14].[7] The lack of mobility of polymer chains in a material which is held below its glass-transition temperature [8] is the most logical explanation for entrapment of free radicals on the end of polymer chains. Termination reactions of such radicals are extremely slow due to such low mobility, and the slow diffusion of oxygen and other gaseous materials into such a mass would also severely limit the rate of reaction of these materials with the active parts of the polymer in the interior of the sample.

The presence of styrene monomer in the polymer apparently augments the degradation of the polymer chain, as well as producing monomer oxidation products, such as formaldehyde and benzaldehyde through free radical reactions [15, 16]. In the case studied here, the addition of styrene monomer to the polymer has resulted in degradation of the sample, as followed by ultraviolet transmission measurements, at a rate almost double that of the pure polymer (see table 2 and fig. 17). Infrared measurements made on the films after the total exposure of 290 hr to ultraviolet radiant energy from an S–1 sunlamp showed a very appreciable difference between the two films; the carbonyl and hydroxyl absorption bands of the monomer-containing film are almost double those of the pure film. Figure 20 illustrates these differences as well as the other spectral changes which occurred. The carbonyl group absorptance is shown in the region of 5.7 to 6.0μ and that of the hydroxyl in the region of 2.85μ. The spectrum of each film after 290 hr of S–1 sunlamp radiation is shown in this figure along with a spectrum of an untreated film which is common to both. This comparison is possible because the monomer that was added and remained in the one film was insufficient to cause any change in the infrared spectrum of the untreated polymer, although sufficient to effect an appreciable change in the degradation. The increase in degradation caused by the addition of monomer is not noticeable in the rates computed from the ultraviolet transmission measurements after approximately 200 hr of exposure to S–1 sunlamp radiant energy. This change in rate indicates that the added monomer had probably completely reacted by that time and thence the degradation of this film proceeded as in the pure film.

[7] Such evidence was summarized by William O. Baker of the Bell Telephone Laboratories, Murray Hill, N. J., in a lecture at the Polytechnic Institute of Brooklyn on January 17, 1953, entitled "Entrapped Polymer Radicals."

[8] Sometimes called second-order transition temperature.

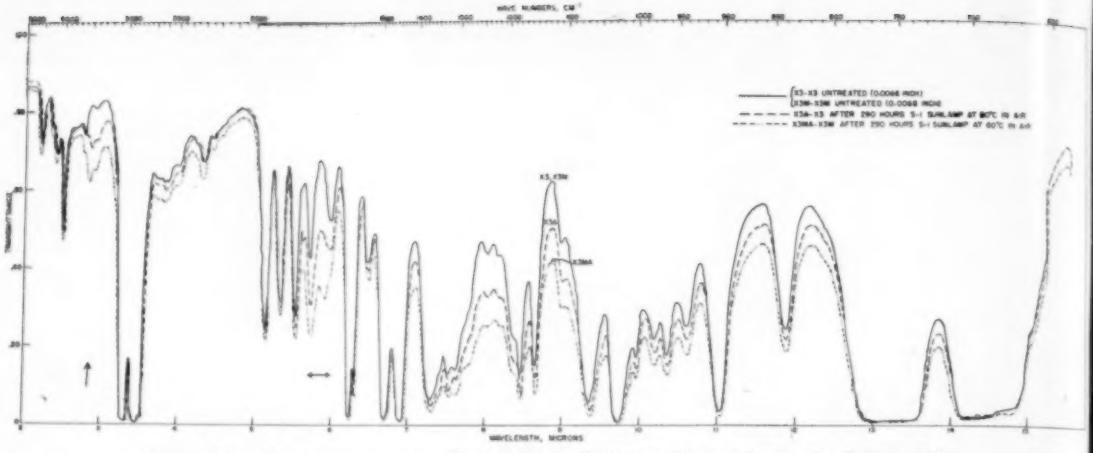

FIGURE 20. *Effect of exposure to radiant energy on the infrared transmittance of polystyrene films.*

8.4. Oxidation Products

The mechanisms that have been postulated for the degradation of polystyrene in ultraviolet radiant energy, however, are probably not all the possible reactions because polystyrene most likely is not a linear hydrocarbon polymer. It has been shown to contain oxygen in the chain [17]. Portions of catalysts, when used, are also part of the chain. All these factors offer weak links for the initiation of degradation and also can alter the products formed on exposure to ultraviolet radiant energy, depending on their type and number. The presence of a multicomponent system is borne out in part by the fact that the absorption curve in the region 290 to 400 mμ for the exposed samples does not exhibit a sharp absorption peak, but rather a broad band, indicating a mixture of compounds absorbing in this general region.

Boyer [18] has described many of the factors affecting the ultraviolet absorbance of a degraded halogen-containing copolymer. Those factors applicable to the explanation of the absorbances noted in the present case of degraded polystyrene include an inductive effect of the conjugated systems on each other, the influence of the presence of a mixture of isomers, the coexistence of many degrees of conjugation, and the positional isomerization of double bonds. However, because of the presence of the phenyl groups and the oxidized structures in polystyrene, a long linear conjugated system is not required to produce the absorbance noted above 300 mμ as is necessary in aliphatic polymers in the absence of air. Boyer also states that in the case of exposure to light, it will be those regions of the chain that have already developed unsaturation and conjugation that will absorb radiant energy most strongly and over a progressively widening spectral band. Although the oxidation and production of unsaturation may be a random process initially, the localization of absorbed energy probably then promotes unsaturation in adjacent monomer units leading to the formation of further conjugated systems.

The most reasonable approach to understanding the steps of the reaction in ultraviolet radiant energy would be to study more simple parent compounds than polystyrene. Styrene monomer, cumene, and benzaldehyde appear to be the most likely compounds for initial study of oxidation mechanisms promoted by ultraviolet radiant energy. Investigations of the reactions occurring in the dark following exposure to radiant energy should be studied with pure materials of definitely known structure which are solids at the temperatures used. Such compounds are typified by *n*-dotriacontane and a similar branched saturated hydrocarbon. Materials whose glass-transition temperatures are above room temperature would be desirable at the start. This factor would increase the possibility of obtaining entrapped free radicals in the mass of the material.

9. Effect of Thermal Energy on Transmittance

The initiation of degradation in these experiments was apparently induced by the ultraviolet radiant energy and not by the approximately 60° C temperature at which the exposures were conducted. It has been pointed out previously that 2 hr of heat at 60° C in air following a storage period in which absorption occurred will not eliminate any of the absorption band formed during storage. Heating at this temperature in the absence of ultraviolet radiant energy will not cause degradation of the polystyrene such as that caused by exposure to ultraviolet radiant energy at 60° C.

Specimens of the pure film and of the monomer-containing film which had been stored for 4 months

in the dark at room temperature were heated in an air oven at 60 to 63° C for a total of 290 hr. Ultraviolet transmission measurements after intermittent heat and storage periods showed no long wavelength absorption band and almost no change at all in the over-all spectrum. The films also did not exhibit any discoloration. Previous infrared measurements on films subjected to 100° C for 200 hr [2] did not show any production of carbonyl or hydroxyl absorption bands or any other spectral change.

10. Summary and Conclusions

Pure polystyrene film exposed to 290 hr of ultraviolet radiant energy from an S–1 sunlamp at 60° C in air was degraded as shown by decreased ultraviolet transmittance. The absorbance increased linearly with exposure time and the greatest rate of increase was calculated to be at wavelengths shorter than 300 mμ.

Storage of pure polystyrene film in the dark in air at room temperature following exposure to an S–1 sunlamp caused the development of a definite broad absorption band with a maximum at 340 mμ. Subsequent exposure to ultraviolet radiant energy caused the elimination of the absorption band developed on storage.

The formation of the post-radiation products was governed by the S–1 radiant energy; storage without previous ultraviolet exposure caused no change in the ultraviolet spectrum. The formation of the storage products, however, did not alter the rate of degradation by ultraviolet radiant energy.

Exposure of the polymer film to heat at 60° C in air for 290 hr with intermittent storage caused no change in the ultraviolet spectrum, the degradation shown by films exposed to S–1 radiant energy at this temperature being induced by the S–1 radiant energy and not by the accompanying heat.

The addition of monomer to pure polymer did not change the pattern of degradation, as shown by ultraviolet spectrophotometry, but did cause the over-all degradation to occur at an increased rate; the accelerated rate held until all the monomer was apparently spent and thence the reaction proceeded as for pure polymer.

Reactions of the type that may account for the absorption curves noted on exposure to ultraviolet radiant energy and on subsequent storage are postulated.

The shape of the ultraviolet absorption curves of the purified polymer after exposure to ultraviolet radiant energy and subsequent storage closely resembles the shape of the initial spectra obtained on commercial polystyrene samples, which indicates that the impurities in the commercial products are of the same chemical types as those produced on exposure of pure polymer to ultraviolet radiant energy and subsequent storage. In most cases the commercial samples absorbed more strongly than the degraded purified polymer.

The authors express their appreciation to Shigeru Ishihara for valuable suggestions during the conduct of the work and to C. Brown and H. A. Baker for preparation of the figures.

This investigation was sponsored by, and conducted with financial assistance from the Office of the Quartermaster General, Department of the Army.

11. References

[1] L. A. Matheson and R. F. Boyer, Light stability of polystyrene and polyvinylidene chloride, Ind. Eng. Chem. **44,** 867–74 (1952).

[2] B. G. Achhammer, M. J. Reiney, and F. W. Reinhart, Study of degradation of polystyrene, using infrared spectrophotometry, J. Research NBS **47,** 116 (1951) RP2235.

[3] B. G. Achhammer, M. J. Reiney, L. A. Wall, and F. W. Reinhart, Study of degradation of polystyrene by means of mass spectrometry, J. Polymer Sci. **VIII,** No. 5, 555 (1952).

[4] Plastics, organic: general specifications, test methods. Federal Specification L–P–406a (Government Printing Office, Washington 25, D. C., Jan. 24, 1944).

[5] A. Smakula, Zur Bestimmung der Molekulargewichte von Polystyrolen, Angew. Chem. **47,** 777 (1934).

[6] J. J. McGovern, J. M. Grim, and W. C. Teach, Determination of monomer in polystyrene. Spectrophotometric and solubility methods, Anal. Chem. **20,** 312 (1948).

[7] E. J. Meehan, Spectrophotometric determination of the styrene content of butadiene-styrene copolymers, J. Polymer Sci. **I,** 175 (1946); Rubber Chem. and Tech. **19,** 1077 (1946).

[8] J. E. Newell, Residual monomer in polystyrene. Spectrophotometric analysis, Anal. Chem. **23,** 445 (1951).

[9] T. W. Campbell, S. Linden, S. Godshalk, and W. G. Young, The absorption spectra of some benzene derivatives with unsaturated side chains, J. Am. Chem. Soc. **69,** 880 (1947).

[10] N. Hadden and J. A. Perry, Ultraviolet spectrophotometric determination of styrene in ethylbenzene, Anal. Chem. **23,** 1337 (1951).

[11] Catalog of ultraviolet absorption spectrograms, issued by the American Petroleum Institute Research, Project 44 at the NBS.

[12] R. A. Friedel and M. Orchin, Ultraviolet spectra of aromatic compounds (John Wiley & Sons, Inc., New York, N. Y., and Chapman & Hall, Ltd., London, 1951).

[13] H. L. J. Backstrom, Der Kettenmechanismus bei der Autoxydation von Aldehyden, Z. physik. Chem. **B25,** 99–121 (1934).

[14] L. A. Wall and M. Magat, Dégradation des polymères par les rayons γ et les neutrons, J. chim. phys. **50,** 308 (1953); also, Effects of atomic radiation on polymers, Modern Plastics **30,** No. 11, 111 (1953).

[15] S. Medvedev and P. Zeitlin, Oxidation and polymerization of styrene, Acta Physicochim. URSS **20,** 3 (1945).

[16] H. Boardman and P. W. Selwood, The oxidation of styrene, J. Am. Chem. Soc. **72,** 1372 (1950).

[17] F. A. Bovey and I. M. Kolthoff, The mechanism of emulsion polymerization III. Oxgyen as a comonomer in the emulsion polymerization of styrene, J. Am. Chem. Soc. **69,** 2143 (1947).

[18] R. F. Boyer, A statistical theory of discoloration for halogen-containing polymers and copolymers, J. Phys. and Colloid Chem. **51,** 80 (1947).

WASHINGTON, May 22, 1953.

UNITED STATES
GOVERNMENT PRINTING OFFICE
SUPERINTENDENT OF PUBLIC DOCUMENTS
WASHINGTON 25, D. C.
OFFICIAL BUSINESS

PENALTY FOR PRIVATE USE TO AVOID PAYMENT OF POSTAGE, $300

Journal of Research of the National Bureau of Standards Vol. 29, No. 3 September 1942

Contents

	Page
Refractive index of cesium bromide for ultraviolet, visible, and infrared wavelengths. William S. Rodney and Robert J. Spindler. RP2440	123
An expansion method for parabolic partial differential equations. J. W. Green. RP2441	127
Characteristics of internal solitary waves. Garbis H. Keulegan. RP2442	133
Becker value of manila rope by photoelastic reflectometry. Sanford B. Newman, Harry K. Hammond, III, and Helen F. Riddell. RP2443	141
Dielectric relaxation in a styrene-acrylonitrile copolymer during and after its polymerization. Paul Ehrlich and Nicholas J. De Lollis. RP2444	145
Study of degradation of polystyrene by ultraviolet spectrophotometry. Mary Jane Reiney, Max Tryon, and H. G. Achlenmeier. RP2445	155

Single copies of the above Research Papers are not available for sale, but the Superintendent of Documents, U. S. Government Printing Office, Washington 25, D. C., will furnish 100 or more copies, cash payment for the purchase price should be mailed promptly without delay.

For sale by the Superintendent of Documents, U. S. Government Printing Office, Washington, D. C. Price 15 cents
Subscription price $3.00 a year; $1.25 additional for foreign mailing. Remittance should be by money order
UNITED STATES GOVERNMENT PRINTING OFFICE: WASHINGTON: 1942